Australian Government
Department of Defence
Defence Science and
Technology Organisation

A Review of Australian and New Zealand Investigations on Aeronautical Fatigue During the Period April 2013 to March 2015

Editors: Phil Jackson and Chris Wallbrink

Aerospace Division

Defence Science and Technology Organisation

ABSTRACT

This document has been prepared by the Australain national delegate to ICAF Phil Jackson, supported by Chris Wallbrink, for presentation to the 34th Conference of the International Committee on Aeronautical Fatigue and Structural Integrity (ICAF) scheduled to be held in Helsinki, Finland, June 1st to 2nd 2015. The report contains summaries of the research and associated activities in the field of aircraft fatigue and structrural integrity at research laboratories, universities and aerospace companies in Australia and New Zealand during the period April 2013 to March 2015. The review covers structural integrity and fatigue-related research programs as well as fatigue investigations on specific military and civil aircraft.

A report of the same name will be published by the Defence Science and Technology Organisation and available for public release.

Approved for public release

Contents

1. INTRODUCTION

This document presents a review of Australian and New Zealand work in fields relating to aeronautical fatigue and structural integrity in the period April 2013 to March 2015, and is made up from inputs from the organisations listed below. The editor acknowledges these contributions with appreciation. Enquiries should be addressed to the person identified against the item of interest.

DSTO	Defence Science and Technology Organisation, 506 Lorimer Street, Fishermans Bend, VIC 3207, Australia
DTA	Defence Technology Agency, Auckland Naval Base, New Zealand
QinetiQ Australia	Level 3, 210 Kings Way, South Melbourne, VIC 3205, Australia.
Monash University	Dept of Mechanical Engineering, PO Box 72, Monash University, VIC 3800, Australia.
RMIT University	Dept of Aerospace, Mechanical and Manufacturing Engineering, PO Box 71 Bundoora, VIC 3083, Australia
The University of Sydney	School of Aerospace, Mechanical and Mechatronic Engineering, The University of Sydney, NSW 2006, Australia
The University of Adelaide	School of Mechanical Engineering, The University of Adelaide, Engineering South, L1, SA 5005, Australia
Civil Aviation Safety Authority	Aviation House, PO Box 2005 Canberra, ACT 2601, Australia
Royal Australian Air Force	Deputy Director ASI, Directorate General Technical Airworthiness, RAAF Williams, Laverton, VIC 3027, Australia

2. RESEARCH ACTIVITIES

2.1 A Constant-Stress Coupon For Fatigue Testing (Witold Waldman [DSTO])

Fatigue testing of coupons is routinely used at DSTO to provide data to be used in the fatigue life management of RAAF airframes. In order to help maximise test machine usage efficiency, and to provide the necessary statistical data for accurate estimation of fatigue life, it is desirable to be able to test the occurrence of many short cracks on a single specimen. To achieve this, it is necessary for coupons to have a notch with a large surface area where the stress remains relatively uniform.

The benefit of a constant-stress coupon is that a large area along the notch surface is subjected to the peak stress. As a result, the incidence of fatigue cracking from small naturally-occurring surface imperfections or discontinuities, which are inherent to the material and the production of the component [1, 2], will be increased, as well as potentially being more uniformly distributed over the region of constant stress. This can serve to reduce the number of coupons that need to be tested, resulting in significant time savings and greatly reduced costs in conducting fatigue testing programs to study the initiation and growth of small cracks from edge notches. The desired outcome from such fatigue testing at DSTO is to improve the fundamental understanding of the probabilistic growth of fatigue cracks from small naturally-occurring defects, where the in-service fatigue life of the component is assumed to be governed by the most severe defect that is present [3].

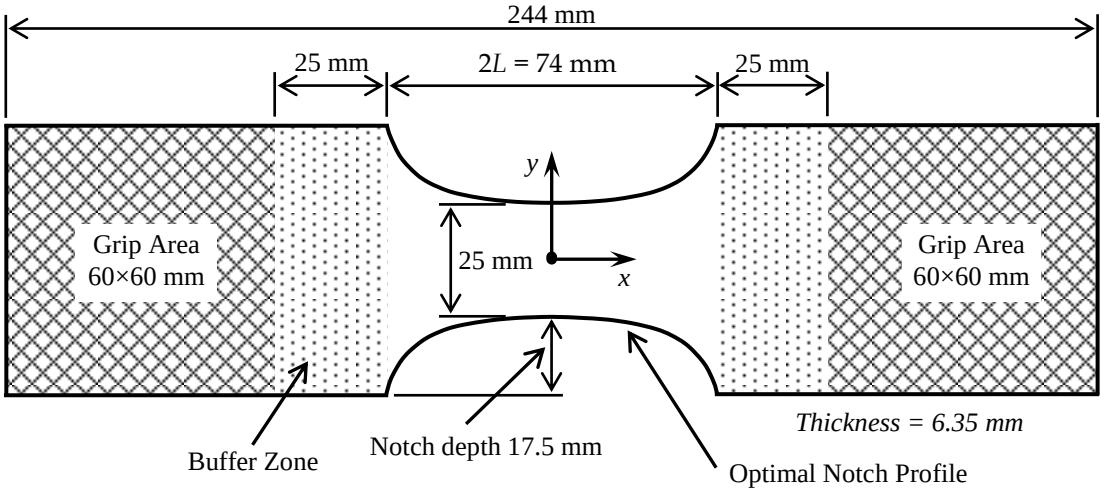

Figure 1: General shape and dimensions of optimised Constant-Stress Coupon.

To meet those special needs, a constant-stress coupon for use in fatigue testing has been designed at DSTO [4] using an in-house general-purpose shape optimisation code [5]. This coupon was produced after stress distributions were computed for various other coupon profiles composed of straight lines and/or circular arcs [6], and it was evident that such coupons could not be expected to meet the constant-stress requirement. The general shape and dimensions of this special constant-stress coupon are shown in Figure 1, where the length of the notch region is $2L$ = 74 mm. The contours of maximum principal stress obtained for a 1/8-

symmetry finite element model of the coupon loaded in uniaxial tension are shown in Figure 2(a). The distribution along the notch boundary of the maximum principal stress normalised by peak stress is shown in Figure 2(b). It is clear that the shape optimisation process has produced a long region of constant stress, extending from x/L = 0 out to $\pm x/L$ = 0.68, to within 0.5% of the peak stress. Figure 2(b) also shows the stress distributions produced by other notch geometries, none which have as good performance as the shape-optimised profile.

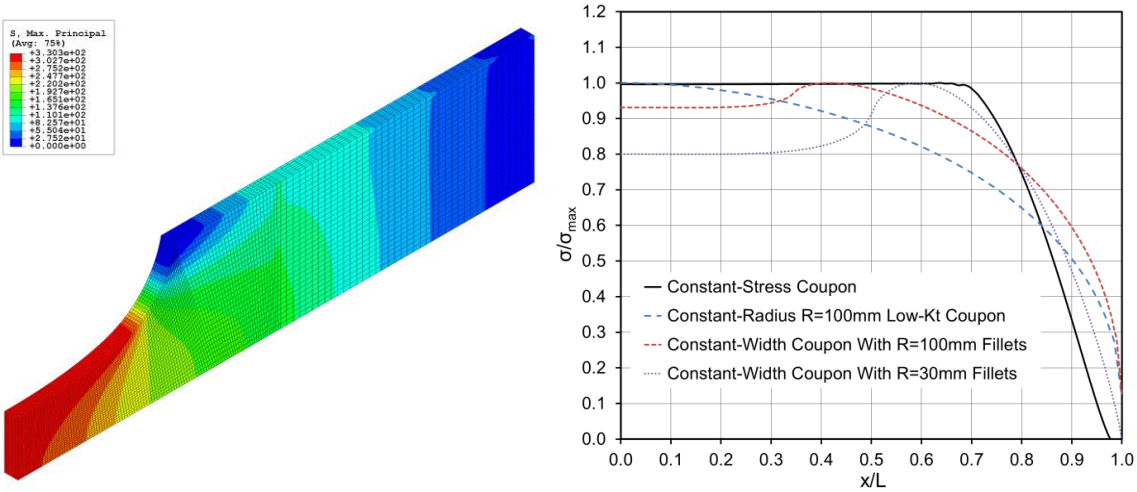

(a) (b)

Figure 2: Stress distribution for optimised Constant-Stress Coupon. (a) Contours of maximum principal stress. (b) Normalised maximum principal stress along optimal notch boundary.

This Constant-Stress Coupon is a new design that has been created to address the issue of undesirable premature failures in the grip region during the testing program. Possible factors contributing to those early failures are the use of oversized test specimen grips and the relatively low gross K_t of the prior design. In order to maintain compatibility with the previous test results, the length of the constant-stress region in the new coupon was made very similar to that of the original design. Hence, when the stresses are matched up appropriately, the two coupons will have similar amounts of surface area exposed to those stress levels.

To aid in crack growth analysis in conjunction with fatigue damage calculations, a 2D boundary element model of the Constant-Stress Coupon was created. Using this model, a number of potential crack growth trajectories were computed, based on the criterion that the crack will grow in a direction perpendicular to the maximum tension stress at the crack tip, together with the associated stress-intensity factors at each crack growth increment. The cracks were simulated as through-thickness edge cracks using the FADD2D boundary element fracture analysis code [7, 8]. The crack starting locations were distributed along the constant-stress zone of the notch boundary. As the locations of the cracks moved away from the centre of the coupon, the computed crack trajectories progressively became more curved (see Figure 3). This computationally-determined body of crack trajectory data can be compared to the crack growth trajectories obtained from fatigue testing, and should help to provide valuable insights for use in crack growth studies.

When the crack trajectories were being computed, the FADD2D boundary element code was also calculating the corresponding stress-intensity factors, K, based on the particular crack trajectory that was present at each crack growth increment. For a through-thickness edge- crack

located at any point along the notch boundary of the Constant-Stress Coupon, the stress-intensity factor can be written as

$$K = S\sqrt{\pi a}F$$

where S is the local tangential stress at the notch surface, a is the crack length as measured along the curved crack trajectory, and F is the boundary correction factor (β factor).

Figure 4 shows the stress-intensity boundary correction factor, F, as a function of distance along the notch boundary for edge-cracks of varying lengths for the Constant-Stress Coupon. For reference, the crack-length-independent boundary correction factor for a through-thickness edge-crack in a semi-infinite plate is represented by the dashed horizontal line at $F = 1.1215$ (this value of F is also known as the free-edge correction factor). For very short cracks with $a \leq 0.1$ mm, F is within 1.0% of that theoretical edge-crack solution over the entire length of the constant-stress region. For short cracks with $a \leq 1.0$ mm, the boundary correction factor is within 3.3% of $F = 1.1215$ along 84% of the constant-stress region, dropping by 7.5% at the end of the constant-stress zone.

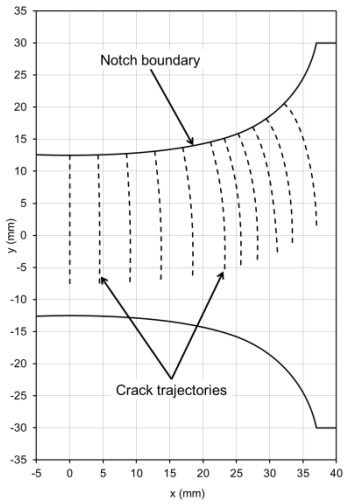

Figure 3: Simulated crack trajectories for through-thickness edge-cracks starting from different points on the notch boundary of Constant-Stress Coupon.

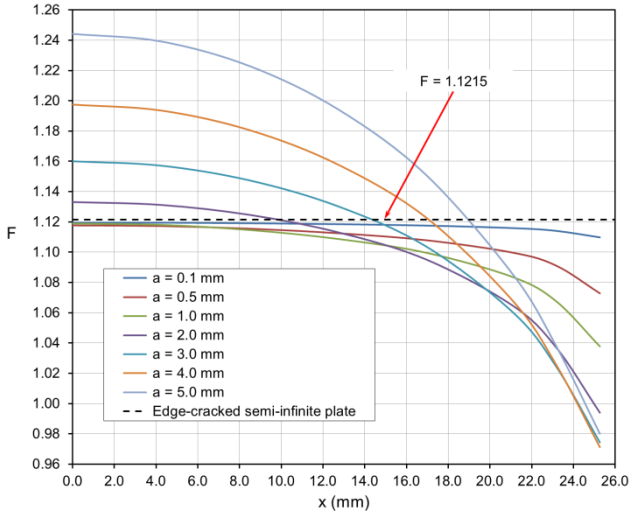

Figure 4: Boundary correction factors, F, for the Constant-Stress Coupon as a function of the distance along the notch boundary for cracks of varying lengths.

References

[1] L Molent, SA Barter, RJH Wanhill. The lead crack fatigue lifing framework. *International Journal of Fatigue*, Vol 33, 2011, pp 323–331.

[2] SA Barter, L Molent, RJH Wanhill. Typical fatigue-initiating discontinuities in metallic aircraft structures. *International Journal of Fatigue*, Vol 41, 2012, pp 11–22.

[3] A Cetin, G Härkegård, A Naess. The fatigue limit: An analytical solution to a Monte Carlo problem. *International Journal of Fatigue*, Vol 55, 2013, pp 194–201.

[4] W Waldman. A modified constant-stress coupon for fatigue testing. DSTO Minute, File B2/129/Pt4, Melbourne, 14/10/2014.

[5] W Waldman, M Heller, G Chen. Optimal free-form fillet shapes for tension and bending. *International Journal of Fatigue*, Vol 23, 2001, pp 509–523.

[6] M McDonald. FEA-COUPON-001 (OPT), Rev 2, Coupons Stress Analysis, 12/06/2009.
[7] C Chang, ME Mear. A boundary element method for two dimensional linear elastic fracture analysis. *International Journal of Fracture*, Vol 74, 1995, pages 219–251.
[8] JC Newman Jr, C Chang, L Xiao, ME Mear, VJ Kale. FADD2D: Fracture Analysis by Distributed Dislocations, Version 1.0, User Guide for Personal Computers with Demonstration Example. October 2006.

2.2 Minimised K_t Values and Boundary Shapes for Quasi-Rectangular Holes (Witold Waldman [DSTO])

DSTO continues to be extensively involved in developing technologies that reduce the cost of ownership of RAFF aircraft extending the fatigue lives of airframe structural components. A free-form shape optimisation technology, based on iterative finite element analysis techniques, has been developed and used to determine optimal repair profiles that have been applied to areas where stress concentrations caused locations to become fatigue critical [1, 2]. Optimised shapes produce significant reductions in peak stress compared to typical non-optimal circular holes. However, the method is very computationally intensive and time consuming. This makes it important to have at hand other methods of producing stress-minimised shapes that can be readily used to design holes for repair applications.

A series of transferable solutions for stress-minimised quasi-rectangular holes in a two-dimensional infinite plate has been produced by DSTO [3]. The analytical equations describing the shape and stress distribution for these quasi-rectangular holes was obtained from [4], and they are applicable to general biaxial remote loadings. The shape equations are shown in Figure 1, where θ is the polar angle that changes from 0° to 360° when going around the boundary of the hole, α and ε are hole shape parameters that can take on values in the range $0 < \alpha \leq 1$ and $-0.12 \leq \varepsilon \leq 0$, and a is the semimajor axis of the hole. For general values of α and ε, the opening is elongated in the x-direction. When $\alpha = 1$ and $\varepsilon = 0$, a circular hole of radius a is obtained. An elliptical hole shape results when $\varepsilon = 0$ and $\alpha < 1$.

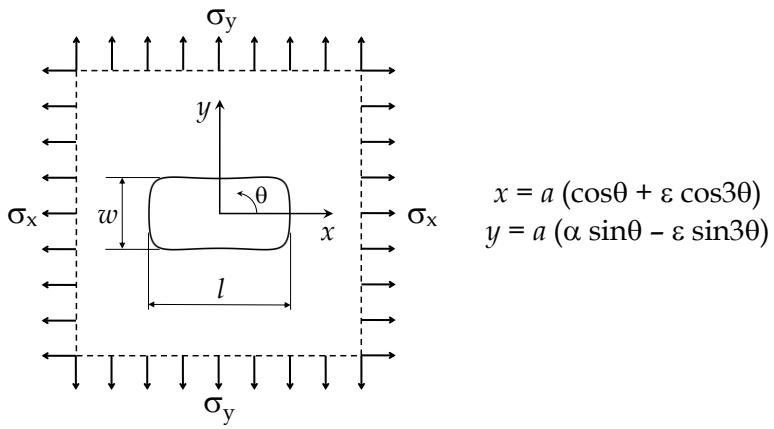

Figure 1: Idealised geometry and loading for a quasi-rectangular hole of aspect ratio $\lambda = l/w$ in a biaxially-loaded infinite plate.

The stress-minimised quasi-rectangular hole shapes were determined for a selected range of remote loading conditions (σ_x:σ_y = 1:0, 0:1, 1:1, 2:1, –1:1, and 1:–1) and a wide range of hole aspect ratios ($\lambda = l/w$ = 1 to 4). The analysis was conducted using a custom-written FORTRAN program, supported by a set of functions suitable for use in spreadsheets. The availability of these tools now provides an automated procedure that enables designers to set up biaxial loading conditions of interest and then determine sets of stress-minimised quasi-rectangular hole shapes that vary as a function of hole aspect ratio. Extensive tables and plots of shape parameters (α and ε) and stress concentration factors were determined, which enables the stress-minimised shapes to be readily used by designers. Examples of the shapes and K_t distributions for holes of aspect ratio λ = 1 and 2 under uniaxial loading are shown in Figure 2. The variation in K_t values and shape parameters as a function of hole aspect ratio for the σ_x:σ_y = 1:0 uniaxial loading case are shown in Figure 3.

These quasi-rectangular shapes produce peak stresses that are typically within 10% of those obtained using DSTO's free-form shape optimisation techniques (see Figure 3a). The parametric studies have produced families of quasi-rectangular hole shapes that offer valuable insights into the effectiveness of stress-minimised hole shapes. They have resulted in an improved capability for rapidly designing rework shapes for use in RAAF structural repairs while significantly reducing the amplitudes of the peak stresses that can lead to early fatigue failures. The shapes have a generous minimum radius of curvature, and so are very amenable to manufacture using numerically-controlled machining techniques. Structural engineers trying to utilise lightening holes to create lightweight, structurally-efficient designs can also easily apply these shapes to improve the performance of their structures.

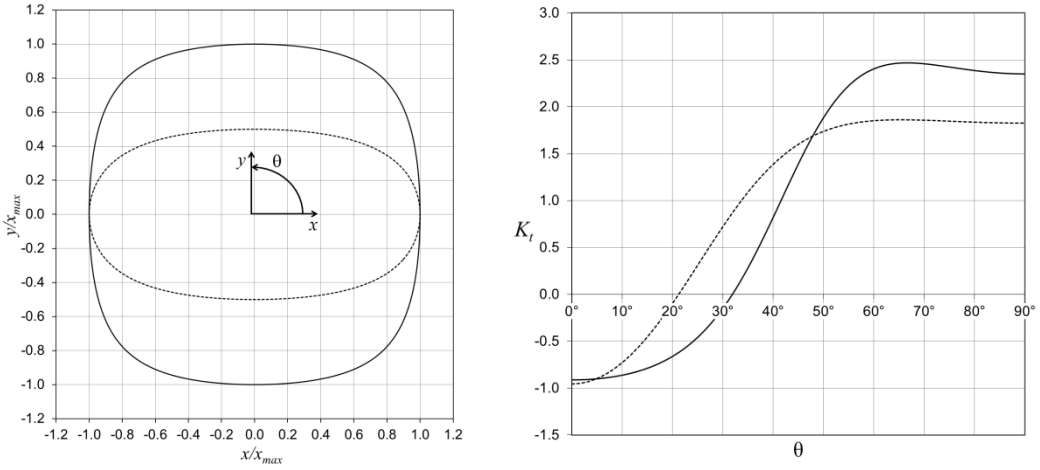

(a) (b)

Figure 2: Quasi-rectangular holes with minimised peak K_t for hole aspect ratios of $\lambda = 1$ (solid line) and $\lambda = 2$ (dashed line) in an infinite plate under a uniaxial remote loading of $\sigma_x{:}\sigma_y = 1{:}0$. (a) Shapes. (b) K_t distributions around the hole boundaries.

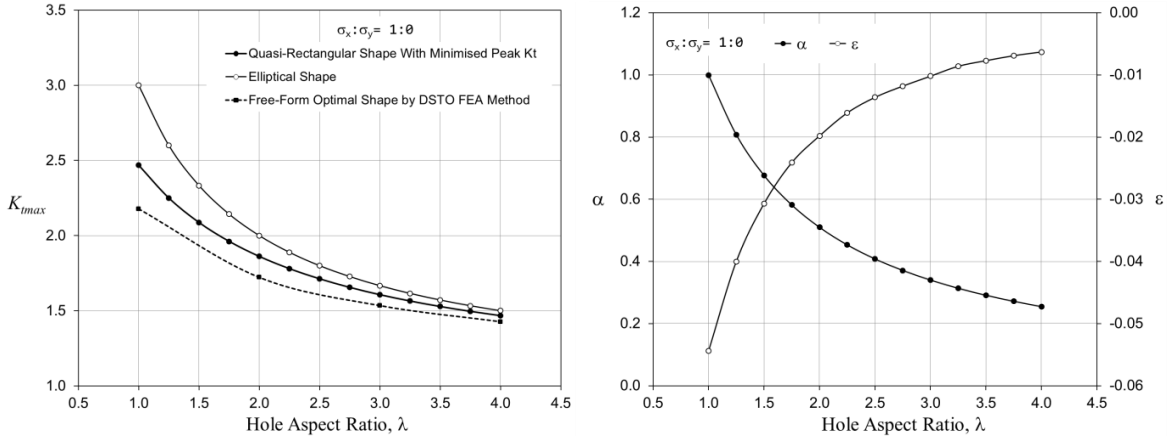

(a) (b)

Figure 3: (a) K_t values for stress-minimised quasi-rectangular holes, elliptical holes and FEA-optimised holes of various aspect ratios in an infinite plate under a uniaxial remote loading of $\sigma_x{:}\sigma_y = 1{:}0$. (b) Corresponding shape parameters α and ε for the quasi-rectangular holes.

References

[1] M Burchill, M Heller. Optimal free-form shapes for holes in flat plates under uniaxial and biaxial loading. *Journal of Strain Analysis for Engineering Design*, Vol 39, No 6, 2004, pp 595–614.

[2] W Waldman, M Heller. Shape optimisation of holes for multi-peak stress minimisation. *Australian Journal of Mechanical Engineering*, Vol 3, No 1, 2006, pp 61–71.

[3] W Waldman. Determination of minimised K_t values and boundary shapes for a class of quasi-rectangular holes in infinite plates. DSTO Technical Report, 2015 (to be published).

[4] K Rajaiah, NK Naik. Hole shapes with minimum stress concentration in infinite isotropic plates using conformal transformation. *ISME Journal of Engineering Design*, Vol 1, No 1, April 1983, pp 15–19.

2.3 Creep Effects on the Structural Performance of Hypersonic Vehicles (G.A. Vio and D. Verstraete, [The University of Sydney]).

There is resurgence in the study of hypersonic vehicles given the attraction of greatly reduced antipodal travel times. The hypersonic environment is extremely complex and the design of any aircraft requires a multidisciplinary approach to successfully create a viable vehicle.

When travelling at hypersonics speed, aircraft are subjected to extreme aerodynamic heating. This induces large stresses which are transferred throughout the airframe of the flight vehicle. The design process for such an aircraft involves optimising the structure to minimise weight while satisfying the driving design parameters. In this study the LAPCAT MR2 configuration was used with a pillow tank configuration for the internal structure, as highlighted in figure 1. The design is aimed at a cruise speed of Mach 8.

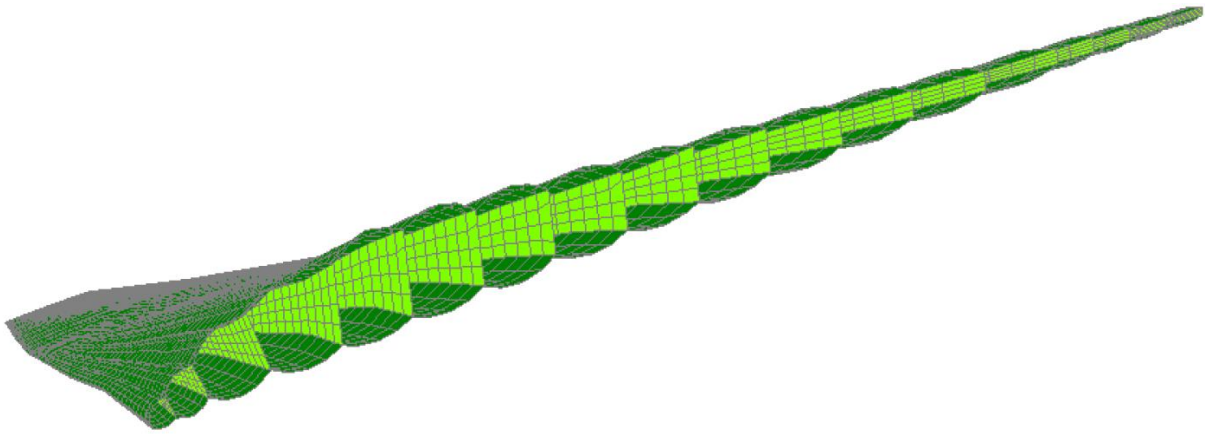

Figure 1: LAPCAT MR2 Pillow Tank Configuration

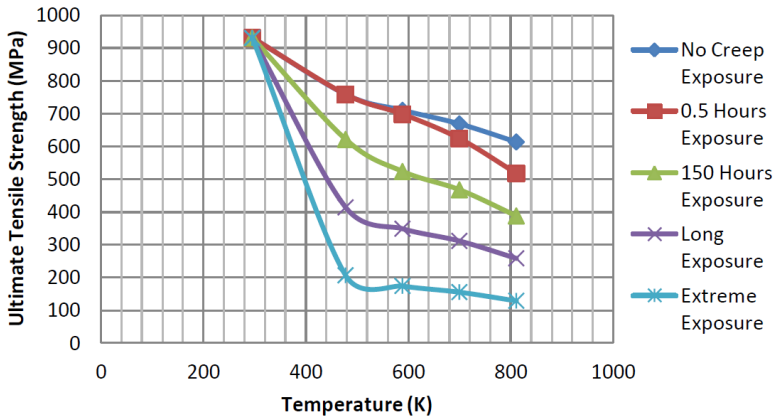

Figure 2: Changes in ultimate tensile strength at sustained elevated temperatures

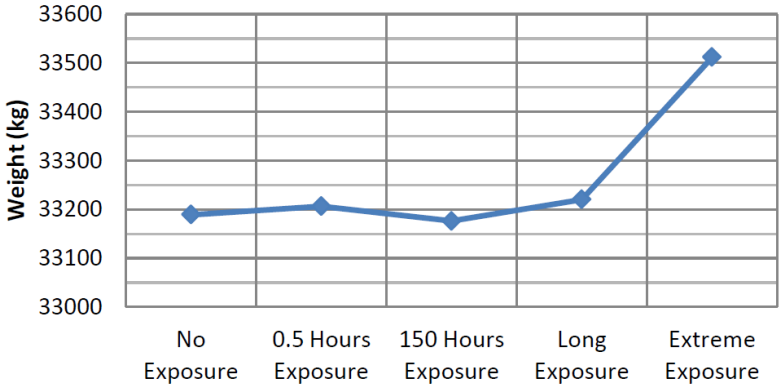

Figure 3: Changes in Structural Weight when Creep is Considered

The sustained thermal loading of the material in the outer skin of the vehicle in question leads to permanent deformation of material due to creep. For hypersonic aircraft the issue is compounded due to the long term exposure to high temperatures. This study looks at the effect of heat on the structural stability of Ti-6Al-25n-4Zr-2Mo applied to the outer skin, as an indication of the overall trend. Figure 2 shows the changes in ultimate tensile strength for a range of termperatures and exposure times. The reduction in strength requires to be compesated by an increase in material, hence a weight increase of the structure is a necessary requirement. For this particular platform there is a 1% change in structural weight even at extreme cases of creep (Figure 3). This is due to the structure already being overdesigned, hence a buffer is already in place from satysfying bucling loads requirements. This study hasn't looked at the effect on the internal structure and the rest of the vehicle, i.e. fuselage and fin.

Email: gareth.vio@sydney.edu.au

2.4 Theoretical and Experimental Study of Fatigue Growth of Interacting Cracks (Andrei Kotousov, Donghoon Chang and John Codrington [The University of Adelaide])

Despite many investigations on the fatigue behaviour of structural components weakened by closely spaced cracks being conducted in the past, the accurate prediction of lifetime in these situations still represents a very complex problem [1]. As a result, many industrial standards typically provide some crude rules to identify whether the particular cracks interact or not, and if yes, then the interacting cracks are normally treated as a single crack with some effective dimensions, which disregard the presence of ligaments between the cracks. Such an oversimplified approach typically leads to large errors and unrealistic estimates of the actual fatigue life of the components.

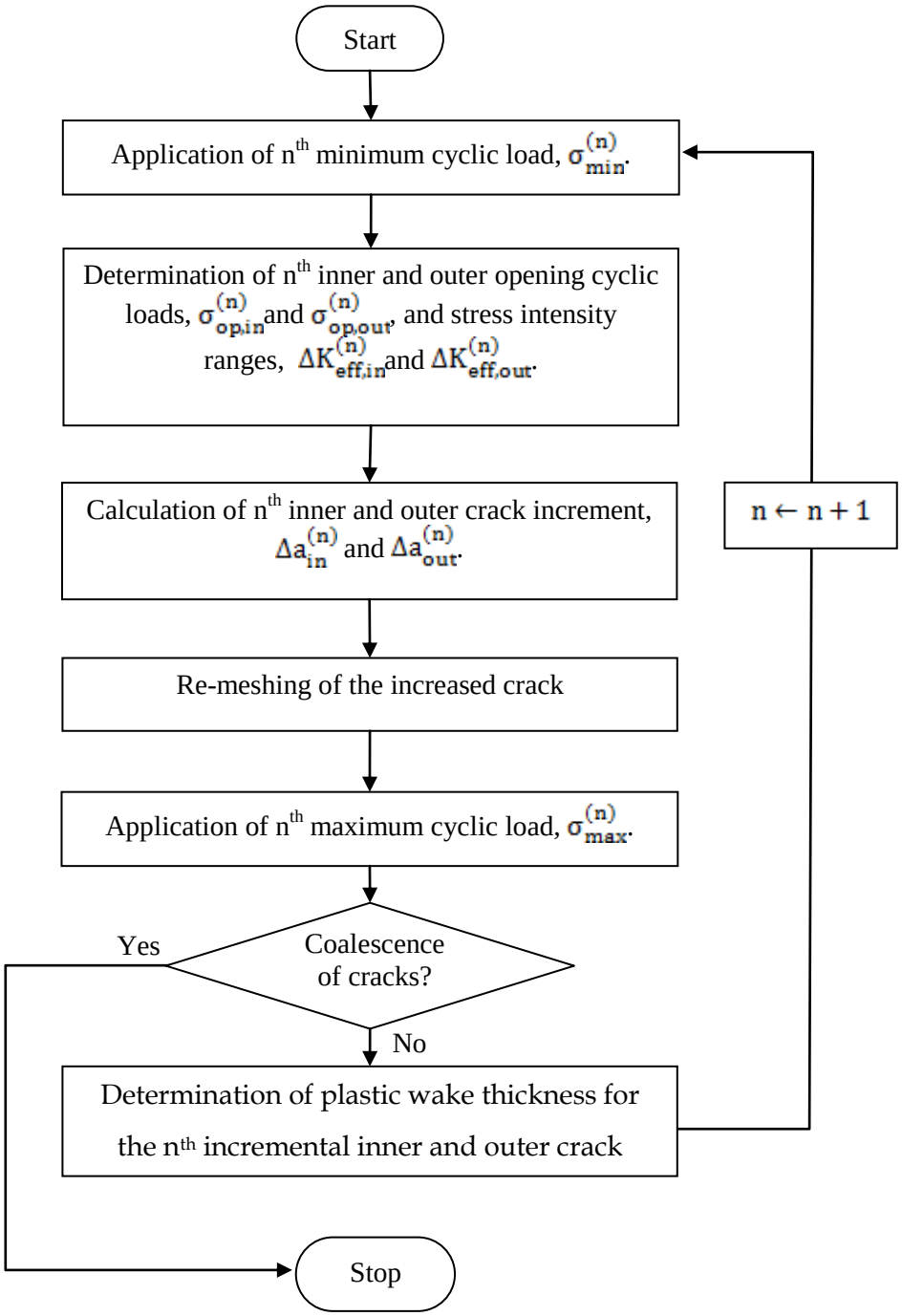

Figure 1: Numerical algorithm for calculation of crack advance

The objective of this work was to develop and validate an advanced technique for the evaluation of fatigue behaviour of closely spaced cracks. The developed technique is based on the classical strip-yield model and plasticity-induced crack closure concept, which has been widely utilised for modelling crack propagation and other fatigue phenomena. The technique is also utilises the distributed dislocation technique (DDT) and 3D fundamental solution for an edge dislocation [2]. This solution allows evaluating the thickness effect and the change of constraint conditions at the crack tips as a result of crack propagation. The crack advance scheme (see Fig.1) adopts cycle-by-cycle calculations of the crack opening stress at the crack tips and effective stress intensity factor range (or crack growth driving force) based on the loading history.

An experimental study was conducted for two collinear interacting cracks in wide plates with different thicknesses subjected to a constant amplitude cycling loading, Fig. 2. A relatively good correlation has been obtained between the theoretical predictions and experimental results [3], as shown in Fig.3. This particular geometry configuration and loading conditions represent the simplest case of interacting cracks; however, the developed technique and computational procedures can be relatively easily extended to analyse more practical problems, which could incorporate more complex geometries as well as more complex loading conditions.

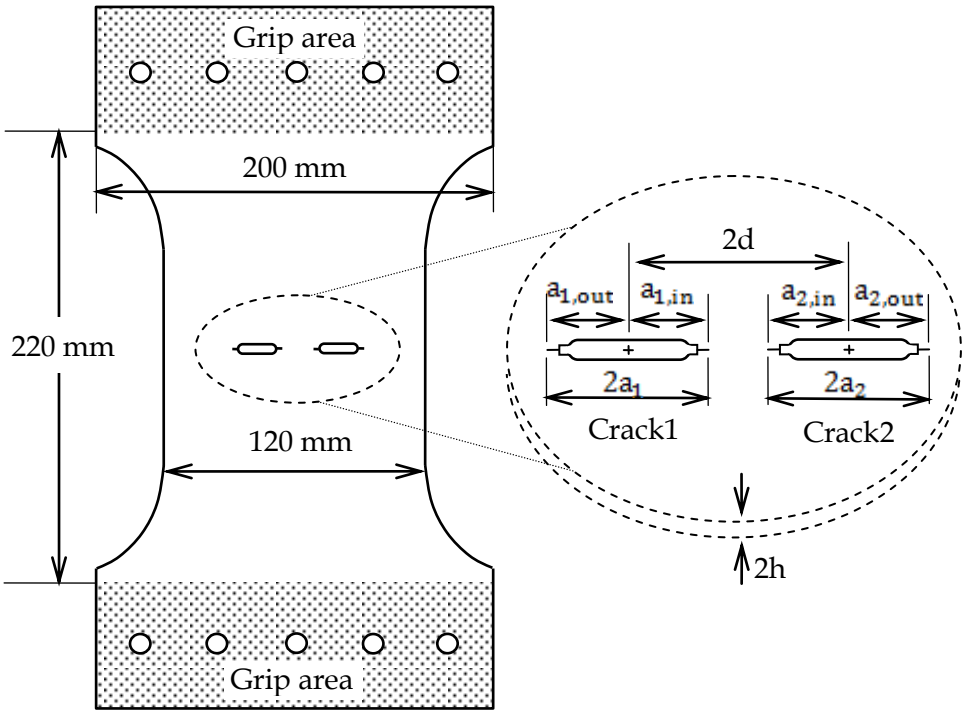

Figure 2: Fatigue specimens [3]

It was found that the plate thickness effect leads to earlier crack opening, during loading for a thicker plate specimen [3]. This highlights the importance of the plasticity induced crack closure concept in explaining fatigue behaviour. Furthermore, the strong relationship between the specimen thickness and growth rate justifies the use of the three-dimensional crack growth model in the current study. It is interesting to note that the fatigue life of a plate with two collinear cracks decreases with increasing plate thickness under a fixed cyclic loading conditions, while the resistance of the same plate to local plastic collapse increases with increasing plate thickness [4]. In other words, thicker plates weakened with two collinear cracks have lower fatigue life but higher strength against local plastic collapse.

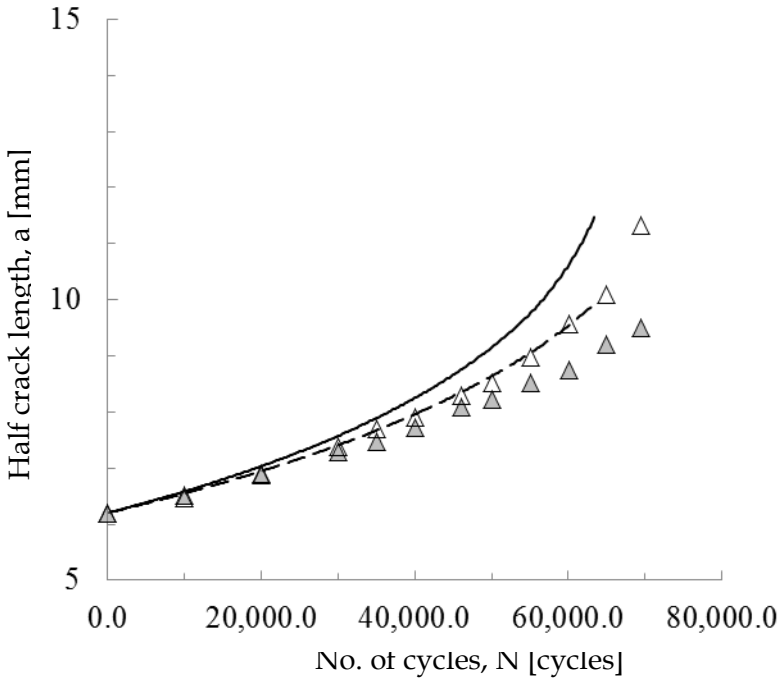

Figure 3: Measured and predicted crack growth for two tested samples [3].

References

[1] O Pártl and J Schijve. Multiple-site damate in 2024-T3 alloy sheet, International Journal of Fatigue . Vol. 15, 1993, pp. 293-299.

[2] A Kotousov. Fracture in plates of finite thickness, International Journal of Solids and Structures. Vol. 44, 2007, pp.8259 – 8273.

[3] A Kotousov and D Chang. Theoretical and experimental study of fatigue growth of interacting cracks. International Journal of Fatigue. Vol. 70, 2015, pp. 130-136.

[4] A Kotousov and D Chang .Local plastic collapse conditions for a plate weakened by two closely spaced collinear cracks. Engineering Fracture Mechanics,. Vol. 127, 2014), pp. 1-11.

[5] D Chang and Kotousov A. A fatigue crack growth model for interacting cracks in a plate of arbitrary thickness. Fatigue and Fracture of Engineering Materials and Structures. Vol. 37, 2014, pp. 1254-1267.

[6] D Chang and A Kotousov. A strip yield model for two collinear cracks. Engineering Fracture Mechanics, Vol. 90, 2012, pp. 121-128.

[7] D Chang and Kotousov A. A strip yield model for two collinear cracks in plates of arbitrary thickness. International Journal of Fracture. Vol. 176(1), 2012, pp. 39-47.

[8] A Kotousov and J Codrington. Application of refined plate theory to fracture and fatigue. In Sook Ying Ho (Ed.), Structural Analysis and Prediction Methods for Aerospace Vehicles and Structures, (pp. 96-132). Online: Bentham Science Publishers, 2010.

2.5 CGAP fatigue life developments with improved elastoplastic constitutive modelling (Dylan Agius [RMIT], Kyriakos I. Kourousis [RMIT, University of Limerick], Chris Wallbrink [DSTO] and Weiping Hu [DSTO])

Safe-life methodologies such as the strain-life method require an accurate understanding of the notch root stress-strain evolution for accurate fatigue life estimation. Oversimplification of the local notch root stress-strain material behaviour can lead to inaccurate fatigue life estimation particularly for complex spectra containing a large number of cycles. Preliminary work by Hu and Wallbrink [1] has highlighted the need for cyclic plasticity models to consider cyclic plasticity phenomena such as mean stress relaxation and ratcheting for large complex spectra for practical application. Their work demonstrated a clear deficiency in using the Masing's hypothesis [2] which is incapable of modelling these complex cyclic behaviours. Their initial work considered the implementation of the Chaboche [3] model (MAF) demonstrating improved fatigue life predictions. However it is known that the Chaboche model does not accurately model the rate of ratcheting for low stress amplitudes [4]. Therefore, the potential simulation improvement from the application of more advanced kinematic hardening models was investigated.

In rate-independent plasticity theory, the fundamental components of the constitutive model include: the yield criterion, flow rule and hardening rule. The strain-life algorithm used for simulations included the von Mises yield criterion and an associative flow rule (where the strain rate tensor is assumed to be normal to the yield surface). Hardening rules are used to describe the transformation of the yield surface with plastic flow where isotropic hardening describes the expansion of the yield surface and kinematic hardening describes the translation of the yield surface. The kinematic models implemented in the strain-life code included the Chaboche–threshold model (CH-T), the multiplicative Armstrong-Frederick model (MAFM) and the Ohno-Wang model (O-W). For the present simulations, isotropic hardening was not included.

These models were implemented in the CGAP strain-life module using parameters gathered from data obtained from specimens of 7075-T6 aluminium alloy. Fatigue analysis was conducted using clipped and unclipped versions of a load spectrum taken from a fatigue-critical location of a transport aircraft. The results of the strain-life simulations are presented in Fig 1.

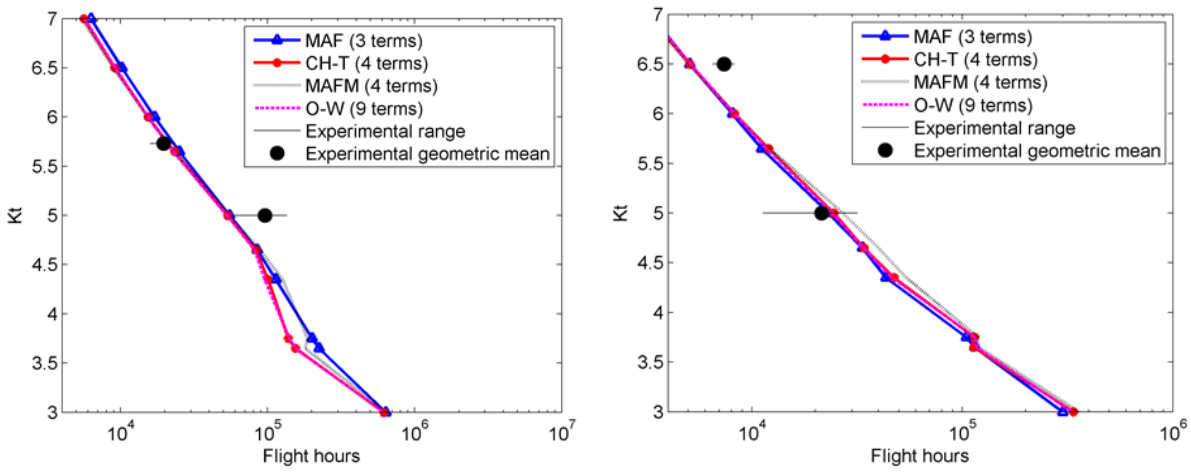

Figure 1 Fatigue calculation comparisons for clipped (a) and unclipped (b) spectra

As can be seen from the results, although fatigue simulations have demonstrated that the CH-T, MAFM and O-W provide improvements to the MAF model in ratcheting and mean stress relaxation calculations, these models appear to provide only slight improvements to the fatigue life predictions with the complex load spectra considered in this study.

Upon closer inspection of the models, a deficiency in the MAF, CH-T, MAFM and O-W models ability to simulate mean stress relaxation was discovered. Asymmetric constant amplitude strain-controlled simulations were performed using the MAF, CH-T, MAFM and O-W models to determine their ability to capture the extent of mean stress relaxation for various strain amplitudes for aluminium 7075-T6. The results of the analysis are summarised in Fig. 2.

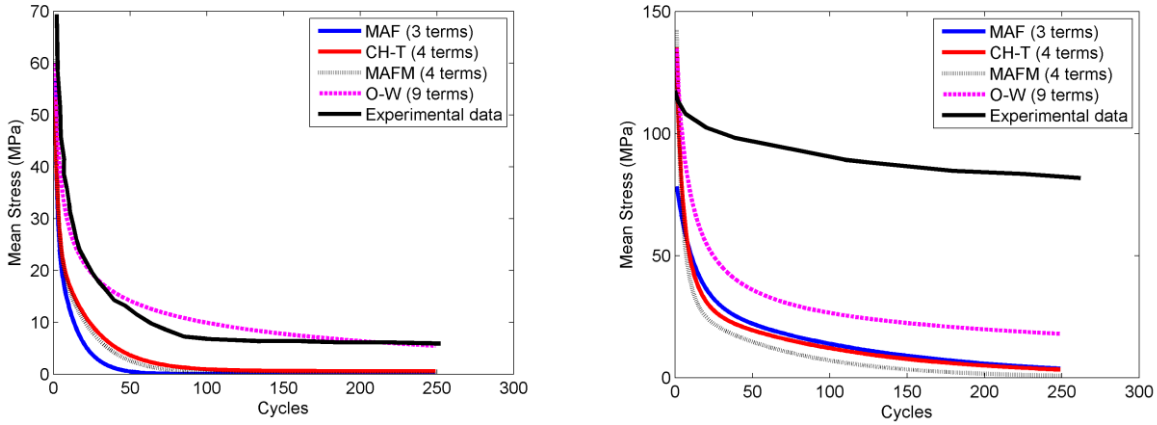

Figure 2 Comparison of the models simulating mean stress relaxation with strain amplitudes of (a) 0.85% and (b) 0.675% (experimental data from [5])

As can be seen from the results, for the higher strain amplitude Fig 2(a), the models correlate well with experimental data. However, there is a significant over-prediction in the amount of mean stress relaxation for lower strain amplitudes in Fig 2(b). Due to the complexity of real world load spectra and the present spectrum under investigation it is quite conceivable that the advanced plasticity models considered here could easily over-predict the amount of mean stress relaxation. Consequently, further investigation is required to improve the plasticity models for mean stress relaxation in combination with ratcheting effects in order to improve the accuracy and robustness of strain-life algorithms.

References

[1] W. P. Hu and C. Wallbrink, "Fatigue life analysis of specimens subjected to infrequent severe loading using a nonlinear kinematic hardening cyclic plasticity model," presented at the Advanced Materials Research, 2014.

[2] G. Masing, "Self stretching and hardening for brass (in German)," in Second International Congress for Applied Mechanics, Zurich, Switzerland, 1926, pp. 332-335.

[3] J. L. Chaboche, "Time Independent Constitutive Theories for Cyclic Plasticity," International Journal of plasticity, vol. 2, pp. 493-496, 1986.

[4] S. Bari and T. Hassan, "Anatomy of coupled constitutive models for ratcheting simulation," International journal of plasticity, vol. 16, pp. 381-409, 2000.

[5] A. Arcari, R. De Vita, and N. E. Dowling, "Mean stress relaxation during cyclic straining of high strength aluminum alloys," International Journal of Fatigue, vol. 31, pp. 1742-1750, 2009.

2.6 Improved Stress Intensity Factors for Selected Configurations in Cracked Plates (R. Evans[a], A Clarke[b], R. Gravina[b], M. Heller[a], R. Stewart[b]; a DSTO, b QinetiQ Australia)

Based on a review of the literature and the authors' experience in developing and applying beta solutions for airframe life assessment, four generic cases were identified as needing improvement. These cases are uniaxially loaded plates with either: (i) a through edge crack, (ii) a through crack approaching a hole, (iii) a through crack propagating from a hole after ligament failure, or (iv) a through crack in an integral stiffener approaching a junction. In this work accurate normalised stress intensity factors have been developed for these common structural geometries using 2D and 3D p-element FE methods, [1].

For the case of an edge crack under uniform stress with bending unrestrained or under uniform displacement, normalised stress intensity factors were developed and represented by equations. The new solutions cover a greater range of plate size and at a higher fidelity than solutions currently available in the literature. Where comparisons could be made, the new solutions were typically within 2.0% of the handbook solution.

Normalised stress intensity factors for a crack approaching a hole in a large plate were provided in tabular form. The parameters considered extend the range found in the literature. A higher density of solutions was also provided for cracks in close vicinity to the hole. Where comparisons could be made, the new solutions were principally within 1% of available solutions but had a greater difference (of up to 5%) in normalised stress intensity factors for hole-size to crack-distance ratios of 0.5 and 0.7. Refer to Figure 1.

The normalised stress intensity factors for a crack propagating from a hole after ligament failure in a finite width plate were obtained and presented as an equation. Because the hole and ligament were modelled, these analyses are much more representative of the real problem compared to the literature. The results were also used to estimate those for a semi-infinite width plate; which can be easier to apply for certain practical geometries. These were provided in tabular form. Refer to Figures 2 and 3.

Tabulated normalised stress intensity factors were provided for a through crack in a stiffener approaching a junction. A handbook comparison of a crack near a junction of two plates indicated that in approximating this geometry the solution would be over-estimated by up to 20%. Considering the assumptions needed to use the handbook solution as well as the error, it was concluded that there is no suitable handbook solution available for this geometry.

Overall it is considered that these four new solutions are beneficial since they expand the range of solutions currently openly available. They can be used as either stand alone or with compounding to analyse more complex geometries.

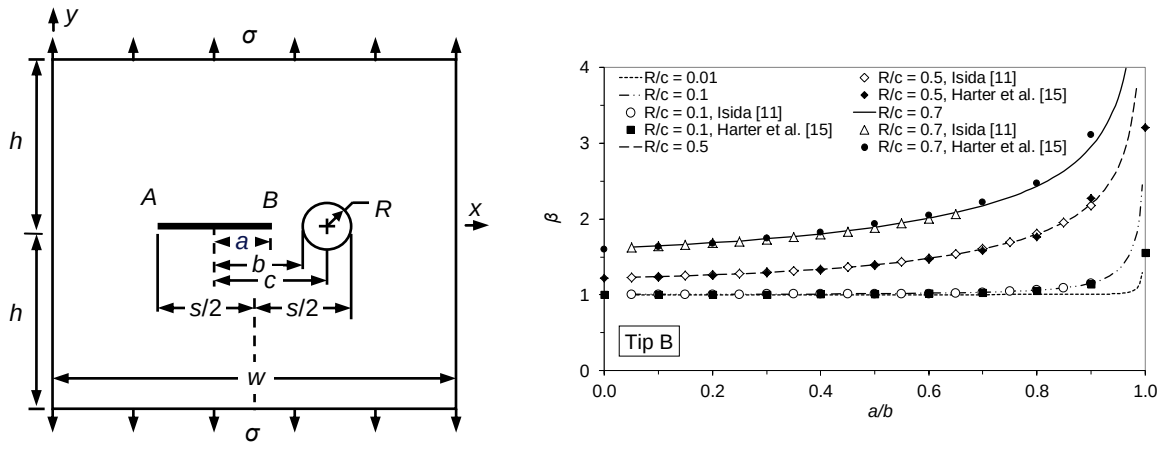

(a) (b)

Figure 1: Crack approaching a circular hole: (a) geometry and notation, (b) comparison of typical beta factors with published solutions.

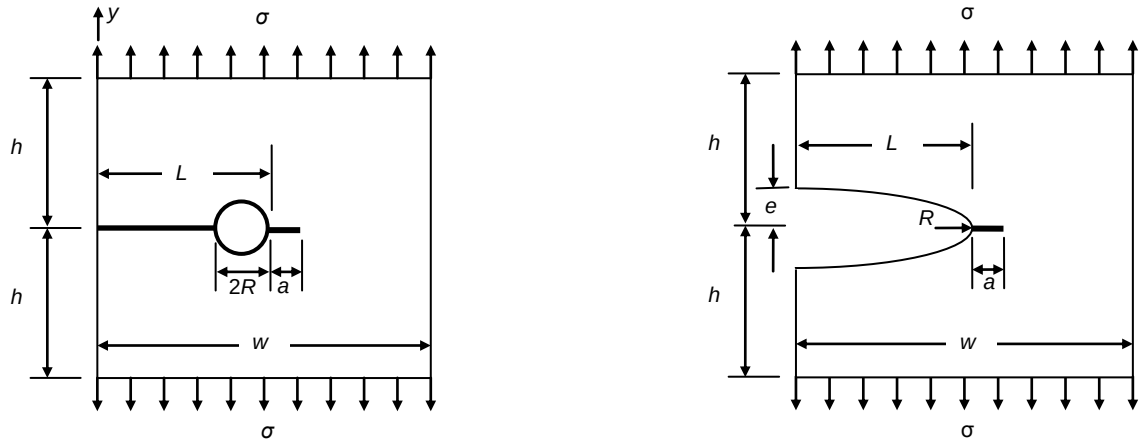

(a) (b)

Figure 2: Geometry and notation for a crack from a hole with ligament failure in a finite width plate: (a) nominal case, (b) simplified representation.

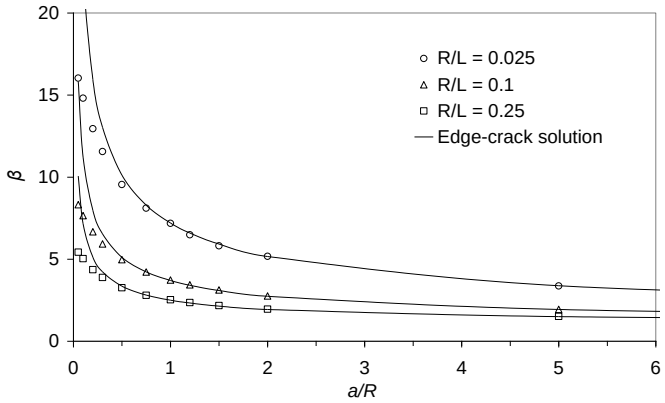

Figure 3: Beta factor results for crack from a hole with ligament failure in a semi-infinite width plate as a function of crack length 'a' compared to the edge-crack solution.

References

[1] R Evans, A Clarke, R Gravina, M Heller and R Stewart, "Improved stress intensity factors for selected configurations in cracked plates", *Engineering Fracture Mechanics*, 127 (2014) pp296-312.

2.7 Improved Stress Intensity Factors for a Single Corner Crack at a Loaded Fastener Hole (R. Evans [a], A Clarke[b], M. Heller[a], R. Stewart[b]; a DSTO, b QinetiQ Australia)

In general, the majority of fatigue cracks found in aircraft originate from loaded fastener holes. There are many published solutions in the literature for corner cracks at an open hole under remote tension loading and pin/fastener loading. Typically the pin loaded hole (or bearing) beta factor solution is developed using superposition of a plate with a hole under remote tension and a wedge solution, as shown in Figure 1.

Improved Mode I stress intensity factors for a large plate containing a single quarter-circle corner crack at a filled fastener hole are determined, [1]. Loads are applied separately to the fastener and remotely to the plate (Figure 2), with out-of-plane bending unrestrained or restrained. It is noted that there are no readily available literature solutions for the bending restrained cases. The case of a steel fastener in an aluminium plate is analysed using p-version 3D FE methods. The solutions are valid for r/t ratios of 0.25 to 1.25 and a/t of 0.02 to 0.95, where $a/c = h/w = 1.0$. Solutions representing the beta factor at an angle around the crack front of 5 and 80 degrees are presented in equation form for ease of use.

As compared to most existing solutions, the key features in the present analysis are:

(i) Contact analysis is used where the fastener and crack are modelled, as opposed to using superposition of open hole solutions and/or using an assumed pressure distribution around the open fastener hole to represent pin loading. Hence the analysis accounts for the hole propping effect which varies with crack length.

(ii) Cases with and without out-of-plane bending are considered since in many practical situations there may be significant reinforcing structure restricting bending.

(iii) Full 3D analyses are conducted to obtain the single crack solution, as opposed to converting from symmetric double corner crack case solutions or compounding using 2D solutions.

The present FEA results for the unrestrained bending case, show some significant differences to those in the existing literature. They generally result in lower beta factor values when compared to available literature solutions, especially at the 80 degree position for both the remote loading and pin loading cases. For the reasons listed above, the new solutions are considered more accurate. As expected, stress intensity factors for the bending restrained cases are lower than those for the corresponding unrestrained bending cases. This effect is most evident at the 5 degree position. Refer to Figure 3.

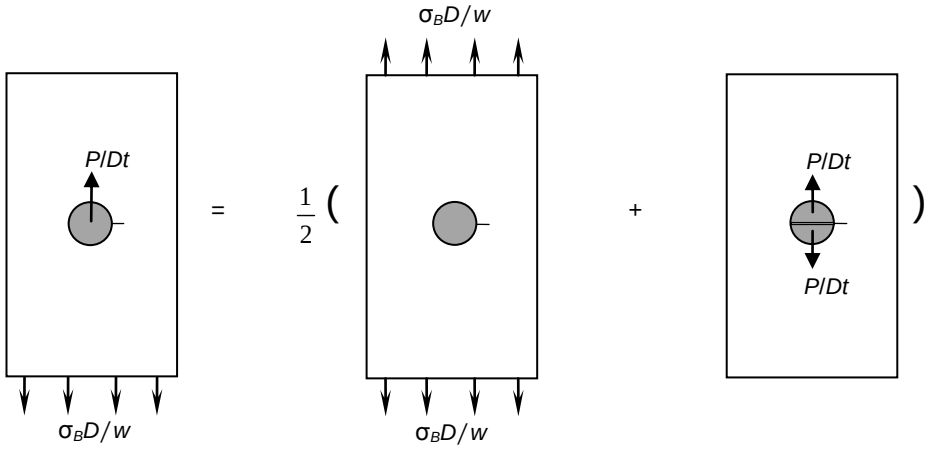

Figure 1: Diagram of the determination of the bearing solution using the principle of superposition (combination of remote tension and wedge solutions).

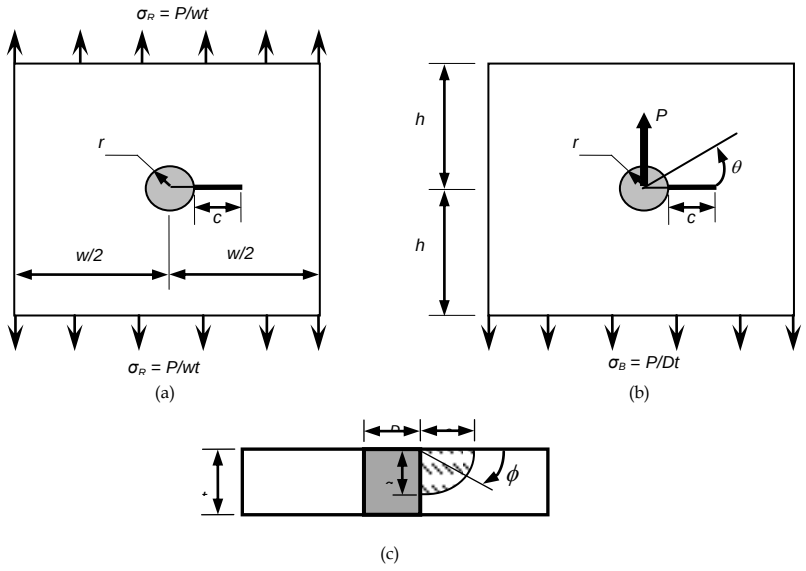

Figure 2: Schematic of relevant notation for the solutions of a single corner crack at a filled fastener hole in a very large plate: (a) remote loading case, (b) pin loading case, (c) cross section.

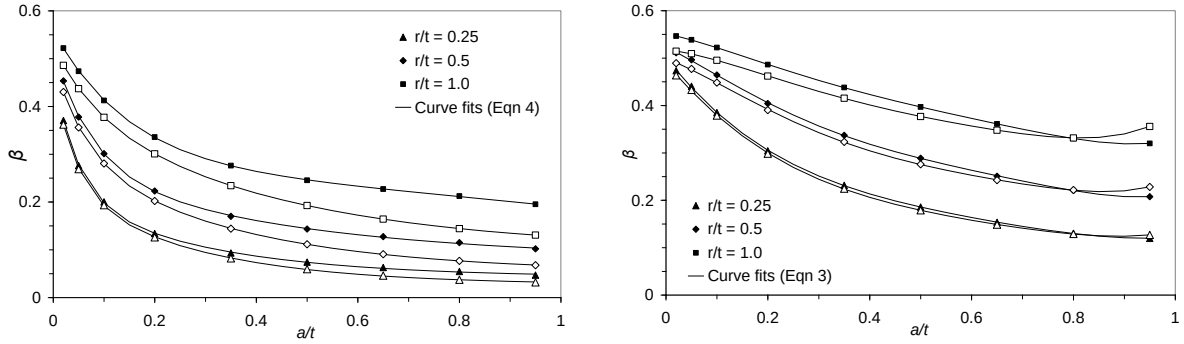

(a) (b)

Figure 3: Comparison of example generic FEA beta values for the pin loaded hole case with bending restrained (open symbols) and unrestrained (filled symbols): (a) ϕ = 5 degrees, (b) ϕ = 80 degrees.

References

[1] R Evans, A Clarke, M Heller and R Stewart, "Improved stress intensity factors for a single corner crack at a loaded fastener hole", *Engineering Fracture Mechanics*, 131 (2014) pp570-86.

2.8 Fatigue Life Analysis of Specimens Subjected to Infrequent Severe Loading using a Nonlinear Kinematic Hardening Cyclic Plasticity Model (Weiping Hu and Chris Wallbrink [DSTO])

For engineering structures subjected to cyclic load, fatigue failure normally occurs at geometrical discontinuities such as holes and notches. In aircraft structures, such locations may experience occasional severe loading that can cause appreciable local plastic deformation. This poses a significant challenge to fatigue life modelling. Modelling fatigue at critical locations subjected to numerous load cycles of varying amplitude requires a reasonably accurate and robust model for cyclic plasticity to accurately determine the stress and strain response in cases where local plasticity may occur. In work conducted in [1], the potential of a nonlinear kinematic hardening model in improving fatigue life analysis was explored. The work is motivated by the inability of an existing strain-life model to capture the difference in fatigue damages caused by an unclipped and a clipped service load spectrum. Preliminary results demonstrate that the new model was able to qualitatively demonstrate the trend in fatigue life for two critical locations analysed. Figure 1 shows the results for one of the locations. Further work is under way to verify the model against more test data and to improve its capability in dealing with cyclic softening or hardening [1].

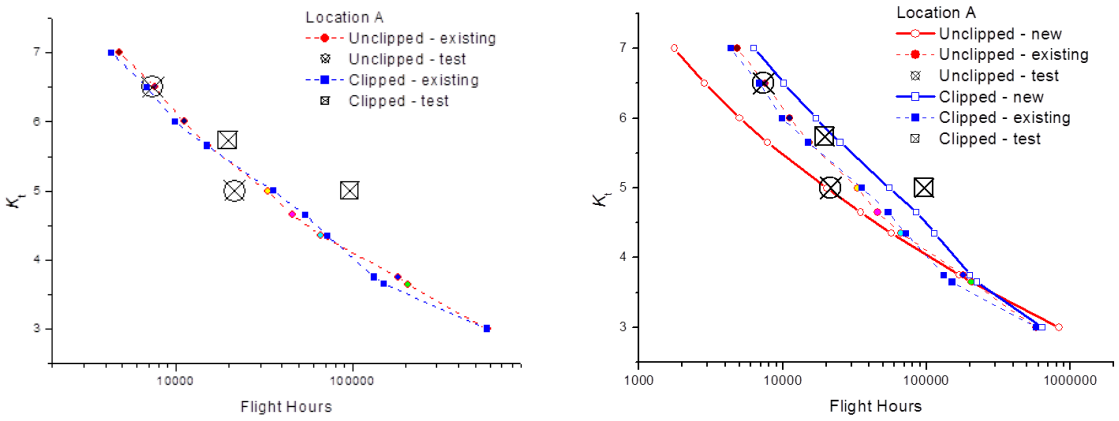

(a) (b)

Figure 1: a) Original Masing strain life model b) the strain life model based on an advanced cyclic plasticity model.

References

[1] W. Hu and C. Wallbrink. Fatigue Life Analysis of Specimens Subjected to Infrequent Severe Loading using a Nonlinear Kinematic Hardening Cyclic Plasticity Model. Advanced Materials Research, Vol. 891-892, 2014, pp. 512-517.

2.9 An Improved Crack Tip Plastic Zone Size Estimate Based on a Bilinear Material Model (Chris Wallbrink [DSTO])

A new simple eqation to describe the plastic zone size ahead of a crack tip based on a bilinear material model under plane stress conditions was developed. The model mirrors the simple approach adopted by Irwin to estimate the plastic zone size, but considers a bilinear material characterisation as opposed to the perfect plasticity assumption. It is envisaged that the present simple method will aid in the development of better fatigue crack growth algorithms.

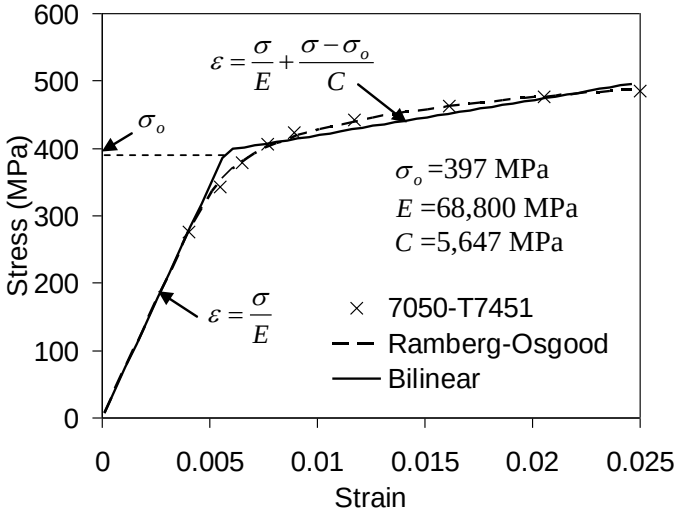

Figure 1: Bilinear cyclic stress strain relationship for 7050-T7451

The bilinear hardening model describes plastic deformation (when $\sigma > \sigma_o$ where σ_o is the yield stress) by an additional plastic strain term characterised by the hardening parameter C, Figure 1. The hardening parameter C is the stress $\sigma - \sigma_o$ per unit amount of plastic strain ε^P.

The elastic-plastic estimate of the plastic zone size r_p for a bilinear hardening material model is obtained with

$$r_p = \frac{\left(\gamma - \sqrt{8+\gamma^2}\right)^2 K^2}{8\pi\sigma_o{}^2},$$

where $\gamma = \sqrt{C/(E+C)}$, K is the mode I stress intensity factor and σ_o is the yield stress [1].

The solution is compared to elastic plastic finite element analysis using bilinear material properties to determine the plastic zone size. Good agreement between the present model and the results from the finite element analysis is achieved and is presented in Figure 2. The present analysis shows that the elastic perfect plastic models predict a larger plastic zone in comparison to both the present model and FEA. Perfect plasticity provides significant mathematical simplifications but does not reflect real material behaviour. In contrast Hutchinson's bilinear linear solution is an attempt to better represent real material behaviour but significantly under-predicts the actual size of the plastic zone. It is interesting to note that the present methodology

will return Hutchinson's bilinear solution if both load redistribution and the elastic component of strain are ignored in the derivation.

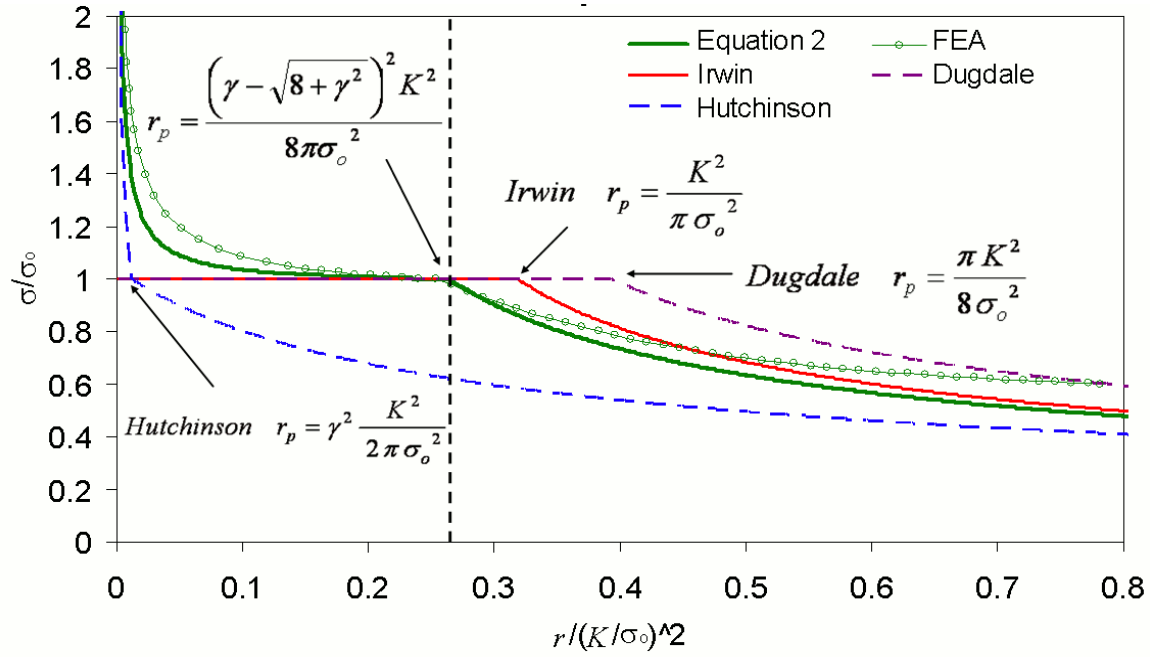

Figure 2: Finite element analysis compared to the present model

References

[1] C. Wallbrink. An Improved Crack Tip Plastic Zone Size Estimate Based on a Bilinear Material Model. In: The 8th International Structural Integrity and Fracture Conference, Melbourne: 2-7 March 2013.

2.10 Unifying Monotonic and Hysteresis Material Properties for Notch Plasticity Analysis under Variable Amplitude Loads (XiaoboYu, Qianchu Liu and Chris Wallbrink [DSTO])

This study was performed in support of accurate notch plasticity analysis under variable amplitude loads. Monotonic and cyclic strain-controlled tests were performed on flat dog-bone coupons machined from 6.35mm thick 7075-T651 aluminium alloy plates. The tests with low-high-low strain amplitude transitions revealed both an instant softening following the high strain amplitude cycle and a gradual recovery during the subsequent low strain amplitude cycles. The transition from monotonic-like to hysteresis-like material behaviour was found to be consistent with an overload induced softening and recovery process. A conceptual consideration is thus proposed to unify the characterisation of monotonic and hysteresis material properties. The implications of the present finding on notch plasticity analysis are also discussed [1].

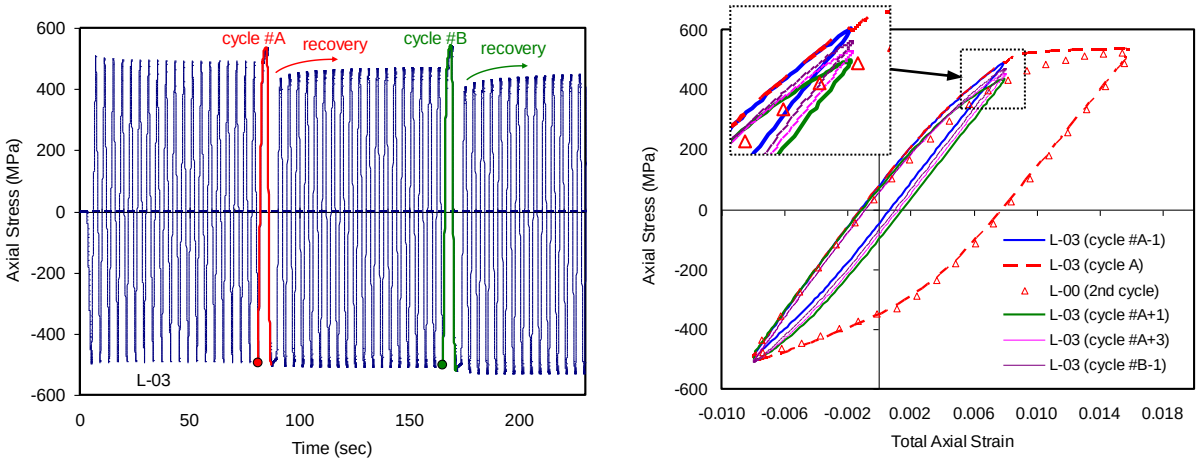

Figure 5: Softening induced by high strain amplitude cycles (cycles #A and #B) and gradual recovering during subsequent low strain amplitude cycles in coupon test L-03. (a) Stress time history; (b) Hysteresis loops.

References

[1] X. Yu, Q, Liu and C. Wallbrink. Unifying monotonic and hysteresis material properties for notch plasticity analysis under variable amplitude loads. Advanced Materials Research, Vol. 891-892, 2014, pp. 500-505.

2.11 The effect of specimen thickness on fatigue crack growth under variable amplitude loading in 7075-T7351 Aluminium (Chris Wallbrink [DSTO])

An investigation has been conducted to examine the effect of material thickness on fatigue crack growth in 7075-T7351 Aluminium under variable amplitude loading. The results of the investigation have demonstrated that a significant effect on fatigue crack growth is observed under variable amplitude loading for specimen thicknesses ranging from 2 mm to 6.4 mm. For all the coupons tested the thinner coupons display longer fatigue lives. The observed behaviour was modelled by modifying the constraint factors used in the FASTRAN crack closure model. The present observation that specimen thickness has a significant effect on fatigue crack growth highlights the importance of selecting appropriate material data and a suitable fatigue crack growth model to use in subsequent fatigue crack growth analysis.

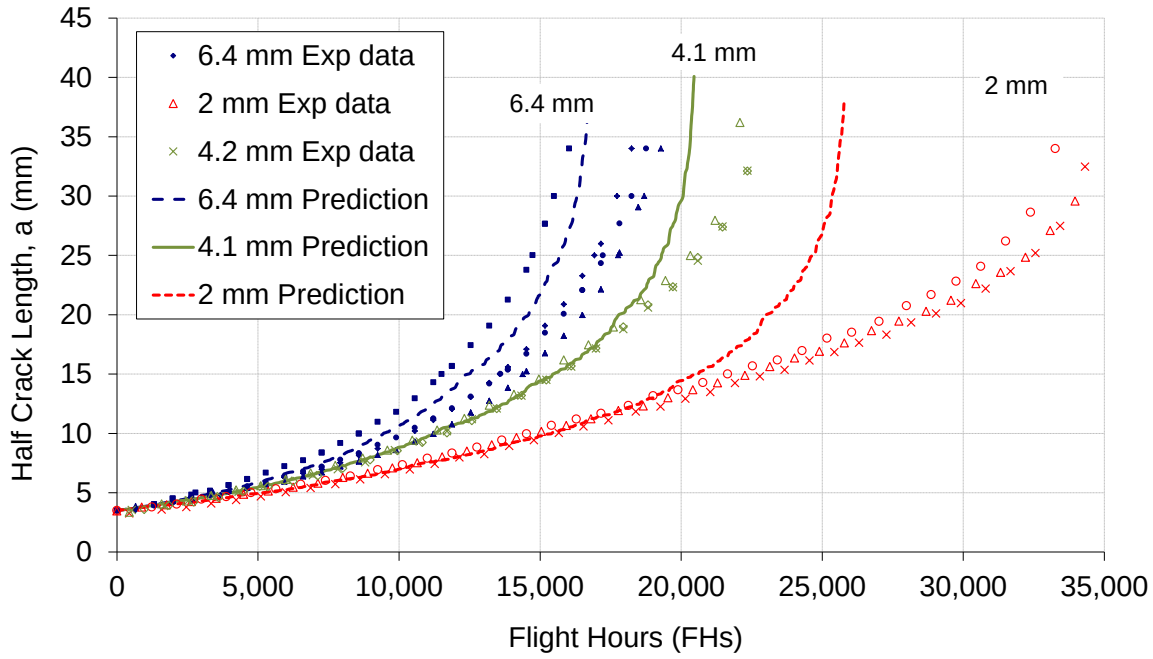

Figure 1: Half length crack growth under the centre wing lower surface spectrum compared to FASTRAN predictions for various specimen thicknesses

References

[1] C. Wallbrink, The effect of specimen thickness on fatigue crack growth under variable amplitude loading in 7075-T7351 Aluminium. In. SIF 2014, Sydney, December 2014.

2.12 Application of FIB to Characterisation of Fracture Resistance of Microstructural Constituencies (Walter Laszlo Costin, Andrei Kotousov and Ian Brown [The University of Adelaide])

The fatigue and fracture resistance of most materials is directly related to their microstructure, which may consist of diverse constituents with characteristic architectures and mechanical properties. However, such features typically occur at micro-length scales and are not directly accessible with conventional fracture tests. Micro-scale fracture testing is a novel tool to overcome such experimental limitations and can be used to investigate the link between the microstructural and bulk properties of materials. This work focuses on the application of miniaturized fracture tests to evaluate the fracture properties of selected microstructural constituents with unique architectures (acicular ferrite). Site specific Focused Ion Beam micro-machining, see Fig.1 (a-d), was used to fabricate sharply notched micro-beams.

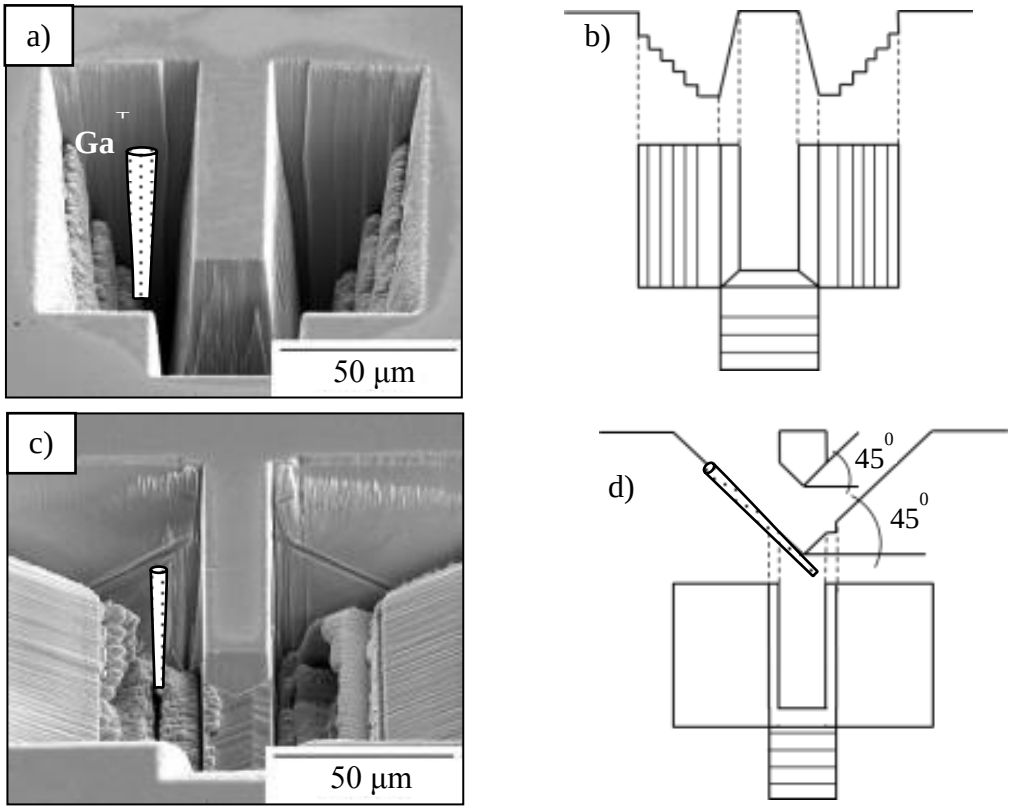

Figure 1(a-c): SE images and schematics illustrate the fabrication procedure for the micro-beams. The milling of the sidewalls was conducted at a glancing angle

The final specimen dimensions of the micro-beam are shown in Fig.2. The deviations of the dimensions between the individual micro-beams were thereby in a range within ±100 nm.

We attempted to probe the fracture properties of acicular ferrite, which is a common constituent in ferrous alloys. It nucleates intergranulary from inclusions inside the prior austenite grains which prevents the formation of parallel ferrite plates and simultaneously restricts their growth due to multiple impingements. All these factors produce an interlocking microstructure that consists of fine plates with different orientations representing a multiple fine interlocking ferrite

plates. The fabricated beam was loaded using nano-indentation with a spherical tip of sufficiently large diameter to avoid local plastic deformations in the vicinity of the contact area.

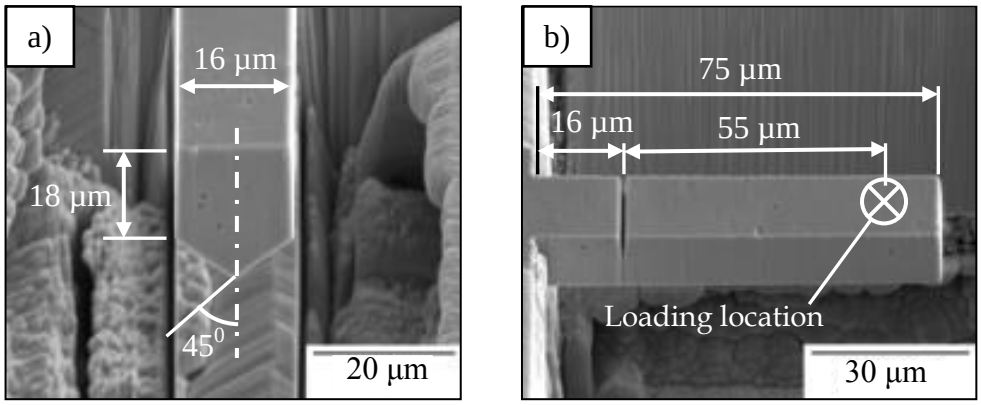

Figure 2: SE images show the final dimensions of the micro-beams

The initial response of the sample to the applied loading was linear (Fig.3), which indicates that the deformations were largely dominated by beam deflections rather than the localised contact. The linear region was followed by a non-linear part indicating the development of large plastic deformations prior to failure. The simplified plastic hinge model was developed to analyse the fracture behaviour, and to calculate non-linear fracture controlling parameters such as CTOD.

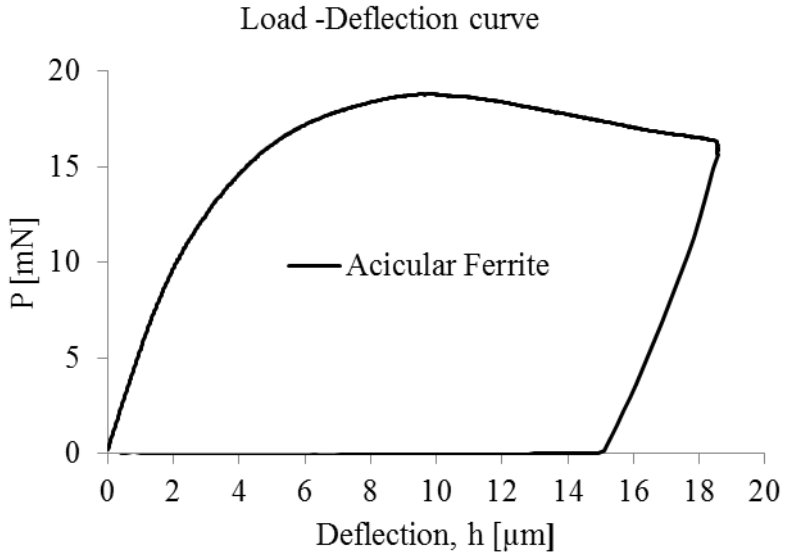

Figure 3: Load-deflection curve

The developed technique and model can be applied to investigate fracture and fatigue properties of various microstructural constituents and architectures within the same material as well as their effect on the overall fracture or fatigue resistance. Ultimately, the described experimental technique can provide a unique insight on how microstructural design can be implemented more efficiently to develop new materials with superior fracture properties.

References

[1] Costin, W. and Kotousov, A. Micro-scale fracture testing in localised microstructural architectures, submitted to Philosophical Magazine, 2014.

2.13 The Hartman Schijve Fatigue Growth Equation Variant (Molent L, Barter S, Walker K [DSTO] and Jones R [Monash University])

The Royal Australian Air Force (RAAF) approach to the management of fatigue cracking in combat and trainer aircraft makes use of the "lead crack" concept [1]. In this approach, the life of the fleet is determined by lead fatigue cracks defined to have, amongst other features, the following characteristics:

Crack growth initiates from small naturally occurring defects or discontinuities, such as broken constituent particles, machining defects and pits, which have dimensions that are equivalent to a fatigue crack-like size typically of about 10 μm in depth;

Crack growth essentially starts from the day that the aircraft is first flown;

The majority of the life is spent in the physically-small crack regime; and

For several types of fatigue initiating discontinuities (e.g. etch pits) their physical depths correlate strongly to their crack-like effectiveness [2].

Therefore, understanding the growth of fatigue cracks from small naturally occurring defects is of fundamental importance to managing the RAAF fleet. This means that it is important to address or overcome the so-called short crack (fatigue) anomaly that is one of the basic problems in materials science and particularly in fatigue crack growth prediction. It should be noted that ASTM 647 (2008) Annex X3 states that "predictions of small crack growth in engineering structures based on laboratory large-crack (near-threshold) data may be extremely non-conservative". ASTM 647 also states: "it is not clear that a measurable threshold exists for small cracks". In such cases it is reasonable to expect that there should be minimal crack closure and therefore R ratio effects, and the short crack fatigue threshold is much smaller than the long crack threshold.

Investigations of a significant range of aerospace metallic alloys have shown that data (long crack, short crack and at various R) collapse to a single line using a variant of the Hartman-Schjive equation [3]:

$$\frac{da}{dN} = D\ [(\Delta K - \Delta K_{thr})/\sqrt{(1-K_{max}/A)}]^{\alpha} \qquad (1)$$

Here K_{max} is the maximum stress intensity produced by the load cycle at each crack's tip, α is a constant, which is determined from the slope of the da/dN versus $[(\Delta K - \Delta K_{thr})/\sqrt{(1-K_{max}/A)}]$ curve and has been found to be approximate 2 for this and several other materials [iv), v)], the parameters A and ΔK_{thr} (for the appropriate short or long crack data, and postulated here to represent the crack growth resistance) are chosen so as to best represent the experimental data

at a particular R. The parameter D is the y-axis intercept at 1 MPa √m. Note that only one data set is required to define equation (1). As noted in [4], the parameter ΔK_{thr} should not be confused with the term ΔK_{th}, which the ASTM 647 fatigue test standard (somewhat arbitrarily) suggests to be the value of ΔK at a crack growth rate da/dN of 10^{-10} m/cycle. In this formulation ΔK_{thr} is so chosen to ensure that equation (1) reproduces the observed crack growth rates over the entire da/dN versus ΔK curve for a given R-ratio, for more details see [4,5]. As such since da/dN is a function of the material, thickness, R ratio and crack length, so (in general) is ΔK_{thr}. However, as discussed above, for short-cracks there is little R ratio dependency so that for the short crack data it is sufficient to approximate ΔK_{thr} to be 0.1 MPa √m.

As such the short-crack anomaly essentially vanishes when fitted with the Hartman-Schjive variant. Importantly scarce and difficult to derive short-crack data can now be extracted for conventional long-crack data. This should contribute significantly to the accurate prediction of crack growth in the short-crack regime which represents a major portion of the total life of a structure.

References

[1] Molent L., Barter S.A., Wanhill R.J.H., The lead crack fatigue lifing framework, International Journal of Fatigue 2011; 33: 323–331.

[2] Molent L. (Invited Review paper), A review of equivalent pre-crack sizes in aluminium alloy 7050-T7451, Fat Fract Eng Mat Struct 2014;37: 1055-74.

[3] Hartman, A. and Schijve J., The effects of environment and load frequency on the crack propagation law for macro fatigue crack growth in aluminum alloys. Engineering Fracture Mechanics 1970;1(4):615-631.

[4] Jones R, Molent L., Walker K., Fatigue crack growth in a diverse range of materials, International Journal of Fatigue 2012; 40: 43-50

[5] Jones R, Molent L and Barter S. Calculating crack growth from small discontinuities in 7050-T7451 under combat aircraft spectra. International Journal of Fatigue 2013; 55: 178-182.

2.14 Closure measurement and analysis for small cracks from natural discontinuities in an aluminium alloy (K. Walker, [DSTO and RMIT University Australia], C.H. Wang, [RMIT University Australia] and J.C. Newman, Jr., [Mississippi State University USA])

Some materials such as 7050-T7451 and β-annealed Ti-6Al-4V exhibit very rough fatigue crack surfaces which suggests that roughness induced crack closure might be a significant issue. The present work examined a range of data for 7050-T7451 material which included experimental results under constant amplitude and variable amplitude/spectrum loading. Further details are available at [1] . Crack closure was either measured directly, or the effects were inferred through results from previous fractographic investigations.

Under pure constant amplitude loading at stress ratio R (min stress/max stress) = 0.1, crack closure in a compact tension (C(T)) coupon was measured using remote compliance based methods as detailed in [2] . The results are compared with FASTRAN analysis in Figure 1. FASTRAN [3] is a strip-yield model based on the Dugdale model but modified to leave a wake of plastically deformed material in the crack wake. A constraint factor (α) is used elevate the flow stress (σ_o) to account for three dimensional effects which influence the stress state ($\alpha\sigma_o$) near the crack tip. Experience with other materials (which do not exhibit significant roughness closure effects) suggested that the appropriate constraint factor α would be about 2.0. This value has been independently verified by elastic-plastic finite element analyses. But as shown in Figure 1, α = 1.0 (plane stress) was required to correlate the crack opening stress in this case.

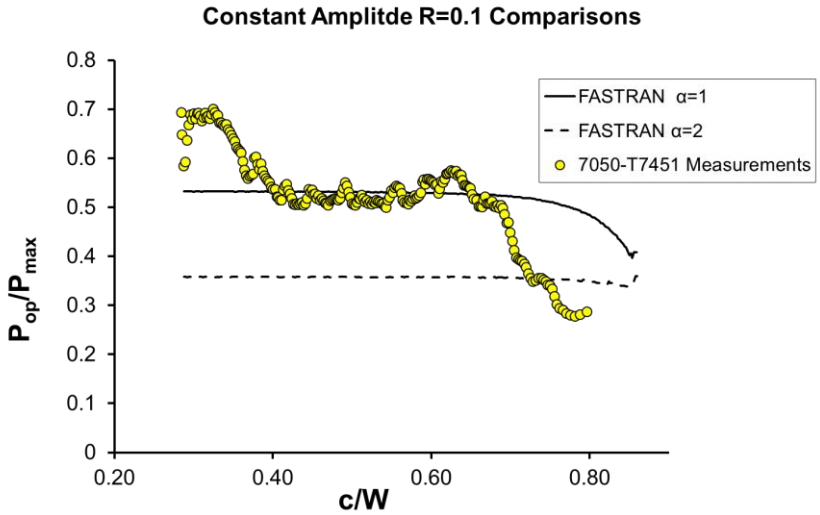

Figure 1 : Crack opening stress comparison

However, FASTRAN analyses for many spectrum loading cases showed that a constraint factor α = 2.0 was required to correlate the data, see Figure 2 for an example.

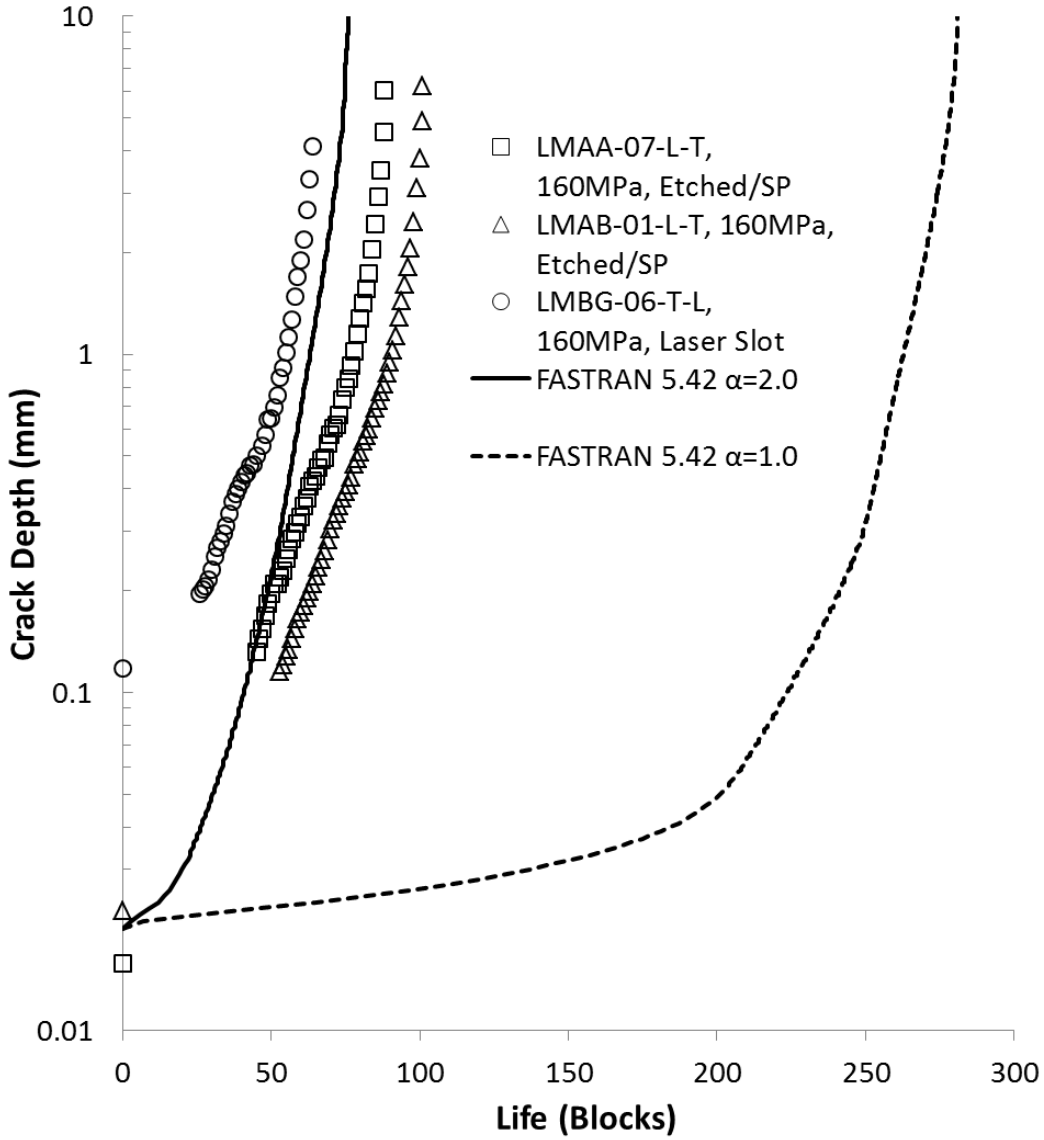

Figure 2 : Crack growth under variable amplitude spectrum loading

Coupons were subjected to a special loading sequence which included spectrum loading with small bands of constant amplitude inserted in between. The fatigue surfaces produced were then examined using an NPFLEX optical profiling microscope, see Figure 3. The crack opening levels were also inferred. It was found that changing to spectrum loading from constant amplitude changed the crack path locally, and the local crack surface characteristics were very different for constant amplitude and spectrum loading. The spectrum loading produced a smoother crack surface, and the rougher surface associated with the constant amplitude loading was associated with an elevation in the crack closure. Thus, the higher constraint factor α is associated with the constant amplitude loading because it compensates for the fact that FASTRAN does not explicitly model roughness-induced crack closure effects. But under spectrum loading the roughness-induced crack closure effects are significantly reduced and the FASTRAN modelling correlates the results well with a constraint value consistent with plasticity effects only.

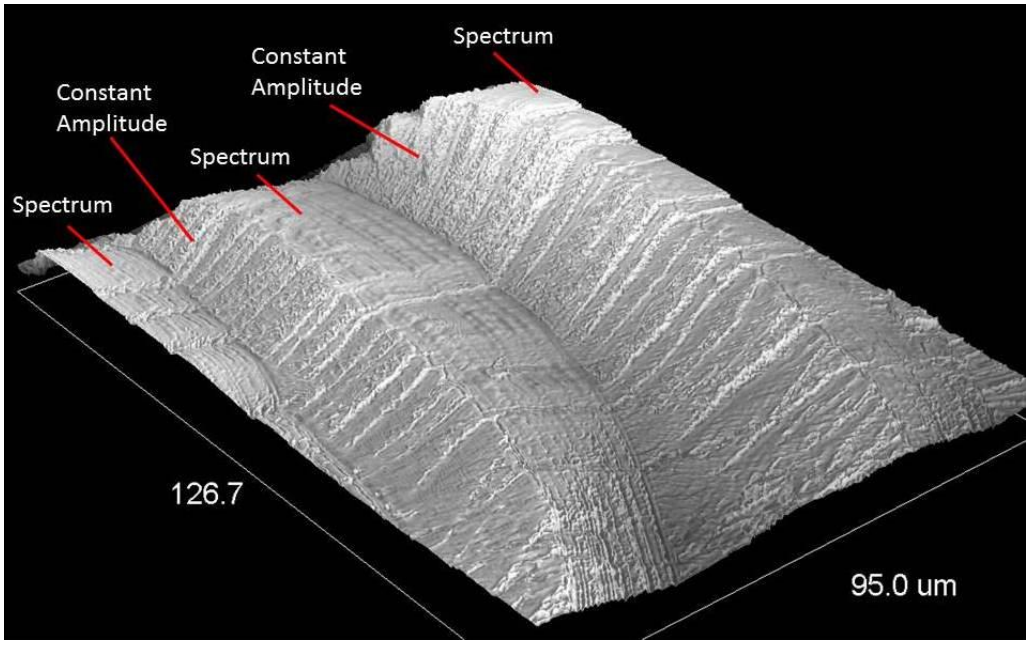

Figure 3 : Crack surface image from NPFLEX optical profiling microscope

Future work will include further testing and analysis to better understand the reasons for the significant differences between constant amplitude and spectrum loading behaviour. Testing will include direct compliance based measurement of crack opening values during small bands of constant amplitude loading inserted into spectrum sequences. Three-dimensional elastic-plastic finite element modelling of a body with a smooth crack and with rough cracks of varying characteristics is also required.

Contact K. Walker at kevin.walker@dsto.defence.gov.au

References

[1]. Walker, K.F., Wang, C.H., and Newman,J.C., Jr., Closure measurement and analysis for small cracks from natural discontinuities in an aluminium alloy. International Journal of Fatigue, Accepted for publication January 2015.
[2]. Anon, Standard Test Method for Measurement of Fatigue Crack Growth Rates, ASTM, Editor. 2011, ASTM International.
[3]. Newman, J.C., Jr., FASTRAN A Fatigue Crack Growth Life-Prediction Code Based on the Crack-Closure Concept Version 5.4. 2013, Fatigue & Fracture Associates LLC.

2.15 An investigation of the extent of crack closure for fatigue crack growth in an aluminium alloy (Barter S, Burchill M, [DSTO] and Jones M. [Fortburn]) [1]

Through the comparison of crack measurements in variable amplitude (VA) loading fatigue tests of metallic airframe alloys, with predictions that utilise the constant amplitude (CA) crack growth rate it has been found that small fatigue crack growth is not well predicted. A number of reasons have been offered in the literature which identify variations in crack closure as the key to poor VA crack growth predictions. Moreover several algorithms and/or adjustments have been proposed to improve correlation with measured VA small crack growth when CA crack growth data via the measurement methods set out in guidance such as in the American Society for Testing and Materials (ASTM) standards, ASTM E647 [2]. These corrections incorporated in fatigue crack growth prediction programs are usually tested by their ability to predict retardation following an overload and for the accuracy of their prediction of lives for long cracks greater than about 1mm. However, to ensure such algorithms are robust, it is crucial that crack growth can be predicted from small sizes and/or small load magnitudes, i.e. on the threshold of crack growth. This would result in predictive models that are more representative of fatigue crack growth in aircraft metallic components, where fatigue cracks typically initiate from small inherent material discontinuities.

Conventional fatigue theory states that only the positive (uploading) part of a load cycle grows a crack, and the closure concept predicts an impediment to the opening of a crack tip from preceding cycles, resulting in only part of a positive cycle being effective. Closure is commonly ascribed to contact between opposing crack faces in the crack tip's wake, resulting from several sources such as: crack wake plasticity, crack surface roughness and wedging from surface oxidation, debris or contaminants in the crack. DSTO's research as part of the Threshold and Short Crack (TASC) program is being carried out to examine the behaviour of very short cracks over a range of stress intensity values ΔK and in a range of airframe structural materials, to identify the onset of closure on the micro scale through the measurement of local crack growth retardation via post-test quantitative fractography (QF).

As a part of the TASC program, several specially engineered spectra were tested on a common aircraft aluminium alloy, AA7050-T7451 to ascertain if the effect of closure could be inferred through the measurements of fatigue crack growth of small cracks. A typical fracture surface that has resulted from the application of one of these DSTO designed test spectra is shown in Figure 1. This spectrum consists of sub-blocks of CA loads with diminishing mean stress but constant stress amplitude, designed to test the extent of closure, (the blue sub-blocks in Figure 1). The spectrum also contains VA (purple) and additional CA (green and red) loads used to assist in positively identifying the crack growth from each sub-block of interest on the fracture surface of the fatigue cracks produced. As shown in the example in Figure 1, the crack growth from one complete block can be readily identified, and under higher magnification can be directly measured (Figure 2b).

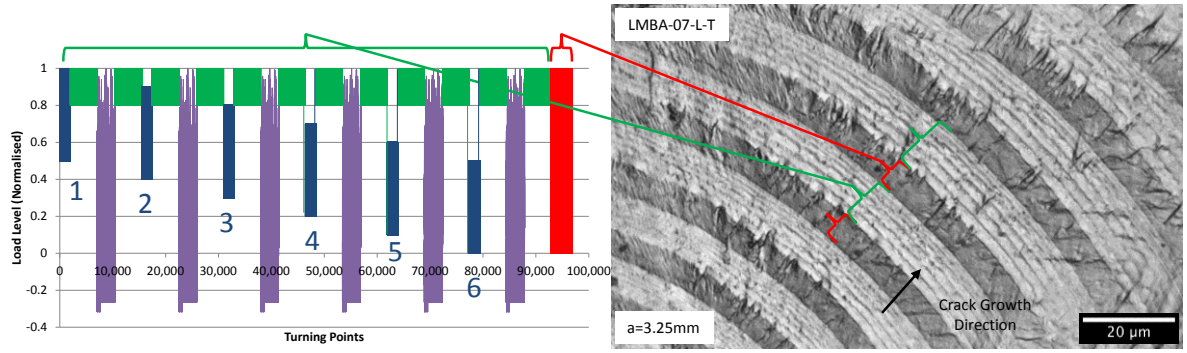

Figure 1 Test spectrum applied to coupons and an overview of the appearance of the fracture surface.

Six coupons tested with this simple spectrum were analysed optically for larger crack lengths (>1mm) and in a field emission scanning electron microscope (FESEM) for shorter crack lengths. The width of each CA test band, those labelled 1 to 6 in Figure 2b, were measured at many locations on the crack surface for each depth and converted to a da/dN values by dividing the band widths by the number of cycles applied (in this example, 1000 cycles). The results were plotted against ΔK as shown in Figure 2a. The results show the effect of the change in mean stress on crack growth rates, that has primarily effected the growth in test bands 4-6. Test bands 1-3 are generally similar in the amount of growth produced, with only a small decrease in the width recorded.

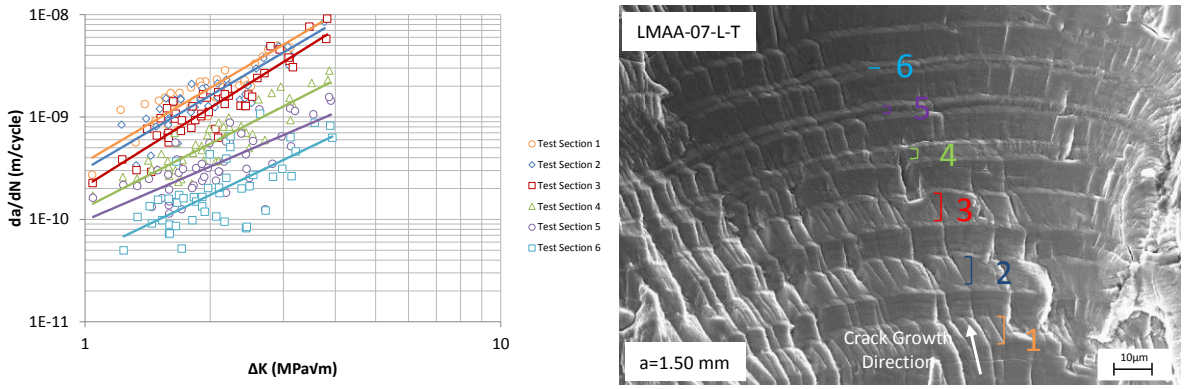

(a) (b)

Figure 2 (a) QF results plotted as ΔK v. da/dN. (b) An example FESEM photograph of one block of loading with the corresponding test bands marked.

The QF results were then compared to four analytical models: FASTRAN [3], AFGROW using the Willenborg retardation model, AFGROW using no retardation, and a simple effective stress intensity calculation methodology based on Elber [4]. The results of the four analytical models, compared to the QF results, are presented in Figure 3a, Figure 3b presents this data as a percentage of the growth predicted in test band 1. The results show the Willenborg AFGROW predictions are relatively accurate for only the first three test bands. The FASTRAN results appear to under predict the crack growth for test sub-blocks 2-6, although the effect becomes less pronounced for lower Kmax values. The simple calculations appear to be the most accurate, showing that, as a rough guide for crack opening stress, this case seems reasonable.

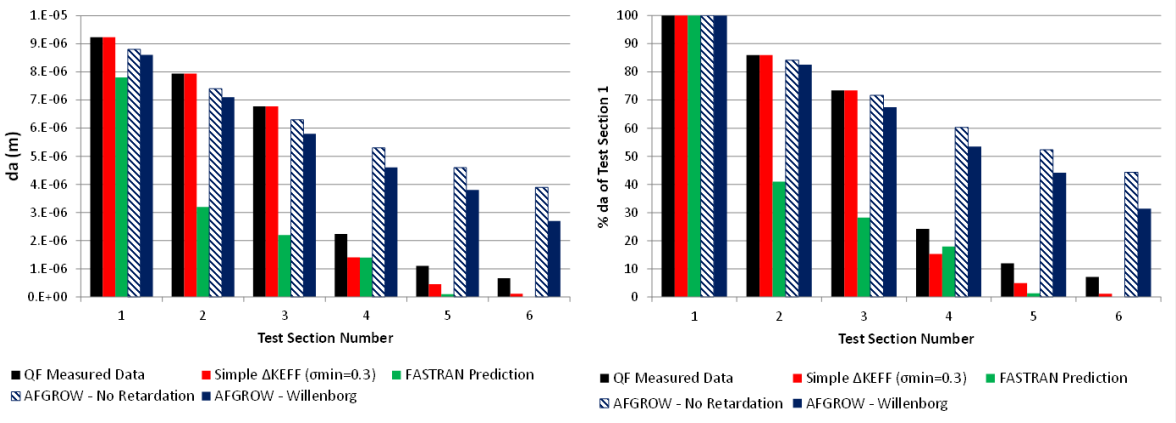

Figure 3 Comparative results of the four predictions compared with the measured growth per band.

The results from this study showed that, with the settings described [1] that the analytical models did not accurately predict the growth of the constant ΔK sub-blocks with the closure algorithms tested. Whilst it must be clearly stated that the predictive models will continue to be refined and the data from these and further testing will be use in this refinement, this investigation has highlighted the difficulty of predicting the magnitude and onset of closure and its subsequent effect on crack growth predictions. Further investigations including testing different spectra and improving the analytical models are ongoing.

References

[1] Barter, S., Burchill, M. and Jones, M., An investigation of the extent of crack closure for crack growth in an aluminium alloy, AIAC, Melbourne, AUSTRALIA, 2014.

[2] ASTM E647-05 - Standard test methods for measurement of fatigue crack growth rates, ed: American Society for Testing and Materials, 2005.

[3] Newman, J.C., Jr., Yamada, Y., and Newman, J. A., Crack-closure behaviour of 7050 aluminum alloy near threshold conditions for wide range in load ratios and constant Kmax tests. Journal of ASTM International, 2010. 7(4).

[4] Elber, W., The significance of fatigue crack closure. ASTM STP486 American Society for Testing and Materials, West Conshohocken, Pennsylvania, USA, 1971, pp230-242.

2.16 The effect of crack growth retardation when comparing constant amplitude to variable amplitude loading in an aluminium alloy. (M. Burchill, S. Barter[DSTO], M. Jones [Fortburn])

Through crack growth measurements from the fatigue testing of metallic airframe alloys it has often been observed that growth of small fatigue cracks under variable amplitude (VA) cyclic loading is not well predicted when utilising standard crack growth rate/stress intensity data. Such data is often generated using the ASTM E647-00 (2005) "Standard test method for measurement of fatigue crack growth rates" which is designed to produce constant amplitude (CA) data for predicting fatigue crack growth that includes that produced by VA (and warns against using long data for predicting short cracks). Small cracks are often observed to grow faster at lower stress intensity factors than predicted by long crack CA data and this appears to be amplified to give inconsistencies over greater ranges when the loading is VA. While a lack of crack closure and microstructural effects (two influencing factors that probably act in unison) have been put forward as possible reasons to explain this for small cracks when loaded with CA cycles, it is harder to explain why VA loading should extend further and produce bigger differences. Research suggests that this maybe because VA is more efficient at extending the crack than CA [2].

Studies undertaken at the Defence Science and Technology Organisation (DSTO) [1] to minutely examine fatigue fracture surfaces suggest that crack growth is more efficient under VA cyclic loading for small to medium sized cracks <3mm in typical aircraft structural alloys. In a series of coupon fatigue tests with a common aircraft aluminium alloy, AA7050-T7451, a possible CA crack growth retardation effect was investigated by applying load sequences of both VA cycles, and CA with a high mean stress (or high R, the ratio of σ_{min} /σ_{max} in a cycle) and a range of cycles to produce growth for close examination. An example of a crack surface produced with this type of loading is shown in Figure 1a. From such a test spectrum (insert Figure 1a) measurements were taken via quantitative fractographic examination that included the individual crack growth bands for each load sequence sub-block. The average crack growth rate per cycle could then be calculated for the CA crack growth and compared, Figure 1b.

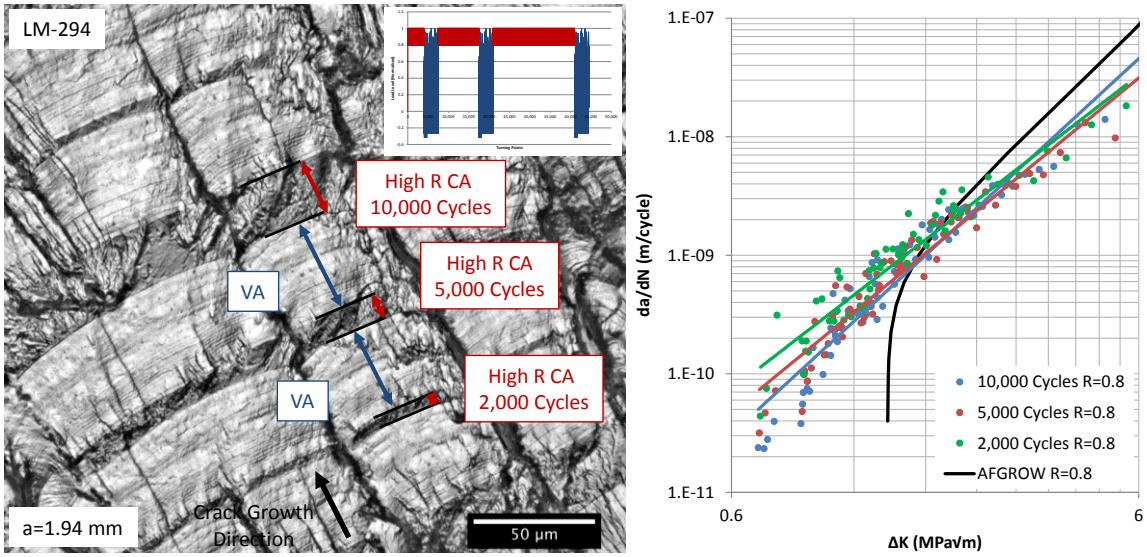

(a) (b)

Figure 1 Results from DSTO retardation test coupons a) example of a fracture surface from loading with a spectrum of VA and varying cycles of high R CA; and b) crack growth da/dN v □K data calculated from QF measurements of individual CA crack growth bands compared to standard material data available in crack growth code AFGROW.

The investigation found that the average crack growth rate varied inversely with the number of cycles in the CA sequences; that is, increasing the number of CA cycles in a band reduced the average crack growth rate as shown in Figure 1b. Further, from crack front features identified during the examination it is postulated that a variation or deviation from an efficient crack path is a driver of retardation in growth under cumulative CA cycles, examples of this are shown in Figure 2. This appears to be one source of error that can lead to inaccuracies in analytical predictions of crack growth under VA spectra, particularly while cracks are small. This research is continuing, including examination and measurement of the crack front morphology after CA bands, and testing with various under and overloads.

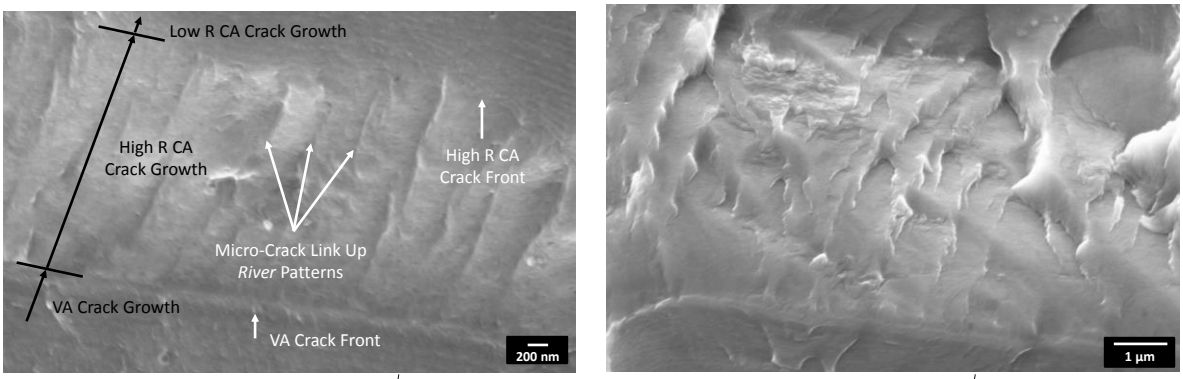

a) a ~ 0.93mm; □K~1.66MPa√m; 2000 cycles *b) a ~ 0.92mm; □K~1.65MPa√m; 5000 cycles*

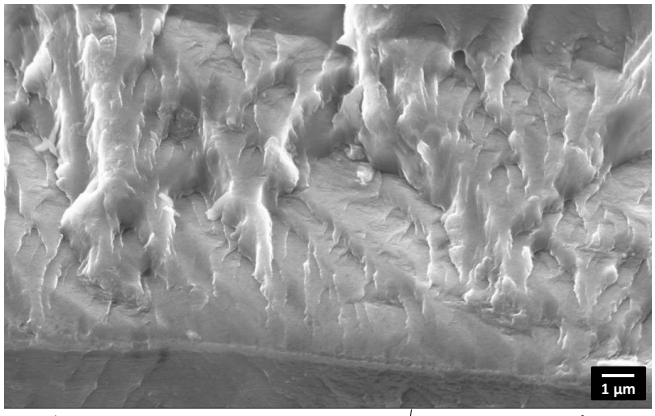

c) a ~ 0.89mm; □K~1.62MPa√m; 10000 cycles

Fig. 2 Scanning electron microscopic images showing various details in fatigue fracture surface morphologies, and the changing appearance of the crack front at the end of each CA load sequence, becoming discontinuous with increasing repetitions of numbers of CA cycles (note scale varies).

References

[1] Burchill, M., Barter, S., Jones, M. (2014) The effect of crack growth retardation when comparing constant amplitude to variable amplitude loading in an aluminium alloy. *Advanced Materials Research Vols. 891-892, pp 948-954*.

[2] White, P., Barter, S. A., and Molent, L. (2008) Observations of crack path changes caused by periodic underloads in AA7050-T7451, *International Journal of Fatigue,* vol. 30, n.7, p.1267-1278.

2.17 Improvements to predicting fatigue crack growth rates in aluminium alloy (AA7050-T7541) loaded with a standard transport spectrum (Burchill M, Walker K, Barter S [DSTO], Wang C, Khadka A. [RMIT])

Accurate prediction of fatigue crack growth is vital to design, maintaining structural airworthiness, reducing the cost-of-ownership and increasing aircraft availability, and hence of great interest to manufacturers, fleet operators and maintainers. Previous work by many researchers have identified deficiencies in standard material data when used with fatigue life prediction codes based on linear elastic fracture mechanics principles, including under predicting the short crack (near threshold) growth rates when compared to empirical long crack measurements from coupon or component fatigue testing.

Researchers at Defence Science and Technology Organisation (DSTO) and Royal Melbourne Institute of Technology (RMIT) have proposed improvements to life prediction through the development of new fatigue material data for AA7050-T7451 [1]. This data was then used in two typical fatigue life prediction codes (AFGROW and FASTRAN) to assess any improvement when using either a non-closure or closure corrected algorithms to carry out the predictions. Previously these data had been found to improve the prediction of fatigue crack growth in coupons tested with a combat aircraft spectrum, which typically contain many large peak loads [2]. To increase confidence in the robustness of the new data to different types of loading spectra, a coupon test and quantitative crack growth measurement program was undertaken using the standard transport spectrum, mini-TWIST (The Transport Wing Standard Load Programme) for the purposes of comparing the predictions to actual crack growth. The emphasis here being that the predictions should not only predict lives but also the growth rates over several orders of magnitude of crack depth generated during the testing.

Fifteen coupons of a low Kt design used in previous studies were tested to failure with the mini-TWIST spectrum, five each at three different peak stress levels (peak spectrum stress of 250, 300, 350 MPa). The test spectrum contained a series of unique marker band load sequences which created visible marker bands on fatigue crack's fracture surfaces and were measured using quantitative fractography (QF); an example is shown in Figure 1. The presence of such marker bands greatly aided the post-test QF examination that was used to obtain accurate measurements of crack depth, down to very short crack growth depths; an example of the coupon crack growth data is shown in Figure 1b.

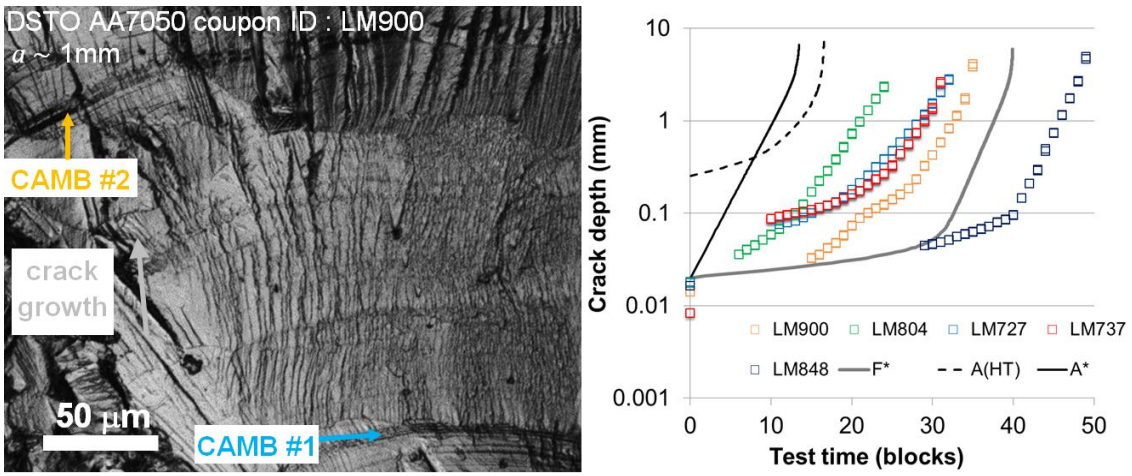

(a) (b)

Figure 1 Results from the mini-TWIST coupon tests, a) fatigue crack fracture surface with marker bands (labelled CAMB), b) 250MPa test crack growth data and analytical growth curves.

AFGROW analyses were conducted using two different rate data sets. The standard data provided with the AFGROW code, labelled in the figures as A(HT). The other, labelled A* was generated in DSTO's threshold and short crack program using QF data obtained from small blocks of constant amplitude loading separated by sub-blocks of a different (typically lower) mean stress [2]. The QF data were obtained from naturally occurring small cracks in a series of coupon tests, from which a rate curve was derived. This data provided evidence of a much lower crack growth threshold than standard test methods predicted. The rate curve for the FASTRAN analyses (F*) were also based in part on similar DSTO QF data, but also informed by long crack testing performed after compression pre-cracking and minimal load reduction testing. In this case, compliance based crack opening data were used to determine the effective (ΔK_{eff}) rate curve. The results from recent related research into roughness closure and the appropriate 3-D constraint factor were also applied [3].

A summary of all coupon and analytical results is shown in Figure 2, where the crack growth per block of test loading is compared at increasing crack depths. As expected, at the longer crack depths, all analytical models predict similar crack growth rates per block of loading. However, for short cracks (less than ~0.5mm in these cases), the use of standard material data, ie A(HT), with AFGROW results in a significant under prediction of the measured crack growth per block. The FASTRAN based predictions were a marked improvement, accurately representing the average crack growth rates. The use of the DSTO A* data on the other hand resulted in conservative results through over prediction of these threshold crack growth rates.

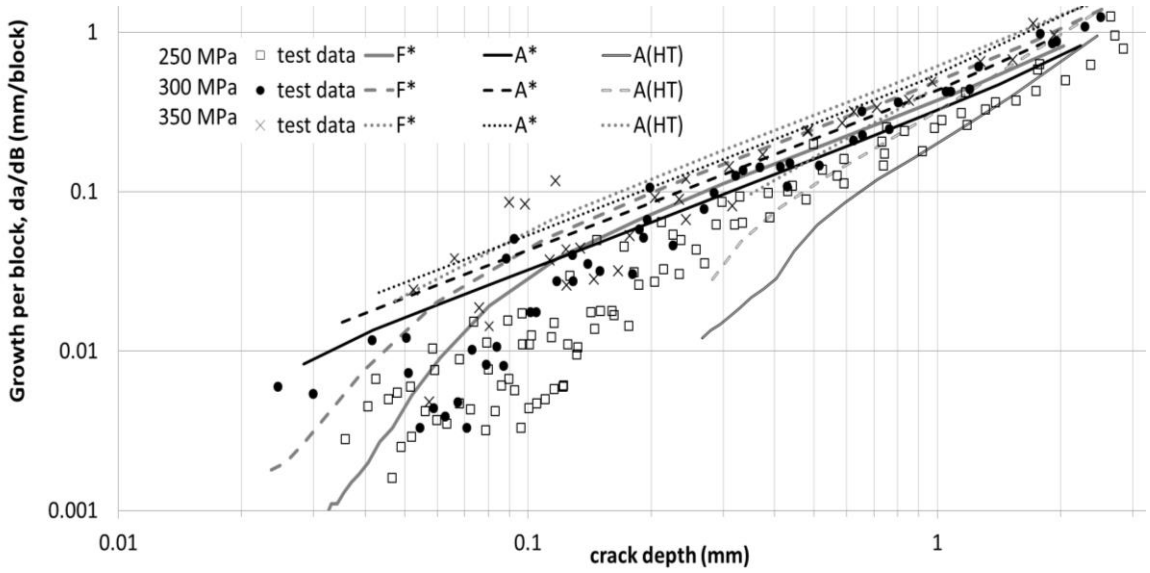

Figure 2 Summary of crack growth rate per block data from test and analyses.

Testing and analysis continues at DSTO in refining the AA7050 material models, in particular for very short cracks, as well as complementary research into developing a better understanding of the growth mechanisms of fatigue cracks, through the examination of crystalline slip, damage accumulation ahead of fatigue crack tips and subtle sources of crack closure while cracks are small, among other issues that have been identified as important to good predictions.

References

[1] Burchill M, Walker K, Barter S, Wang C, and Khadka, A. Improvements to predicting fatigue crack growth rates in aluminium alloy (AA7050-T7451) loaded with a standard transport aircraft spectrum. *International Conference on Structural Integrity and Failure, APCFS-SIF*, Sydney, 2014.

[2] Burchill M, Barter S and Amsterdam E. Improved fatigue life predictions for combat aircraft from a novel testing program. *AIAC Australian International Aerospace Congress* 2013, Melbourne Australia.

[3] Walker K F, Barter S A. The Critical Importance of Correctly Characterising Fatigue Crack Growth Rates in the Threshold Regime. *26th ICAF Symposium,* Rotterdam, 2011.

2.18 Effect of models and derivation methods for initial flaw size distribution on probability of failure of airframes (Ribelito Torregosa and Weiping Hu , DSTO)

Two methods for the derivation of the probability distribution of the equivalent initial flaw size (EIFS) are examined to evaluate their effects on probability of failure (PoF) calculation. The two methods are the direct method and the time to crack size (TTCS) method. For the TTCS method, three baseline crack sizes, 0.10, 0.20 and 0.30 inches, are selected to study their effects on the PoF values, and the log-normal distribution model was used to represent the life distribution at these baseline crack sizes. For the direct method, the log-normal distribution model was used to fit the regressed flaw sizes. The resulting EIFS distributions are shown in Figure 1a, and the right tails of the distributions are shown in an enlarged view in Figure 1b.

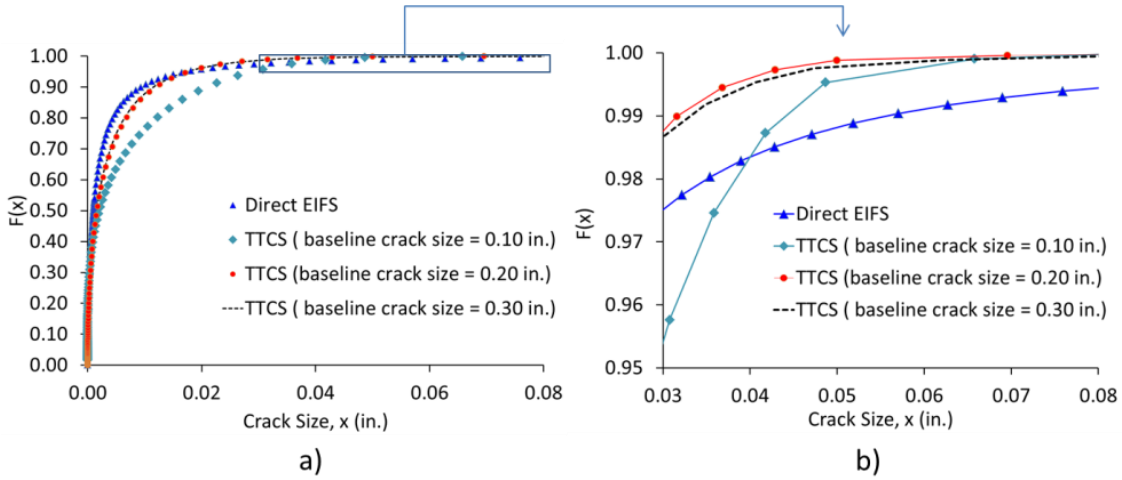

Figure 1 EIFS distributions derived using the direct method and the TTCS method corresponding to baseline crack sizes of 0.10, 0.20 and 0.30 inches, a) CDF curves; and b) the right tail of the distribution.

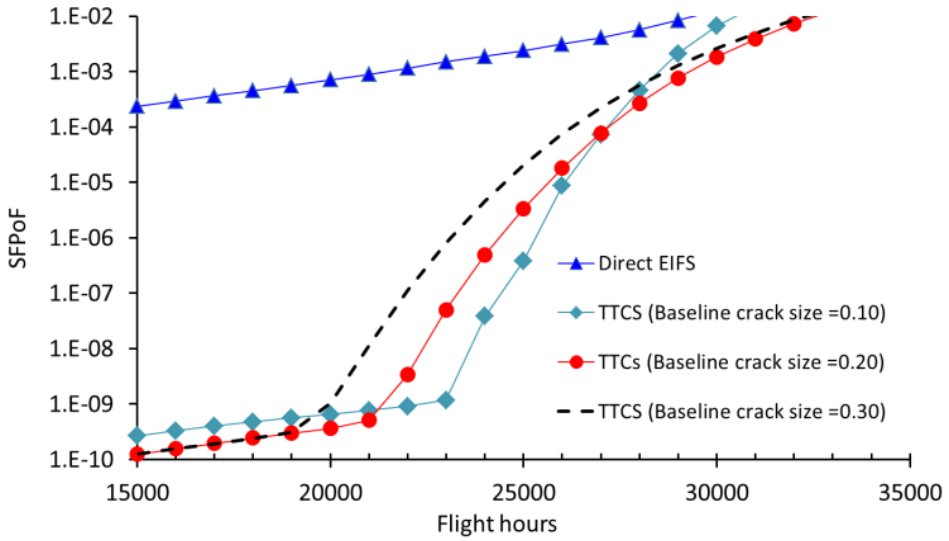

Figure 2 Comparison of SFPoF for different EIFS methods and baseline crack sizes

Figure 2 shows the PoF curves using different EIFS derivation methods. The following may be concluded:

1. The EIFS distribution derived using the direct method may lead to a very high probability of failure, especially when an unbounded distribution model is used.

2. The EIFS distribution derived using the TTCS method give probability of failure which are sensitive to the assumed baseline crack size. The baseline size should correspond to the actual condition of the location being analysed so as not to produce unrealistic EIFS values.

3. The mean of the EIFS distribution is less sensitive than the right-tail of the distribution for PoF predictions.

Reference

[1] Torregosa, R. and Hu, W., *Effect of models and derivation methods for initial flaw size distribution on probability of failure of airframes*, 9th International Conference on Structural Integrity and Fracture , 9-12 Dec. 2014 Sydney, Australia.

2.19 Crack Growth Variability and Its Effect to Risk Analysis of Fracture Prediction (Ribelito Torregosa, Beau Krieg and Weiping Hu, [DSTO])

Using the test results of 85 specimens of 7075-T7351 aluminium alloy, the relationship between the coefficient of variation of fatigue life and flight hours is shown in in Figure 1a, Using the derived equation of the coefficient of variation, a second order probabilistic risk analysis of fracture was conducted to investigate the effect of the variability of the crack growth on the probability of fracture (PoF) prediction. It was assumed that the crack growth curve used in previous analysis is the mean crack size which corresponds to a 50% confidence level. Three confidence levels (CLs) were considered in the analysis. These are the 90%, 95% and 99% CLs and shown in Figure 1b.

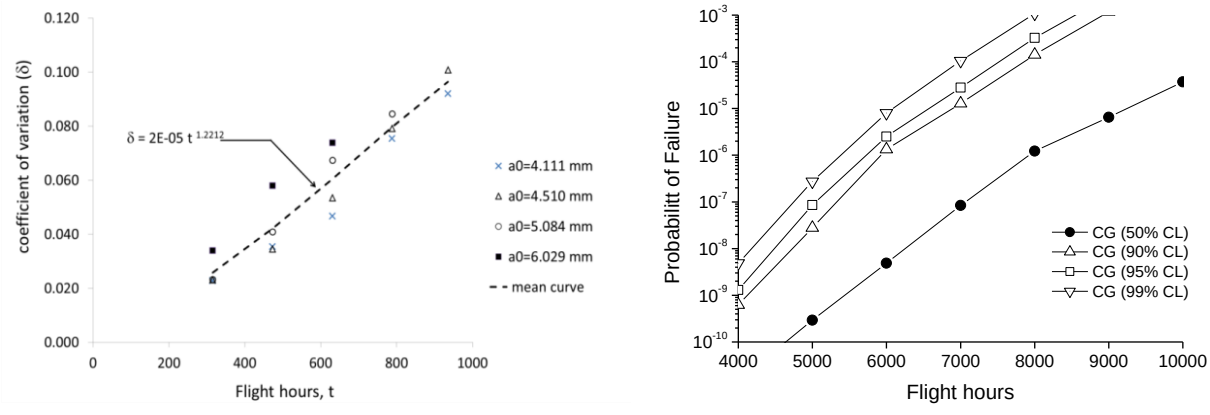

(a) (b)

Figure 1 a) Coefficient of variation of crack sizes corresponding to fatgiue life (i.e., flight hours), b) Probability of Failure corresponding with different confidence levels.

Figure 1b shows that specifying confidence levels of a crack growth curve in the risk analysis will result in a significant difference in the predicted risk values. It is observed that increasing

the confidence from 90% to 99% increases the risk prediction by approximately a magnitude. As a consequence, given the observed coefficient of variation from the test results, increasing the confidence levels of the risk predictions of fracture resulted in a significant increase in risk values. The varying risk values corresponding to confidence levels show that probability of failure itself is variable. The confidence level is a good measure of the sensitivity of risk predictions. Also, if crack growth is treated as a deterministic process, a suitable growth curve rather than the mean should be used.

References

[1] Torregosa, R.F., and Hu, W. Crack Growth Variability and Its Effect to Risk Analysis of Fracture Prediction, 28th ICAF Symposium 3-5 June 2015. Helsinki, Finland.

[2] Hu, W., B. Krieg, and R. Torregosa, Material Scatter in Crack Growth Rates of 7075-T7351 under Spectrum Loading, in Eleventh International Fatigue Congress. 2014: Melbourne, Australia.

2.20 Effect of Anodising Treatment on Equivalent Crack Size of the 7XXX Aluminium Alloy (Alex Shekhter [DSTO])

Anodising is an electrochemical process in which the natural oxide layer on the surface of aluminium alloys is artificially thickened. Anodising is carried out in a treatment bath containing a suitable electrolyte (such as chromic acid or sulphuric acid). A voltage is then applied to cause an electrochemical reaction. The component to be anodised is made the anode and either the bath or a non-reactive metal (such as lead) is used as the cathode.

In the case of military aircraft United States Department of Defence MIL-A-8625F 'Anodic Coatings for aluminium and Aluminium alloys' is the most common military process specification. However, there are also United Kingdom Ministry of Defence DEFence STANdard (DEFSTAN), Aerospace Materials Specification (AMS) and aircraft manufacturer propriety standards for anodic coatings.

The Equivalent Crack Size (ECS) method is a modification of the Equivalent Initial Flaw Size (EIFS) method developed by Rudd and Gray [6]. It allows surface damage (inclusions, pits, or damage from the cleaning process during anodising) to be evaluated using the same procedure as used for fatigue cracks. The ECS approach generates that a correlation between initial damage size and an equivalent crack size.

The use of EIFS in assessment of fatigue damage had been extensively examined researchers in the past The original concept of EIFS deliberately ignores short crack effects and assumes instantaneous fatigue crack initiation. The use of crack growth models based on data generated in the test program to calculate an EIFS distribution for fuselage skin joints by fitting a crack growth rule to marker band observations and back projecting to zero cycles, and to generate fatigue crack growth data from marker band observations for use with Air Force Growth AFGROW crack modelling software.

Fatigue test coupons were manufactured from Pechiney supplied bare rolled AA7050-T7451 (6 inch thick) aluminium alloy plate, which had been manufactured to American Materials Society

(AMS) 4050H. A number of coupons were surface–treated using a Type IC anodising process by an authorised surface treatment company. Marker bands were added to the R=0.1 constant amplitude spectrum for post-failure fatigue crack growth analysis. The marker bands consisted of a set of high load ratio cycles (R=0.8), followed by a set of 100 cycles at the same load ratio as the main constant amplitude loads (R=0.1).

Fatigue crack growth rate measurements were performed in two parts. The first using an optical microscope, and the second using a Scanning Electron Microscope (SEM). The marker band positions could easily be identified optically, but the features were too fine to measure accurately at short crack depths. The two parts was as follows: Firstly, the marker band to marker band crack spacing was measured using an optical microscope followed by high-magnification SEM to obtain detailed marker band features. Calibrated image software was used to accurately measure the intra-marker band spacing. Multiple intra-marker band measurements were measured for each image and the average intra-marker band spacing was determined.

The optically derived crack depth measurements were combined with the SEM derived intra-marker band spacing to determine the fatigue crack growth rate for each coupon. The stress intensity factor, ΔK, was calculated at each point from the coordinates of the crack front derived optically. The stress intensity equation for a corner crack was the applied. The measured crack growth rates were then used to plot da/dN versus ΔK to generate a single curve for the different surface finishes.

Table 1 presents the fatigue life results from constant amplitude testing of the baseline coupons and the anodised Type IC coupons, showing a reduction in fatigue life for Type IC anodising as opposed to the baseline coupons

Table 1: Coupon Fatigue Life

Condition	Stress, MPa	Number of coupons	Minimum (cycles)	Maximum (cycles)	Mean (cycles)	Std. Deviation (cycles)
Baseline	340	8	31,653	59,900	47,204	8,523
	270	8	69,914	131,316	94,884	19,330
Type IC	340	8	24,149	40,017	33,381	5,681
	270	8	51,569	84,695	67,469	11,929

Figure 1 shows the relationship between intra-marker band crack growth rates [11] da/dN and the change in stress intensity, ΔK. These were calculated during a test program that included baseline, Type IC, Type IB and Type II anodising and are shown here to demonstrate that anodising has no effect on crack growth rates. Also shown is an average crack growth curve from another DSTO test program "The Threshold and Short Crack Growth (TASC)" [13]. As shown in Figure 2 the results from the TASC program are very similar to experimental data

captured in this program. Therefore it was decided to use the da/dN versus ΔK curve generated from the TASC program [14] as an input into AFGROW for the ECS calculations.

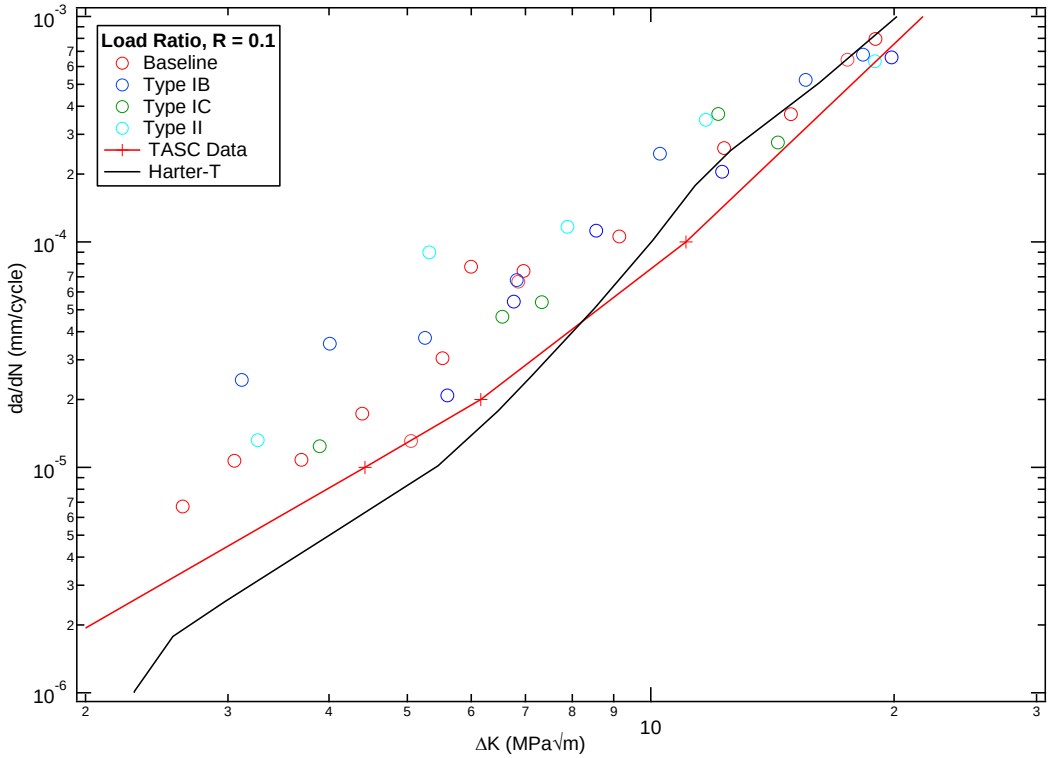

Fig.1 Experimental fatigue crack growth data for various anodising types and two da/dN versus ΔK curves generated from other programs.

Following the modelling of the crack using AFGROW, an exponential curve of the form:

$$y = y_0 + A\, e^{(-invTaux\,x)} \qquad (1)$$

was fitted to predict the ECS for the baseline and Type IC coupons.

From Equation 1, an ECS values were calculated for all fatigue test results. The distributions of the ECS values for both surface conditions were plotted and independently compared to the distributions of measured initiating damage as cumulative probability plots, Figure 2. The correlation between ECS and measured initiating damage is extremely good at a distribution level. With a focus on the ability to characterise the detrimental effect on structural integrity caused by anodising, it is of higher importance to predict the corresponding distribution of fatigue lives than the fatigue lives of individual tests. Further analysis is therefore underway to improve predictive capabilities by including surface crack models and transition to corner cracks to include more realistic coupon geometries and loading conditions.

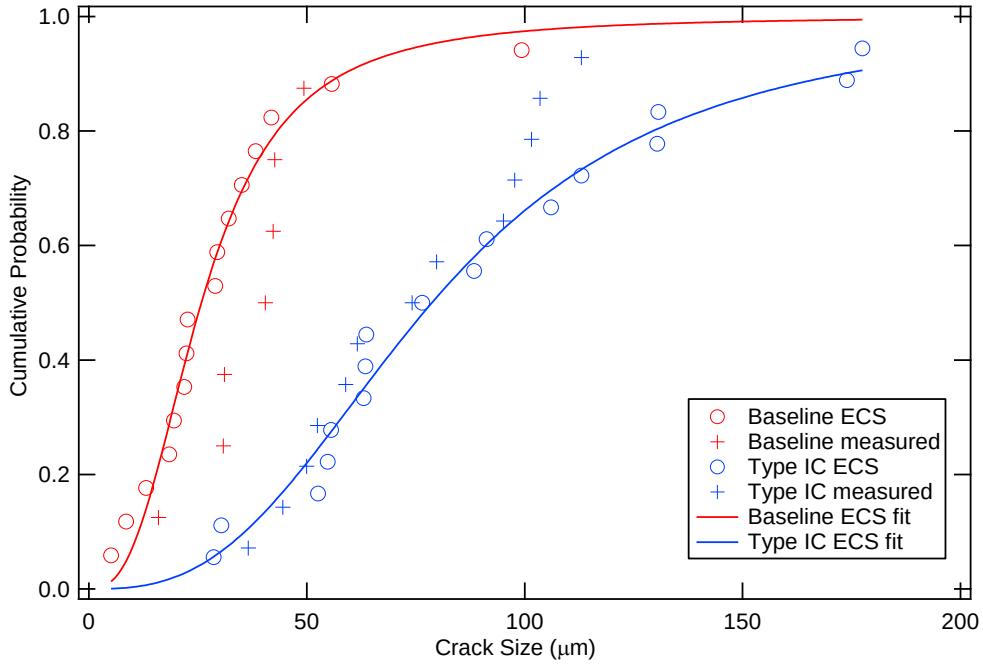

Fig.2 Equivalent Crack Size and measured fatigue cracks initiator size for coupons tested at 340 and 270 MPa

2.21 Interaction of Fatigue and Intergranular Corrosion in AP-3C Dome Nut Holes (C. Loader, [DSTO] T. Harrison, [RMIT University] D. Goudie, B.R. Crawford and A. Walliker [DSTO])

Background

Currently of concern to the Royal Australian Air-force (RAAF) is the issue of Intergranular corrosion (IGC) in the AP-3C Orion maritime patrol aircraft. There have been cases of IGC forming from the bore of particular fastener holes (Dome Nut Holes (DNH)) in the wing skin to depths approaching 10 mm. Due to the large size of the IGC, removal and subsequent repairs are also costly and can reduce aircraft availability.

A research program was developed to investigate the interaction of IGC with fatigue. This program involved an investigation of the causes underlying fatigue initiation from IGC through a combination of an experimental program and a numerical model. This culminated in a PhD thesis being submitted and accepted on 28th of August, 2014. In conjunction with the initiation investigation, a DSTO AP-3C Orion Intergranular Corrosion project investigated the interaction of fatigue cracks growing in the presence of IGC. The results of both programs are presented here.

Fatigue Initiation

The reduction in fatigue lives found in the initiation focused fatigue test program were the result of the features associated with the IGC, rather than the IGC fissure itself (shown in Figure 1). IGC representative of that seen on the aircraft, grows from a corrosion pit down the bore of the

fastener hole. In some cases, the corrosion will grow through an inclusion within the material, corroding it preferentially before continuing. Both these create voids in the material that result in stress concentrations above that of the stress concentration created by the hole itself.

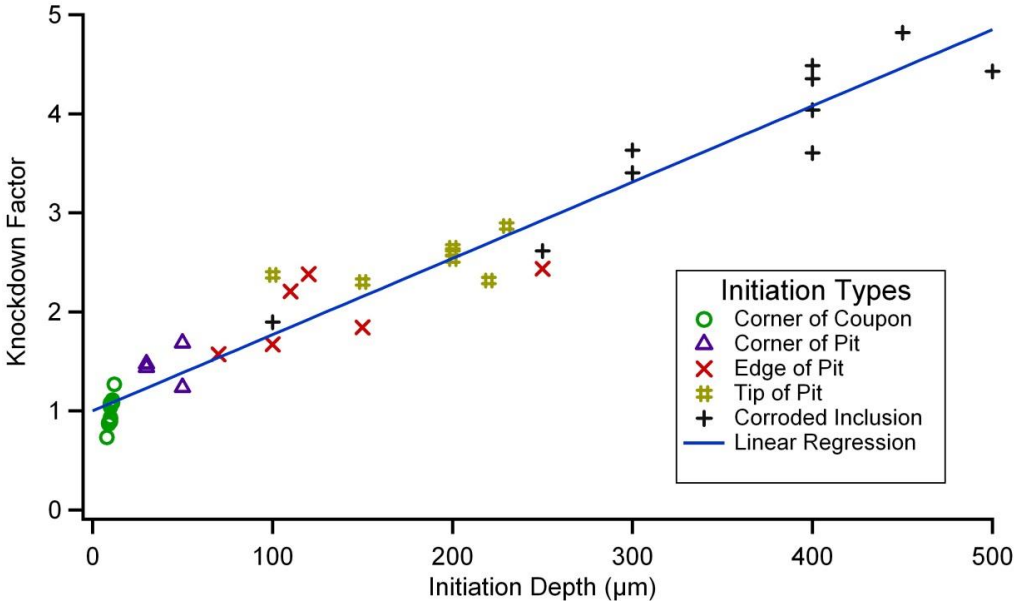

Figure 1: Initiation depth and type and their effect on change in fatigue initiation lives (shown using a knock-down factor)

A competition then exists between these two features, with the feature having the higher stress concentration generally being the initiating feature. This competition results in what was coined the Critical Inclusion Distance (CID), where a corroded inclusion must be within a certain distance for it to be the initiating feature, for a given pit size. The modelled values for CID compared well to the fatigue test results, shown in Figure 2. Following this, a predictive model was developed within Microsoft Excel that predicts the initiation depth, which can be related to a knock-down factor for fatigue crack initiation.

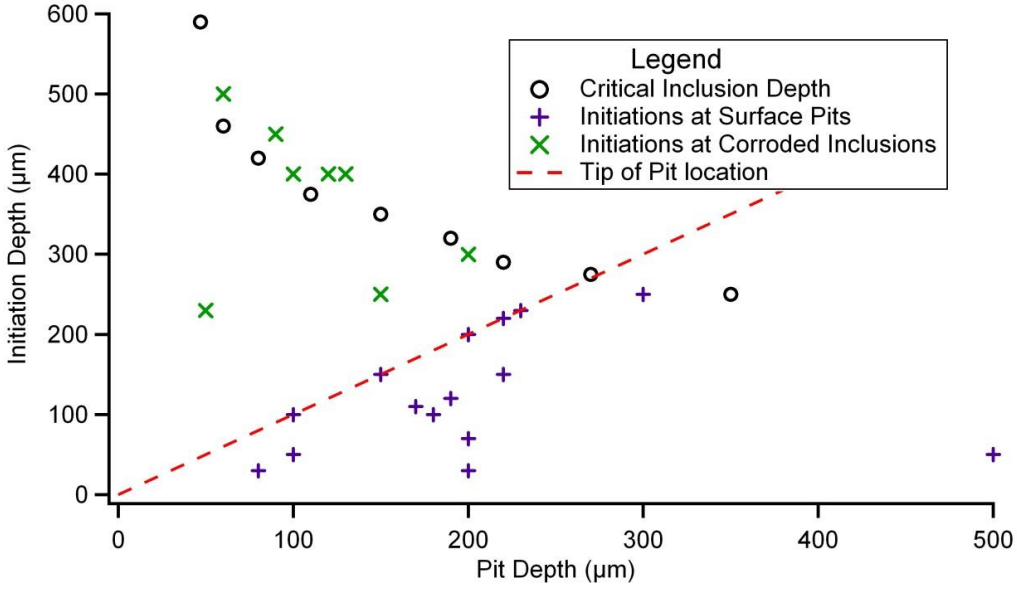

Figure 2: Critical Inclusion Distance values compared against the fatigue test results

Fatigue Crack Growth

The AP-3C Orion wing skins are lifed based on the period between when a fatigue crack reaches a detectable limit until failure. An investigation was carried out to examine the fatigue crack growth of the first ligament between the DNH and a satellite hole. The crack growth life was defined as the time it takes a crack to grow from 1.27mm through to the first ligament failure.

Two extremes of behaviour are possible in the interaction between a fatigue crack front and IGC. In the first extreme, the fatigue crack would ignore the IGC and grow in the same manner as normal for coupons of the given geometry. In the second extreme, the IGC would act as a barrier to fatigue crack growth, confining the fatigue crack to a single ligament and is termed tunnelling. In this investigation, evidence supporting both extremes, and some intermediate behaviour was discovered.

Two spectra were tested, and the crack growth recorded for the area of interest. Examination of the fracture surfaces showed that only for two specimens was there significant tunnelling. An example of this is given in Figure 3.The two specimens, both tested using Spectrum FCA352, showed crack retardation compared to specimens for which no IGC was present (Figure 4).

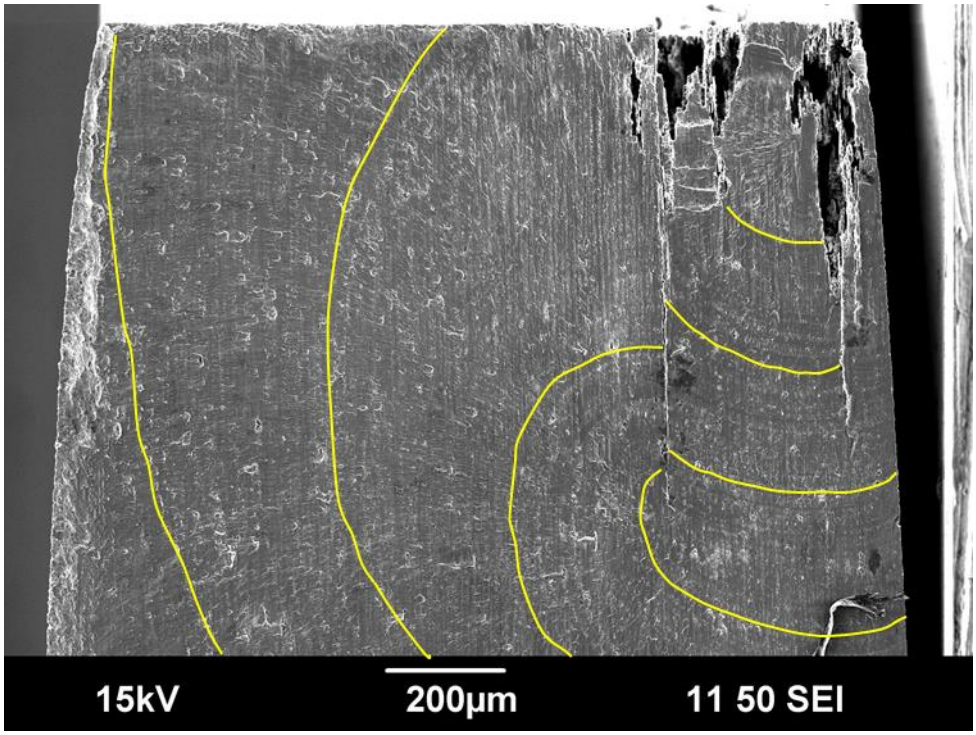

Figure 3: Fracture surface of P3-IG-03 showing 'tunnelling' where the IGC acts as a barrier to the fatigue crack front

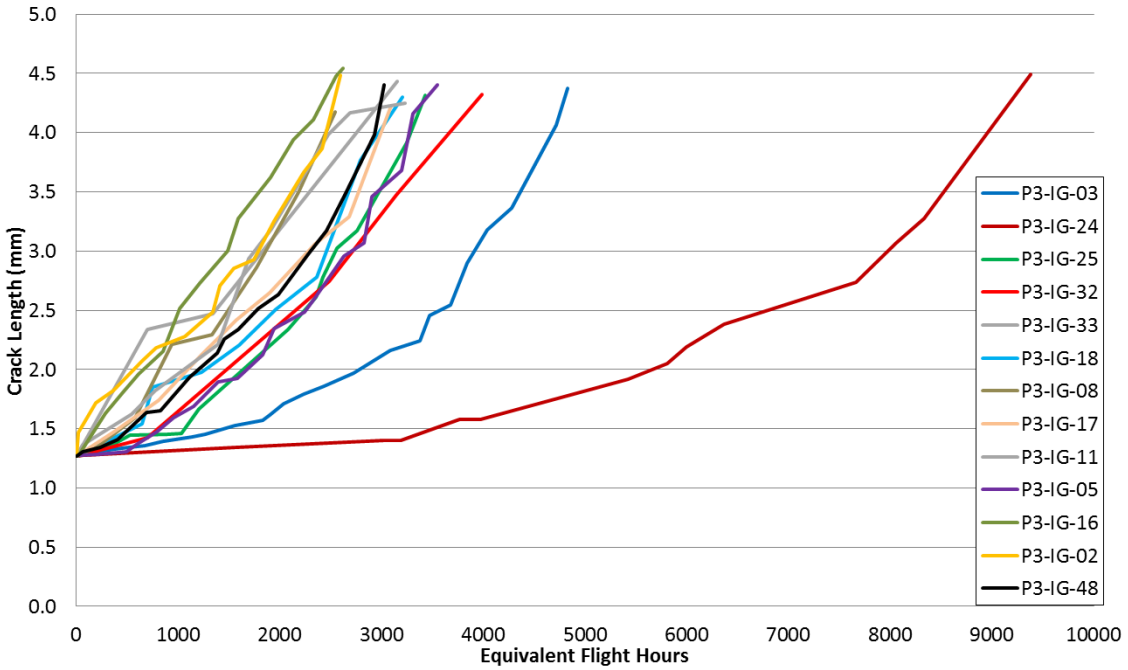

Figure 4: Crack growth for the first ligament with application of FCA352 spectrum loading.

Multiple cases of 'pinning', where the crack front is retarded at the location of the IGC were found (Figure 5). Unfortunately, the surface crack length at the time when the crack front was interacting with the IGC was too small to reliably identify the retardation. The spectra were not blocked or marker banded to allow quantitative fractographic determination of crack growth rates.

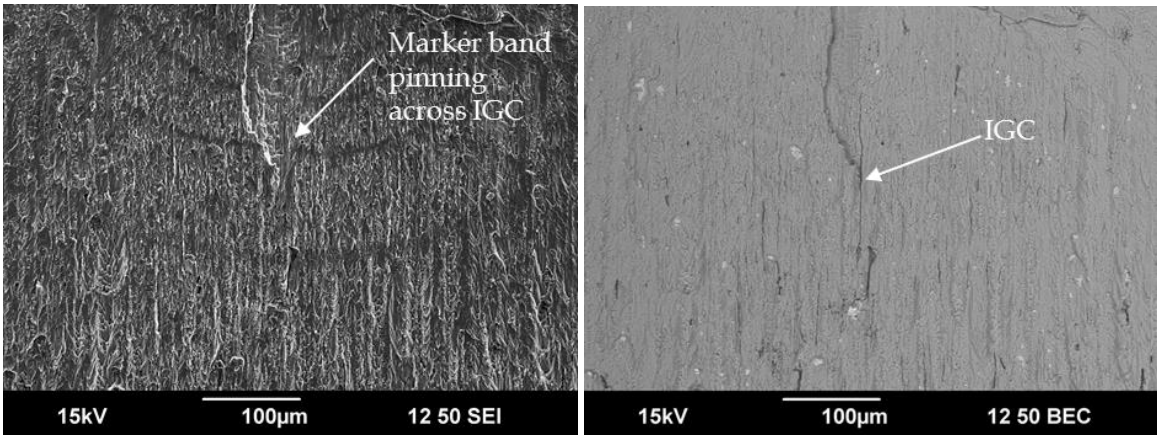

(a) (b)

Figure 5: Fracture surface of coupon P3-IG-49 showing 'pinning' in the marker band each side of the IGC strike using a) secondary electron and b) back scattered imaging

The retardation of the fatigue crack due to mechanisms where the IGC acts as a barrier to crack propagation is attributed to the reduction in constraint for thinner material. As a fatigue crack grows, the plastic zone size eventually becomes comparable with, or greater than, the cross sectional thickness. The decreased constraint leads to plane-stress conditions at the crack tip resulting in an increase in plastically induced crack closure and a resultant reduction in fatigue crack growth rate. This occurs at smaller crack sizes (and at smaller loads) in the material where an IGC strike splits the material into ligaments of smaller thicknesses.

Load shedding to the remaining ligament is a second consequence of the IGC strike acting as a barrier to fatigue crack growth. Although both ligaments would have experience the reduction in constraint, a fatigue crack in one ligament would result in an increase in load in the remaining ligament. This would result in an increased (relative) fatigue crack growth rate in the second ligament which would act to even up the cracks, explaining the 'pinning' phenomena as multiple cracks grow on either side of the IGC. Finite element analysis was conducted that concluded that the pinning phenomena would be more likely to occur when the IGC strike is centrally located, and this was corroborated by Scanning Electron Microscopy observations of the fracture surfaces. The central IGC strikes, however, were not large enough for the pinning to effect the crack growth as measured at the surface at lengths greater than 1.25mm, and so they failed to show up in the crack growth measurements (Figure 4).

Conclusions

Fatigue cracks initiate from Dome Nut Hole locations containing IGC either at pitting corrosion, which is the precursor to IGC, or at corroded inclusions along the IGC fissure. A predictive model was developed that predicts initiation depth and relates this directly to a knock-down factor for fatigue crack initiation. The reductions in fatigue live from the enhanced initiation mechanisms did not impact on the lifing of the DNH locations, which are based on crack growth, and did not invalidate the inspection techniques used in maintenance of the AP-3C by a shifting of the site of fatigue crack initiation.

No increase in fatigue crack growth rates was found associated with IGC at the DNH locations investigated. An investigation of fatigue crack growth for individual coupons was correlated with fractographic observations. This led to the discovery of a mechanism of crack retardation through a combination of decreased constraint leading to an increase in plastically induced closure, and load shedding. These mechanisms led to both tunnelling and pinning of the fatigue crack which was visible via scanning electron microscopy of the fracture surfaces.

2.22 Fatigue of Bonded Joints and Composite Laminates: A Re-examination of the Correlating Parameter (Matthew Donough [RMIT University])

In order to ensure continuing airworthiness, composite and bonded structures must demonstrate no or very slow growth of a pre-existing flaw within the structure. Presently, this is achieved by employing low design allowable strains and full-scale fatigue test validations. Consequently, this places an artificial limit on the design space. In order to fully optimise the advantages of composite materials and adhesive bonding, and also reduce the high cost burden of existing design practice, a fatigue design criterion is needed to predict the evolution of the crack in a bonded composite structure.

The characterisation of fatigue crack growth rates (FCGR) in composite laminates and bonded joints is typically correlated to the strain energy release rate (G) in a Paris law relation. The most prevalent means of characterising FCGR under different load ratios (R) is defined as the difference between the maximum and minimum G, as shown below,

$$\Delta G = G_{\max} - G_{\min} \tag{1}$$

However the ΔG parameter does not maintain similitude principle under fatigue loads (i.e. crack tip conditions are not uniquely defined by a single loading parameter) as discussed in Ref. [1, 2]. ΔG infers FCGR is driven by a specific combination of cyclic load range and mean load without any physical basis. There is also ambiguity for negative load ratios ($R < 0$). For example, ΔG equals zero under fully reversed loading ($R = -1$), because the G_{max} and G_{min} are equal. Hence, for these reasons, ΔG is unable to correctly account for the influence of load ratios under mode I and II loadings in a consistent manner.

Given the lack of physical basis of ΔG, an alternative definition of the cyclic strain energy release rate was used,

$$\Delta G_{eq} = \left(\sqrt{G_{\max}} - \sqrt{G_{\min}}\right)^2 \tag{2}$$

The ΔG_{eq} parameter assumes that FCGR is controlled by the cyclic stress state at crack tip, consistent with the similitude requirement as ΔK for fully open fatigue cracks in metallic alloys. Mode I and II fatigue experimental studies were carried out on double cantilever beam (DCB) and end-notched flexure (ENF) specimens with and without an adhesive bondline at the mid-plane. The FCGR were generated under ambient laboratory conditions and using the load-shedding approach recommended in ASTM E647 [3]. Figure 1 shows the mode I and II experimental results correlated with ΔG_{eq}. The mode I FCGR for both cohesive debonding and delamination can be observed to be significantly influenced by load ratios, similar to metallic alloy's fatigue behaviour when plotted against ΔK. Conversely the mode II FCGR for both crack propagation mechanisms was observed to be independent of load ratios.

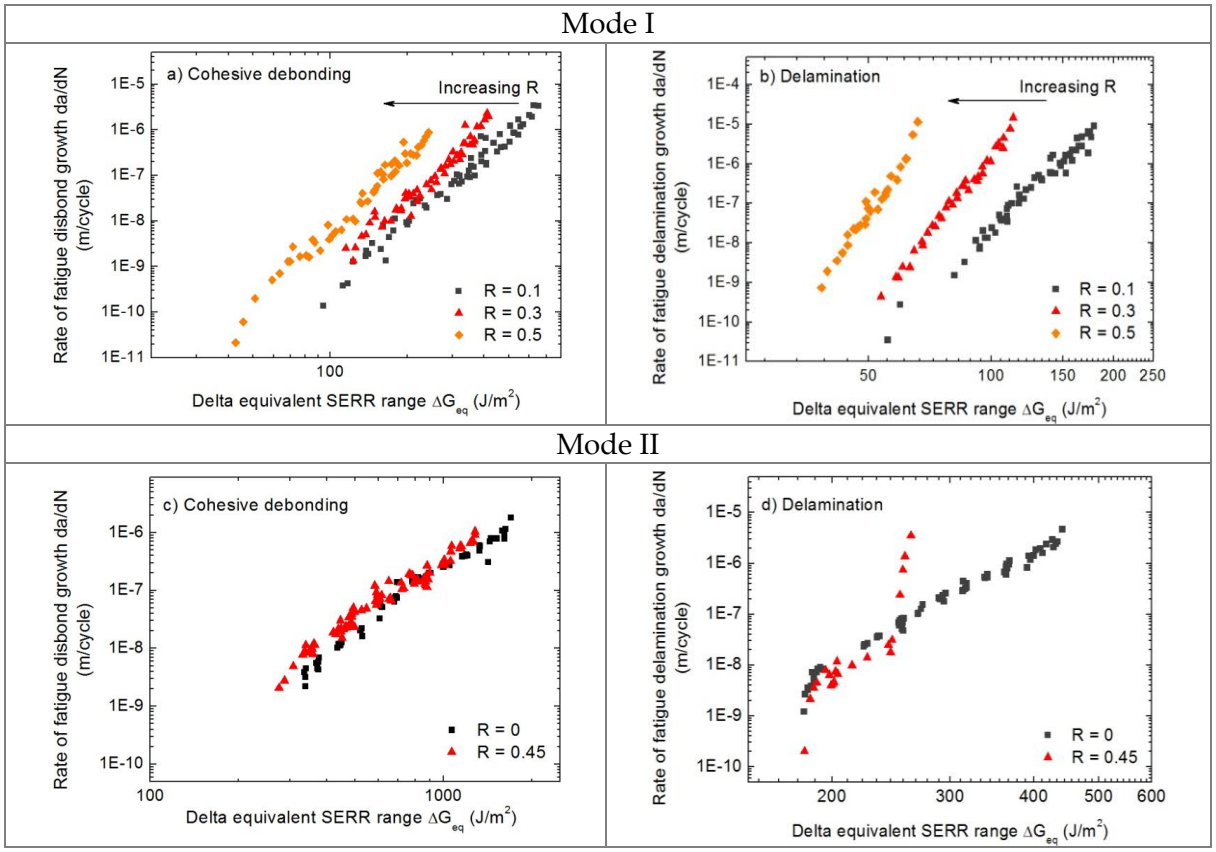

Figure 1: Mode I and II fatigue experimental results of a unidirectional DCB and ENF specimens with/without an adhesive bondline

A plastic zone, as well as a plastic wake, can be observed in the adhesive bondline for the bonded DCB specimens. Given the success of the crack closure concept in accounting for the load ratio effects in metallic alloys fatigue behaviour, the plasticity induced crack closure mechanism was hypothesised to be dominant cause for this observed load ratio dependency behaviour. In order to quantify the effects of crack closure in bonded joints, elastic-plastic analysis of the fatigue crack propagation in a DCB joint was carried out. Such analysis is commonly carried out to analyse the crack closure behaviour of isotropic materials [4, 5]. The results of the numerical analyses showed that small scale yielding condition is valid and the effective load range experienced at the crack tip is shown in Figure 2a. Using the crack closure concept, the effective strain energy release rate is proposed as follows:

$$\Delta G_{eff} = \left(\sqrt{G_{I,\max}} - \sqrt{G_{I,op}}\right)^2 = G_{I,\max}\left(1 - \frac{P_{op}}{P_{\max}}\right)^2 = \Delta G_{I,eq} U^2 \qquad (3)$$

From the numerical results under mode I, the effective load range U, given as $U = \frac{P_{\max} - P_{op}}{P_{\max} - P_{\min}} = \frac{1 - P_{op}/P_{\max}}{1 - R}$, is shown in Figure 2b. Under mode II, crack closure is numerically shown to be a non-issue as the cyclic displacement of the crack flanks occurs parallel to the fracture plane rather than perpendicular to it. Consequently the influence of load ratios in mode I FCGR can be eliminated after the effects of crack closure are accounted for.

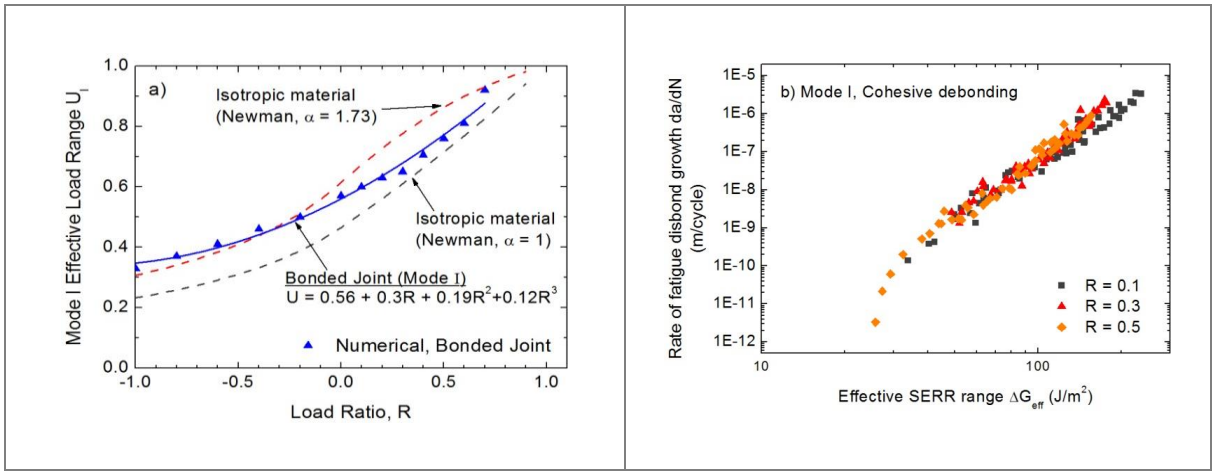

Figure 2: a) Effective load range as a result of plasticity induced crack closure and b) Experimental correlation

Fibre bridging can be observed in the wake of the crack for the composite DCB laminate. Plasticity induced crack closure was shown in numerical simulations to be absent for unidirectional laminates due to the constraints of the fibres [6]. Hence this leaves fibre bridging to be the only plausible mechanism affecting the crack tip stresses.

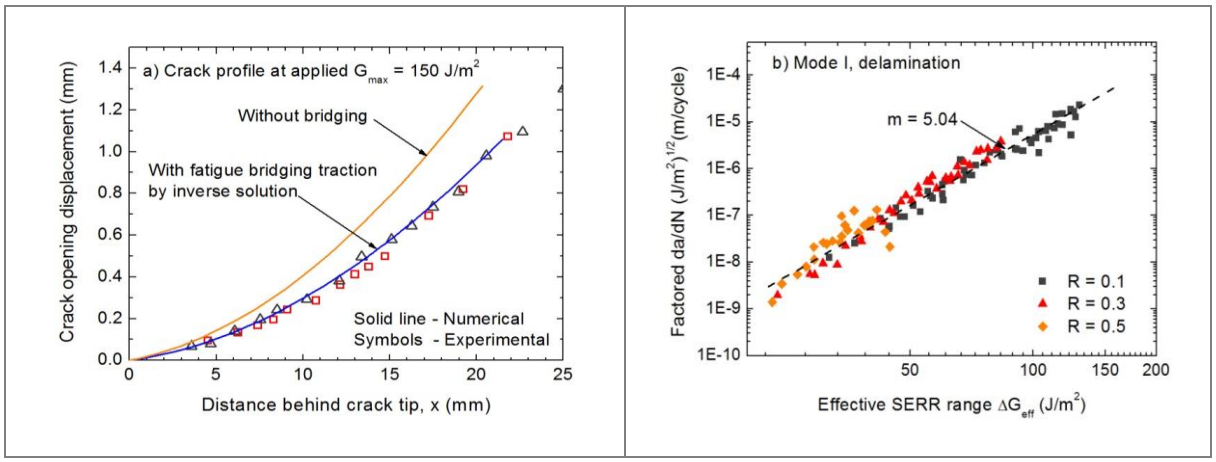

Figure 3: a) Crack profile as a result of fibre bridging and b) Experimental correlation

In order to further investigate this phenomena, a fatigue bridging zone of 20 mm long was developed under cyclic loads, constant applied *G*. The crack opening displacement of the crack profile was measured and the bridging tractions were then identified in an inverse solution procedure. The crack tip shielding provided by the fatigue bridging zone, G_b^f, is determined to be 75 J/m². Hence the following correlating parameter is proposed for fibre bridging in Eqn. (4). Together with the Forman equation to account for the increased influence of G_{max}, a good correlation for the mode I FCGR can be obtained as shown in Figure 3b.

$$\Delta G_{eq} = \left(G_{\max}^{app} - G_b^f\right)(1-R)^2 \qquad (4)$$

A number of approaches had been proposed over the years to characterise the fatigue crack growth in bonded joints and composite laminates. The common theme among these models is that it is phenomenological in basis, designed to fit the observed experimental data. In this work,

the respective mechanisms influencing the FCGR in bonded joints and composite laminates were identified. Correlating parameters are proposed to account for the effects of load ratios in a mechanistic manner. Having achieved this, this paves the way of enabling fatigue life predictions under variable amplitude loading conditions, overcoming the limitations of existing methods.

References

[1] Rans, C., R. Alderliesten, and R. Benedictus, *Misinterpreting the results: How similitude can improve our understanding of fatigue delamination growth.* Composites Science and Technology, 2011. 71(2): p. 230-238.

[2] Donough, M.J., et al., *Plasticity induced crack closure in adhesively bonded joints under fatigue loading.* International Journal of Fatigue, 2015. 70(0): p. 440-450.

[3] ASTM Standard E647, "*Standard test method for Measurement of Fatigue Crack Growth Rates*", 2013, ASTM International, West Conshohocken, PA, 2013, DOI: 10.1520/E0647-13AE01, www.astm.org

[4] Newman Jr, J.C., *A finite-element analysis of fatigue crack closure.* ASTM STP, 1976. 590: p. 281-301.

[5] Zapatero, J., B. Moreno, and A. González-Herrera, *Fatigue crack closure determination by means of finite element analysis.* Engineering Fracture Mechanics, 2008. 75(1): p. 41-57.

[6] Donough, M.J., *Load ratio effects in the fatigue crack propagation of composite laminates and bonded joints*, 2014, RMIT University.

2.23 A Study of Environmentally Induced Fatigue Crack Growth in 7075 Aluminium Alloy (Michael Lo, Monash University)

Ageing aircraft fleets commonly experience environmentally induced degradation. The extended operation of ageing fleets can include certification using the Safety by Inspection approach. The application of Safety by Inspection regime in aviation airworthiness needed an accurate assessment of fatigue crack growth in the presence of environmentally induced degradation. In general there is an urgency to remove corrosion damage on aircraft structures upon detection, thus causing unscheduled downtime and higher upkeep costs. Since the majority of the life of a fatigue crack is spent in propagation of small and short cracks, crack growth laws must ideally capture small (<100 μm) and short (<1 mm) crack behaviour as well as long crack growth for fatigue life assessment.

The current research addresses the effect of environmentally assisted degradation and fatigue crack nucleation and propagation in aircraft structures. Two common forms of localised corrosion are studied, namely, pitting corrosion and intergranular corrosion (IGC). A specific interest of this work is to establish the effect of IGC at a fastener hole representative of the structural geometry on the RAAF AP-3C Orion aircraft [1]. In order to produce IGC at the central hole, a corrosion protocol developed by DSTO was implemented, see [1]. Fatigue tests are conducted with marker band loading with two alternating R ratios (R=0.1 and R=0.8) for identification of crack growth with quantitative fractography.

Figure 1 depicts fatigue cracking in a corroded dome nut hole coupon DNHS-1-4 tested at a peak stress of 80 MPa, see [2]. Multiple out of plane fatigue cracking in the coupon is observed around a region containing corrosion pitting and IGC at the bore of the central hole. These small fatigue cracks propagate collectively and eventually coalesce to form larger cracks. Evidence of IGC of about 0.4mm in depth from the bore of the hole at the base of the corrosion pit is revealed on the SEM fractographs. The presence of IGC may have segregated the crack paths of multiple fatigue cracks up to the depth of the IGC. Beyond the depth of the IGC, the slightly off-plane cracks coalesce and propagate as a single main crack. Under fatigue cracking, IGC can act as a weak plane providing partitioning between two cracking ligaments on either side of the IGC, and has been described as 'pinning' in [3]. The fatigue cracks in both ligaments would crack simultaneously, grow equal progressively and coalesce to form a single crack beyond the depth of the IGC.

The results show that the physical size of discontinuity, particularly corrosion pits, is not the only feature that can strongly dictate fatigue crack growth behaviour. Dynamics such as the morphology and location of the corrosion sites, position of crack origin with respect to the unevenly formed corrosion damage, and properties of the local microstructure, i.e. local fatigue threshold, also have a significant impact on crack propagation [2, 4-7]. Accordingly, the Hartman-Schijve (HS) variant of the NASGRO formulation which can correctly represent the relationship between fatigue crack growth rate da/dN and stress intensity factor ΔK in the AA 7075-T6 and 7075-T651 test coupons [6-7], is given by

$$da/dN = D\left(\frac{\Delta K - \Delta K_{thr}}{\sqrt{1-K_{max}/A}}\right)^2 \quad (1)$$

where D= 1.86×10^{-9}, and A= 47 MPa $m^{1/2}$. In general, it is shown that short cracks exhibit smaller thresholds stress intensity levels than long cracks [7].

The ability of the formulation to model the variation in the crack growth rates associated with both small and long cracks is verified by allowing for small changes in the term ΔK_{thr} [2, 7]. Figure 2 demonstrates that the variability in the small and short crack growth rates seen in these tests can be accurately estimated using Equation (1) and allowing for threshold values [2]. Further, the proposed threshold parameter compatibly accounts for corrosion pits which are usually non-ideal crack starters due to the rough and odd shapes, and often generate multiple cracks which interfere with one another, resulting coarsely formed crack fronts [2, 5]. The initial cracks interact with the irregular corrosion damage and propagate slower than if the pits were ideal semi-elliptical profiles [2, 5]. The presence of intergranular corrosion can have a range of influences on the crack growth behaviour [3]. For the reasons discussed above, a comprehensive fatigue failure analysis requires in-depth understanding of the impact of the morphology of pitting and intergranular corrosions.

In summary, in order to predict the entire scope of the aircraft life and crack growth history, a single formulation should be used, which should be accurate for small cracks, the transition from small to long and capture the long crack growth behaviour. The technique investigated herein confirms that Equation (1) can capture small, short and long crack growth, and the total fatigue life [2]. In circumstances where the life of an aircraft is largely dependent on environmentally initiated fatigue crack growth, the present technique can contribute towards a more effective management approach of structural integrity.

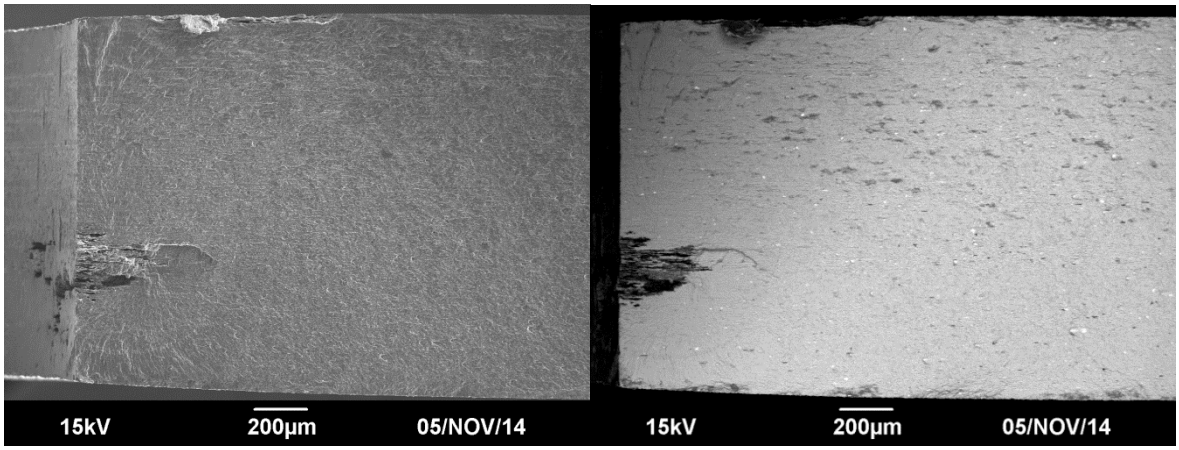

Figure 1. Secondary (SEI) and backscatter (BSE) SEM fractographs showing fatigue cracks in DNHS-1-4 initiating from a corrosion pit at the bore of the central hole [2].

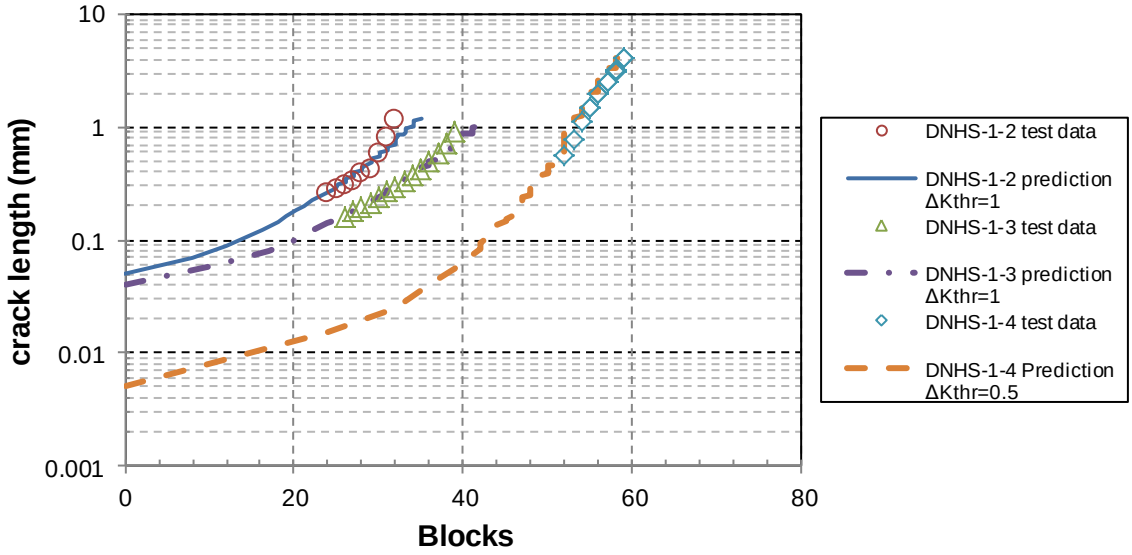

Figure 2. Fatigue crack growth and life prediction of corroded dome nut hole test coupons [2].

References

[1] Salagaras, M., Wythe, A. & Trathen, P., Methodology For Producing Intergranular Corrosion on AA7075-T651, In: Corrosion & Prevention 2012 Paper 120, 2012

[2] Lo, M., Jones, R., Peng, D., Bowler, A., and Edwards, D., Fatigue Crack Growth from Environmentally Induced Damage in 7075 Alloy, International Committee on Aeronautical Fatigue and Structural Integrity, Helsinki, ICAF 2015

[3] Loader, C., Goudie, D., Salagaras, M., Underwood, J. and Walliker, A., RAAF AP-3C Interaction between Integranular Corrosion and Fatigue, DSTO-TR-3048, DSTO, December 2014.

[4] Jones R, Molent L., Barter S., Calculating crack growth from small discontinuities in 7050-T7451 under combat aircraft spectra, International Journal of Fatigue, Volume 55, 2013, pp 178-182.

[5] Barter, S.A., Molent, L., Fatigue cracking from a corrosion pit in an aircraft bulkhead, Engineering Failure Analysis, Volume 39, April 2014, Pages 155-163, ISSN 1350-6307

[6] Jones R., Lo M., Peng D., Bowler A., Dorman M., Janardhana M., Iyyer NS., A study into the interaction of intergranular cracking and cracking at a fastener hole, Meccanica, 2013, Volume 48, Issue 10, doi 10.1007/s11012-013-9849-x
[7] Jones R., Fatigue Crack Growth and Damage Tolerance, Fatigue and Fracture of Engineering Materials and Structures, 2014, Volume 37, Issue 5, pages 463–483.

2.24 Experimental and modeling study of the effect of corrosion pitting on fatigue failure locations in aircraft components (Bruce R. Crawford, Chris Loader, Qianchu Liu, Timothy J. Harrison, P. Khan Sharp [DSTO] and Gunnar Härkegård [Department of Engineering Design and Materials, Norwegian University of Science and Technology, Norway])

Introduction

Corrosion pits reduce the fatigue life of aircraft components. However the effect of pitting corrosion on the location of fatigue failures has been overlooked. This is problematic as corrosion pits have caused fatigue failures in unexpected locations and components, such as the trailing edge flap lug of the F/A-18 [1]. DSTO call this problem 'Corrosion Criticality'.

This report describes the development of Monte-Carlo models of how pitting corrosion affects the location of fatigue failures in two specimen geometries with different stress concentration factors (k_t). These specimens are a low-k_t specimen and a high-k_t specimen with three holes arranged along its centerline. The modeling results for the low-k_t specimen are compared with experimental results for that specimen. The low-k_t model produces good estimates of fatigue life and of the probability of fatigue failure at any given location in the specimen's gauge section. The process that will be used to develop the high-k_t model is outlined.

Low-k_t Fatigue Specimen Model

The Low-k_t Corrosion Criticality Model (CCM) was the first model developed. It was based on fatigue life, crack growth data inclusion size data from Crawford *et al.* [2, 3]. Figure 1 shows the specimen geometry. Corrosion strike offset distances, *d*, of 30, 38 and 45 mm were tested.

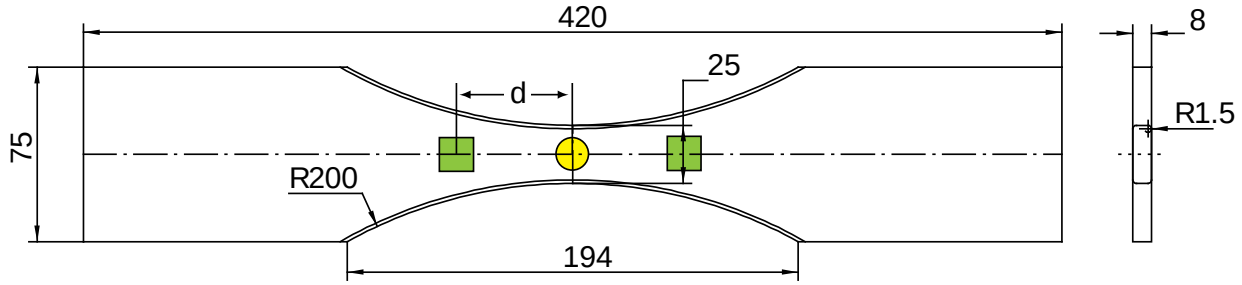

Figure 1: Geometry of low-k_t fatigue specimens. The ● symbol shows the location of the centrally located corrosion strike used in [2, 3] while the ■ symbols are the offset corrosion strikes [4], which are offset a distance d from the specimen's center. Dimensions are in millimeters.

Figure 2 shows the model's fatigue life and failure location predictions. It compares these with experimental results from Crawford et al. [2, 3], which consisted of 300 corroded specimens with

central corrosion strikes and an additional 16 fatigue life tests with offset corrosion strikes. The model's predictions compare well with these results. In predicting the failure locations (Figure 2b) ten replicate runs each simulating 5,000 fatigue life tests with dual corrosion strikes were conducted at d values between zero and 60 mm. Figure 2(b) plots the proportion of the fatigue failures due to corrosion with 90% confidence intervals calculated using the Modified Wald Method [4]. The agreement between the model and the experimental data is good.

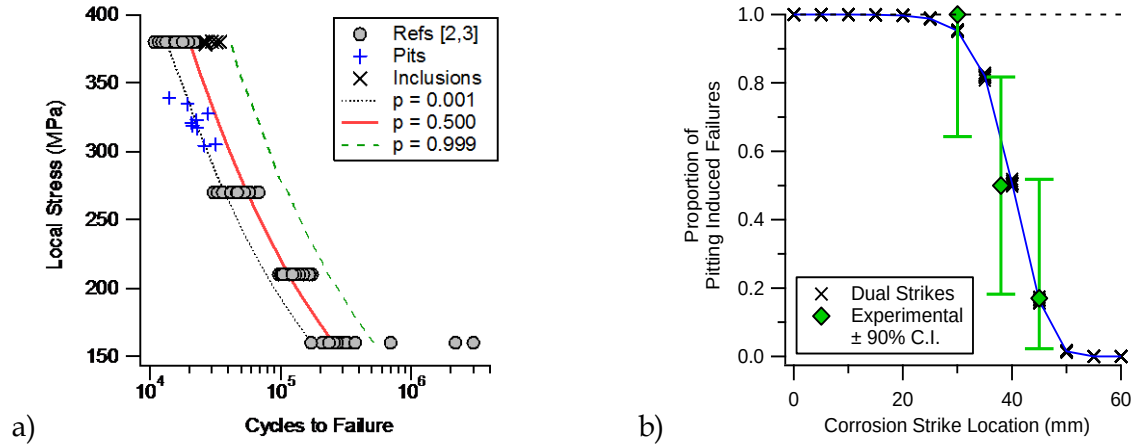

a) b)

Figure 2: (a) Comparison of fatigue life results from [2, 3] with those obtained from the offset tests and the model's predictions. 'Pits' are specimens which failed due to cracks from corrosion pits. 'Inclusions' are specimens that failed from inclusions. (b) Comparison of predicted and observed proportion of fatigue failures induced by pitting corrosion.

Figure 3 illustrates how corrosion alters the fatigue behavior of the low-k_t specimen. A corroded specimen can be divided into three distinct regions. The first of these is the 'Always fatigue critical region' (colored red) which is the highest stress region. In an aircraft this would be the fatigue critical region when corrosion is absent. This region must be periodically monitored for fatigue damage to maintain airworthiness. Once the specimen is corroded the fatigue critical region grows to include the 'Fatigue critical when corroded' region (colored amber). This is where corrosion damage inspections should be concentrated. The size of this region is determined by the size of the pits relative to the material's other fatigue initiators. Larger pits will cause a larger expansion. Finally, there is the green 'Not currently fatigue critical' region where the stress and defect size combination cannot produce a crack driving force large enough to cause fatigue failure. Therefore, it is possible to delay the repair of corrosion damage in this region so long as the growth of the corrosion damage can be slowed or stopped using corrosion inhibiting compounds.

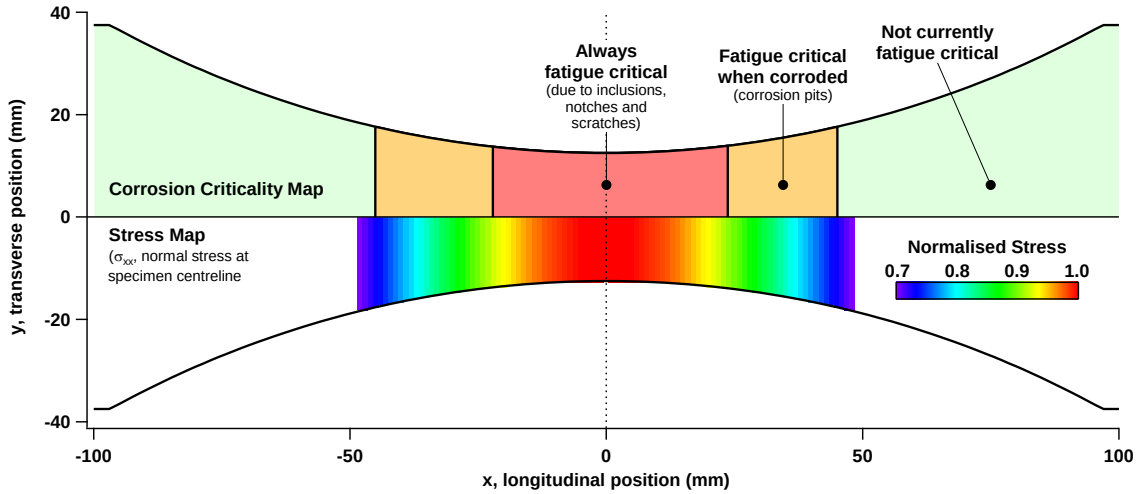

Figure 3: Illustration of how pitting corrosion damage increases the size of the fatigue critical region of the low-k_t fatigue specimen. The figure's upper half shows the criticality of various regions of the specimen while the lower half shows the normalized stress vs. position.

High-k_t Fatigue Specimen Model – Results to Date

The accuracy of the Low-k_t model indicates that the CCM is useful. However, the fatigue critical areas in aircraft are typically associated with stress concentrators. Therefore, it was decided to test the CCM using high-k_t specimens, Figure 4, which have three holes. Opie [5] found that the k_t of the outer holes was 2.69 while that of the central hole was 2.48, which is 7.8% less. Therefore, the central hole is unlikely to initiate a critical fatigue crack.

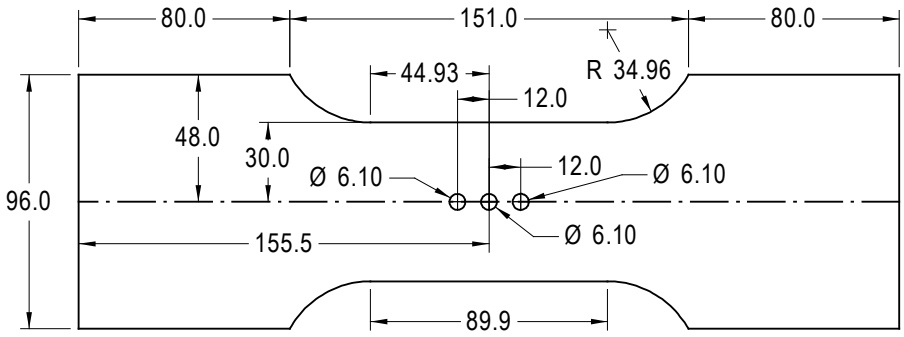

Figure 4: Engineering drawing of the high-k_t fatigue specimens. The specimens were 6.35 mm thick and were machined from 7050-T7451 aluminum alloy. All dimensions are in millimeters.

Constant amplitude fatigue life tests were conducted on ten high-k_t specimens. Six were tested in the as-machined state while the remainder had their central holes corroded before testing. The specimens were tested at a stress of 125 MPa with a load ratio of 0.1. The corroded specimens had shorter and less scattered fatigue lives than the uncorroded specimens, Figure 5. These specimens all failed at the central hole. The uncorroded specimens failed from either the outer hole or ran out.

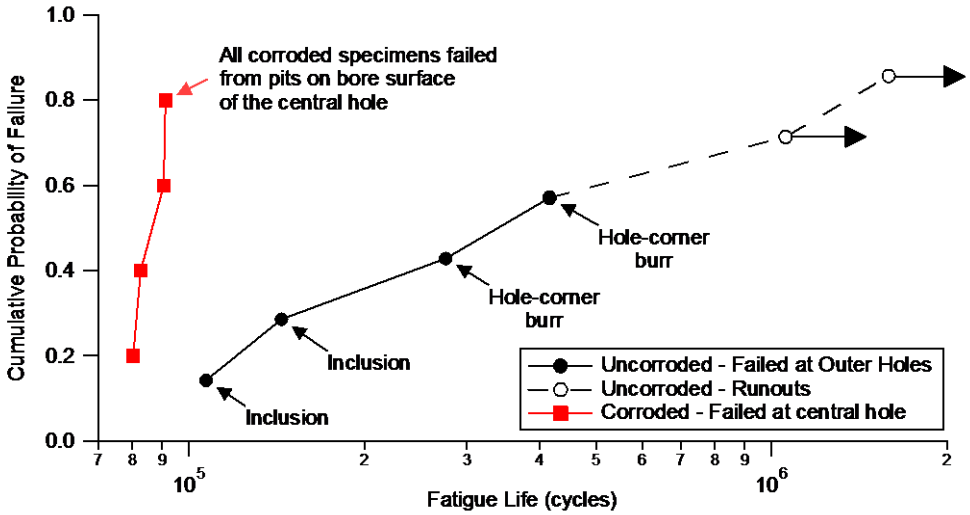

Figure 5: Fatigue life results for corroded and uncorroded high-k_t specimens. Arrows indicate runouts and specimens that failed in the grips. Cumulative probability values were estimated using the formula $p = i/(n+1)$, where i is the i-th data point in the sorted data series and n is the total number of data points in the sorted series.

The initiating features of the primary cracks in each specimen were identified and measured using a scanning electron microscope. The critical corrosion pits had a mean depth of 175 microns compared to 43 microns for the critical inclusions. Two uncorroded specimens, however, failed due to cracks from hole-corner burrs and could not be sized.

High-k_t Fatigue Specimen Model – Future Work

The next stage in this work is to create a Monte Carlo model similar to that developed for the low-k_t specimen. The first step will be to build a Monte Carlo model from first principles as was done with the low-k_t model. Then PFat [6], which was developed by NTNU, will be used to develop an independent model. As part of this a Abaqus was used to make a three-dimensional finite element model of the high-k_t specimen. Figure 6 shows a surface contour plot of the maximum principal stress near the holes. The stresses in this figure are numerically equal to the stress concentration factor. The k_t of the outer holes (2.83) is higher than that the central hole (2.56).

The final stage is to incorporate the FE results into the models being developed. This should be relatively easy for the PFat model as it can directly read Abaqus files. In contrast, the DSTO model will require post-processing of the FE data. Next it will be necessary to characterize the fatigue crack growth and microstructural properties of the 7050-T7451 material from which the specimens have been made. Given these data the models will be used to predict the fatigue life and failure location of corroded and uncorroded high-k_t specimens. These predictions will be compared to the observed fatigue lives and if necessary the models will be revised to improve their accuracy.

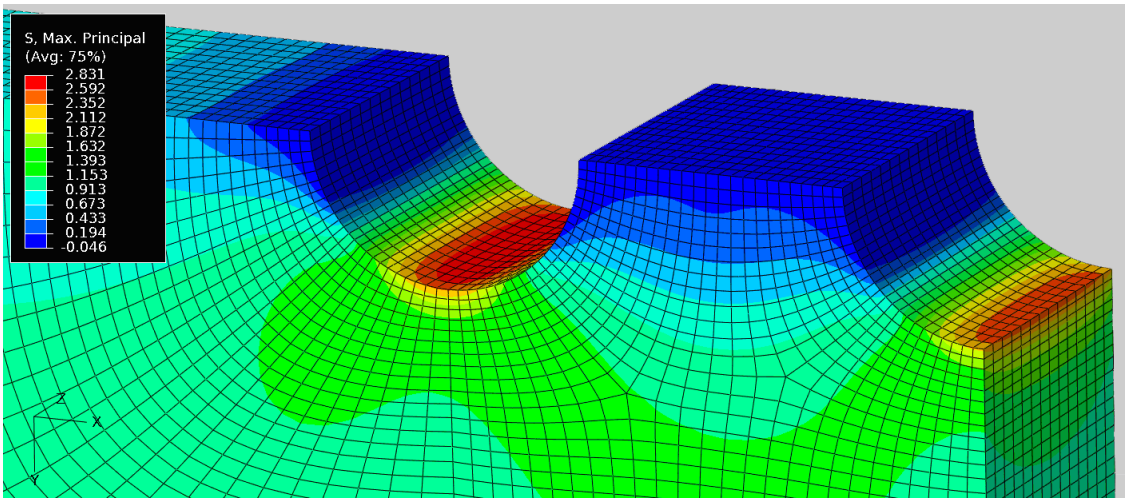

Figure 6: FE model of maximum principal stress in a high-k_t fatigue specimen modeled with XY and XZ symmetry planes.

Summary

This report has described models which predict how corrosion damage affects the fatigue life and failure locations of fatigue specimens of the aluminum alloys 7010-T7651 and 7050-T7451. The first model, which is based on a low-k_t fatigue specimen of 7010-T7651, accurately predict both failure location and fatigue life. It demonstrates clearly that pitting corrosion can shift the location of fatigue failures. The second model, which has been partially developed here, is for high-k_t fatigue specimens of aluminum alloy 7050-T7451. A small experimental trial of ten specimens was conducted. It again showed that pitting corrosion can alter the location of fatigue failures in the high-k_t specimen. The work required to complete the high-k_t model has been outlined.

References

[1] Barter, S. A., Sharp, P. K. and Clark, G. (1994) The failure of an F/A-18 trailing edge flap hinge. *Engineering Failure Analysis* **1** (4) 255-266

[2] Crawford, B. R., Loader, C., Ward, A. R., et al. (2005) The EIFS distribution for anodised and pre-corroded 7010-T7651 under constant amplitude loading. *Fatigue and Fracture of Engineering Materials and Structures* **28** (9) 795-808

[3] Crawford, B. R., Loader, C., Harrison, T. J., et al. (2013) *A Demonstration using Low-k_t Fatigue Specimens of a Method for Predicting the Fatigue Behaviour of Corroded Aircraft Components*. DSTO-RR-0390, Melbourne, DSTO

[4] Agresti, A. and Coull, B. A. (1998) Approximate is better than "Exact" for Interval Estimation of Binomial Proportions. *American Statistician* **52** (2) 119-126

[5] Opie, M. (2013) *2D Plane Stress Finite Element Derivation of Stress Concentration For a 3-Hole Dogbone Coupon in Support of the Corrosion Criticality Project*, DSTO Minute B2/129/PT4, Melbourne, Aerospace Division, November 2013.

[6] Wormsen, A., Fjeldstad, A. and Härkegård, G. (2008) A post-processor for fatigue crack growth analysis based on a finite element stress field. *Computational Methods in Applied Mechanical Engineering* **197** 834-845

3. FULL SCALE TEST ACTIVITIES

3.1 F/A-18A/B Hornet Outer Wing StAtic Testing (HOWSAT) (Wayne Foster [DSTO])

Attempts to develop a through life management strategy for the outer wing of the F/A-18A/B Hornet aircraft, based on direct test interpretation of previous full-scale fatigue tests including FT93L (an Original Equipment Manufacturer's test) and FT245 (International Follow-On Structural Test Project) have proven inconclusive mainly due to variations in the in-service configuration of the wing tip stores and significant aerodynamic buffet.

Loading at the outer wing representative of RAAF usage and store configuration was not achieved on either of the fatigue tests. A strict application of DEFSTAN 00-970 would therefore require the use of severe life reduction factors, which would have led to unacceptably short Safe Life Limits and an extensive Safety-By-Inspection program. To achieve such a program, inspection of most of the critical structure in the outer wing would require substantial disassembly, including removal of the upper wing skin, which would come with significant cost and aircraft availability impact. However, the fatigue tests have been useful in demonstrating the likely fail-safety of the outer wing structure as well as the locations of potential cracking. Both the test wings sustained loads above limit with damage including severed spars. It is thought that this excess load carrying capacity comes from the carbon fibre/epoxy upper and lower wing skins.

A new representative fatigue test would take at least several years to prepare and carry out to allow useful conclusions about the actual fatigue life of the outer wing. Considering that the RAAF F/A-18A/B fleet is currently projected to retire around the 2020 timeframe, the results would be available too late to be useful for the Aircraft Structural Integrity Program.

To address this, the F/A-18A/B Hornet Outer Wing StAtic Testing (HOWSAT) program was developed. It is intended to substantiate a Through Life Management Strategy for the F/A-18A/B Hornet outer wing internal metallic structure by testing it with significant representative damage present [1]. The static test program, which is now nearing completion, uses damage scenarios derived from worldwide structural condition data, in addition to the fatigue damage demonstrated in the previous full-scale fatigue tests, to underpin a fatigue control plan for the outer wing in RAAF service.

Numerous representative damage cases have been successfully applied to the HOWSAT test article using the test rig shown in Figure 1. An overview of the induced damage locations is presented in Figure 2. For the majority of locations, the representative damage was introduced by cutting the structure with a saw, scoring the cut with a sharp knife and then cycling the test article to grow small fatigue cracks at the end of each saw cut tip.

The testing of each representative damage load case involves the application 120% design limit loads for 12 static load cases. Ground vibration testing is also conducted to assess any changes in dynamic response due to the introduction of the representative damage. The deflections

resulting from the maximum wing bending up and maximum wing bending down load cases are shown in the composite photograph of Figure 3.

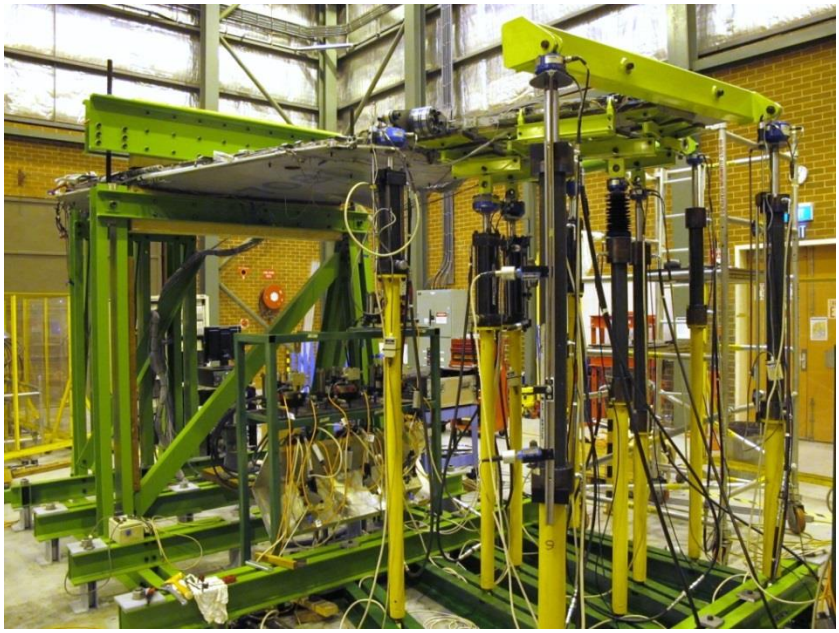

Figure 1 HOWSAT test rig configuration

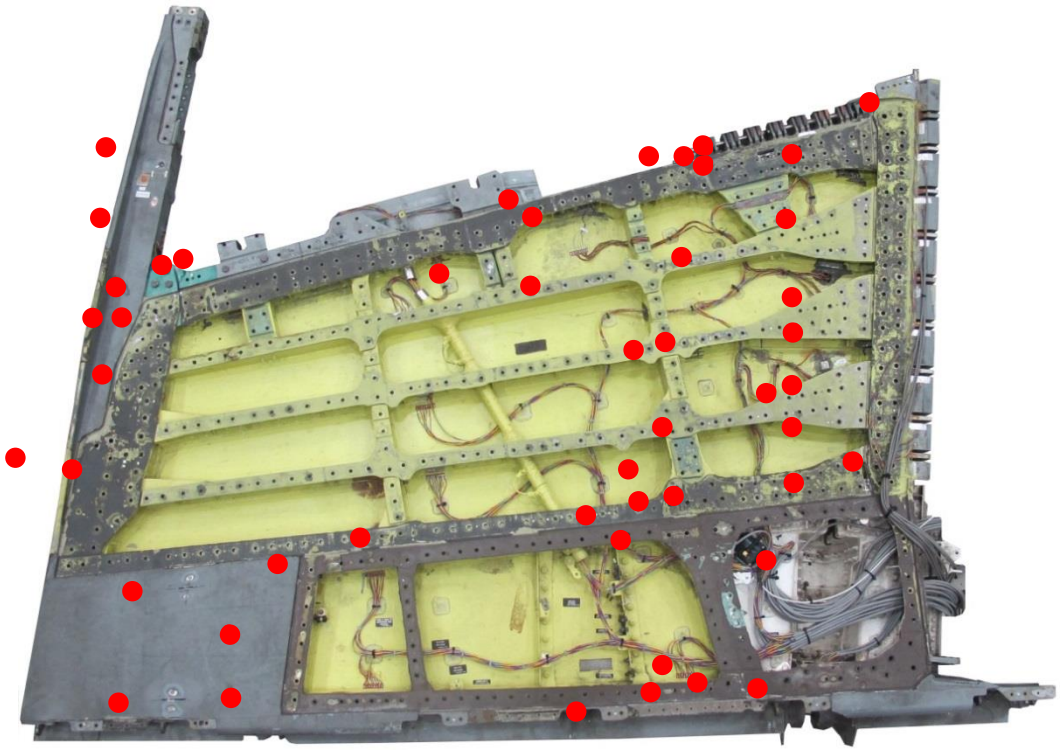

Figure 2 Overview of the introduced HOWSAT damage locations represented by red dots. Only the upper surface is shown. The induced damage may have been on the upper surface, lower surface, web, etc.

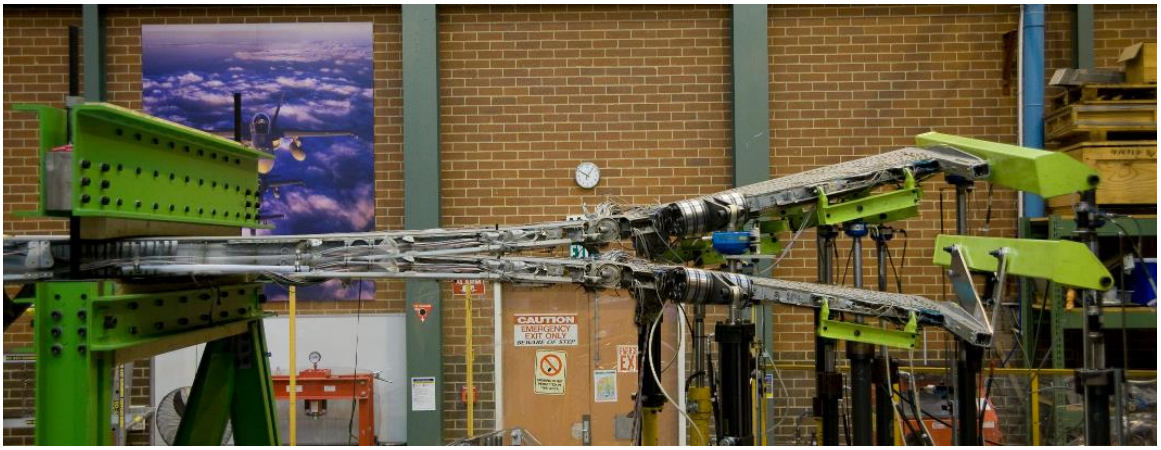

Figure 3 Composite photograph showing the deflections resulting from the maximum wing bending up and maximum wing bending down load cases. A different wing tip loading configuration is required for the wing down bending load cases due to load actuator displacement constraints.

References

[1] FLTLT G. Needham, SQNLDR R. Kloeden, The F/A-18A/B Hornet Outer Wing StAtic Test Program (HOWSAT), proc. Fourteenth Australian International Aerospace Congress, Melbourne, Aust., Mar 2011.

3.2 RAAF C-130J Wing Fatigue Test Interpretation (R. Ogden, K. Maxfield, J. L. Dal Pra [DSTO], SQNLDR L. Pearce and FLTLT W. Scott)

Following the Royal Australia Air Force (RAAF) acquisition of the Lockheed Martin Aeronautics C-130J-30 Hercules an extensive certification compliance finding program was undertaken by the RAAF in order to support the assessment of durability clearance for RAAF representative operations up to the projected planned withdrawal date. The compliance finding program adopted a certification basis appropriate to the role and environment of the RAAF C-130J-30 and in line with the original aircraft design criteria. Ultimately, a series of shortfalls encountered in this certification program led the RAAF to enter into a collaborative C-130J Wing Fatigue Test (WFT) program with the United Kingdom Ministry of Defence. Fundamentally, the WFT program is designed to support substantiation of durability clearance for the RAAF C-130J-30 fleet. However, it is also envisaged that test findings and associated data will support the substantiation of Instructions for Continuing Airworthiness applicable to the RAAF C-130J-30 fleet.

With Marshall Aerospace as the prime contractor, and the Defence Science and Technology Organisation (DSTO) providing technical assurance for the RAAF, the WFT is nearing its sixth year of test cycling. Fifty five thousand flying hours have been completed at Marshall's test facilities in Cambridge, UK (see Figure 1) with an expectation that the test target of sixty two and a half thousand flying hours will be completed by late 2015 or early 2016. Upon completion of this test phase, significant activity will then commence to dismantle, teardown, inspect and

forensically examine the test article for signs of both discrete and widespread fatigue damage. The process of interpreting test damage and translating this into relevant structural integrity management advice is ultimately transferred to the respective RAF and RAAF technical authorities. In the case of the RAAF, this process of performing C-130J WFT Test Interpretation (TI) in accordance with an applicable certification basis is charged to the DSTO (including appropriate support from Australian Industry). The following provides a brief insight into the RAAF C-130J-30 TI process.

Figure 1: C-130J Wing Fatigue Test

Covered in greater detail in [1] the overarching RAAF TI process is presented in the flowchart in Figure 2. Note that this represents a slow crack growth based deterministic damage tolerance analysis approach. Probabilistic based TI analyses will also be considered in subsequent analysis phases.

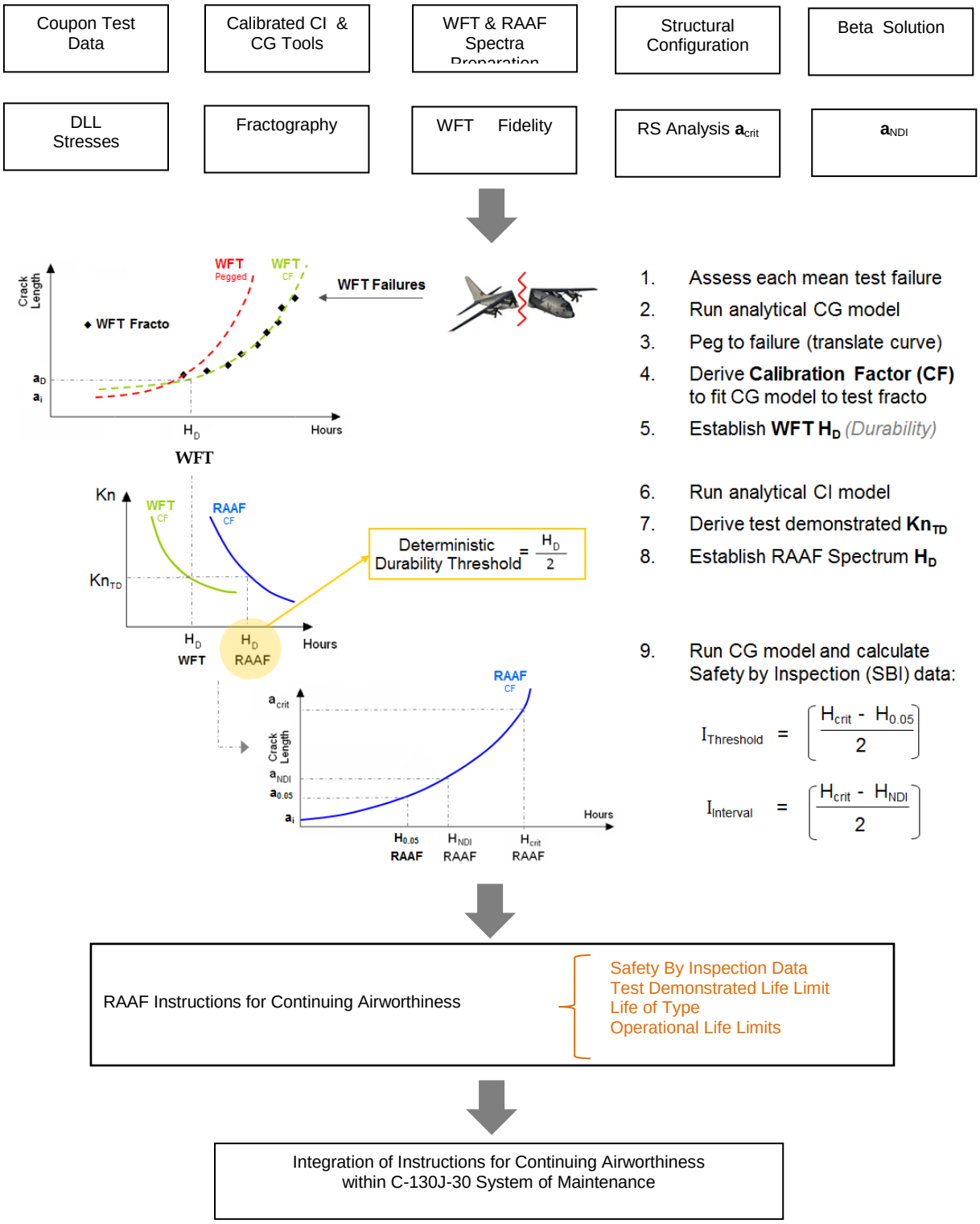

Figure 2: Overarching RAAF C-130J WFT TI Process.

At this stage of the program DSTO is finalising development of the key elements that form the overarching TI process. As such, it is expected that DSTO will be well positioned to interpret test findings and subsequently inform structural integrity management of the RAAF fleet in a timely fashion.

Most significantly, the extensive Al7075-T7351 coupon test program (both crack initiation and crack growth specimens) has been completed in order to calibrate and verify the suitability of the adopted closure based crack growth (CG) analysis tool, FASTRAN and the strain life based analysis tool FAMS. Figure 2 presents an example of the calibrated FASTRAN CG model versus coupon results for both WFT and RAAF spectra.

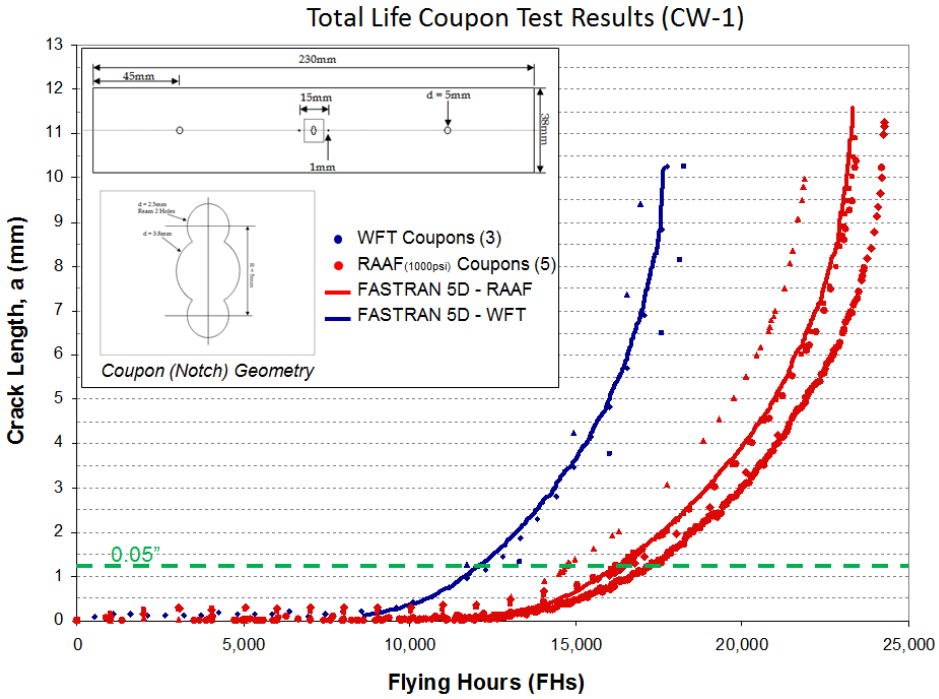

Figure 2: Example FASTRAN vs Coupon Test Results

In addition a significant amount of work has been completed in support of developing tools for building up complex parametric based beta solutions; validating global C-130J FEM for use in supporting TI; developing a RAAF specific spectrum; assessing the representative nature of the WFT spectrum loads; and finally in preparation for the conduct of teardown and subsequent fractographic analyses.

References

[1] Hartley, D. Ogden, R. Maxfield, K. & Meadows, L (2013) Australian Test Interpretation Process Description for the Collaborative Royal Air Force and Royal Australian Air Force C-130 Full-Scale Fatigue Test Program, DSTO-TR-2878, Defence Science and Technology Organisation.

3.3 F/A-18A-D Flaw IdeNtification through the Application of Loads (FINAL) Program, (G. Swanton, DSTO])

2015 marks the 12th year of structural testing of Classic Hornet aluminium alloy (AA) 7050-T7451 "centre barrels" (CBs) via DSTO's "Flaw IdeNtification through the Application of Loads" (FINAL) program. The purposes of the FINAL tests have expanded beyond the original risk mitigation aim for F/A-18s that were to remain in RAAF service without CB changes, to covering a myriad of other goals. These have included: repair testing and certification, life extension, the pooling of results and the demonstration of critical crack sizes, test applications for thermoelastic stress analysis (TSA), novel coating and sensor applications and collaborative modification programs with other F/A-18 operating nations. To date, the test articles have come from the United States Navy, USN (9), Royal Canadian Air Force, RCAF (1), Royal Australian Air Force, RAAF (7) and the FT46 fatigue test article (1). The testing and the following examination of the cracking produced has generated approximately 190 quantitative fractography investigations covering over 1200 individual cracks.

The 18th CB test article is an ex-USN item and has been designated FINAL CB18, see Figure 1. This test is being used to support a collaborative program with the Finnish Air Force which involves fatigue testing of a boron doubler that has been applied to the Y488 bulkhead of the entire Finnish fleet. TSA scans were also conducted on the area with the doubler and the images are shown in Figure 2. Testing of this part of the test article has been completed while the QF investigation and assessment of the doubler has yet to be commenced. A paper on this work has been accepted for presentation at ICAF.

Figure 1: FINAL CB18 in the test rig at DSTO-Melbourne. The circled area shows the area where the Finnish Air Force boron doubler reinforcement was applied. The black paint was for the purpose of conducting TSA scans.

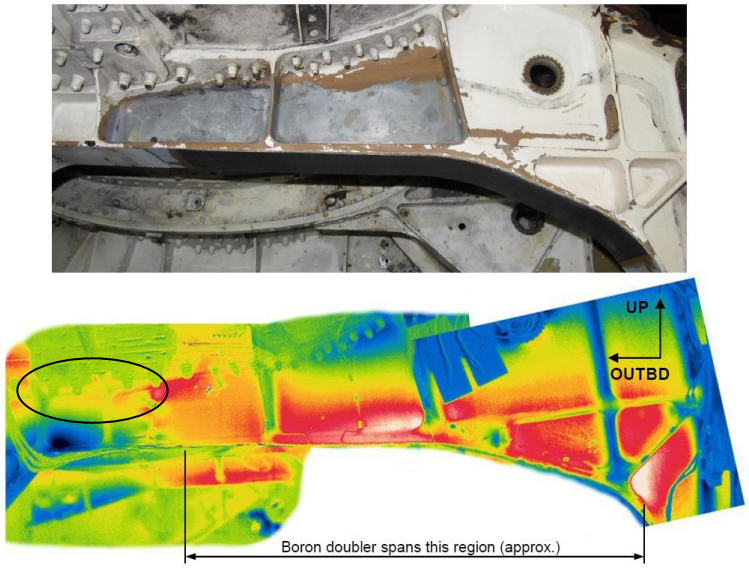

Figure 2: Top image shows a photo looking side on at the Finnish Air Force boron doubler on the lower left hand side of the Y488 bulkhead. The bottom image is a composite of three TSA scans of the same area. The red colour signifies areas of tensile stress and the circled area indicates where the failure point originated.

At the previous ICAF, the FINAL CB19 article was entering testing. Although it has since failed at the Y488 bulkhead, the testing of the remaining bulkheads continues. One aspect of this testing is the assessment of oversizing to damaged fastener holes in otherwise inaccessible locations, in support of a collaborative 'hole salvaging' program with the RCAF, to investigate the fatigue life improvement potential of the oversizing and cold working of holes where crack tips may remain. The rig itself has also undergone a significant modification to facilitate the application of shear loads to the lower Y453 bulkhead, see Figure 3. This change was carried out so as to allow the reproduction of the strains from the full-scale certification test article (designated FT55) at certain critical hotspots, which to date, have not been achievable with the current simple FINAL loading arrangement. The intent is to demonstrate that the loading for this particular area of FT55 was not indicative of the service cracking that has been found to date on retired RAAF CBs.

The FINAL testing is now approaching its end but has been of great use in a number of areas and played a significant role in the Hornet Upgrade Program, resulting in savings of $400M and reducing the impacts of aircraft availability to the RAAF.

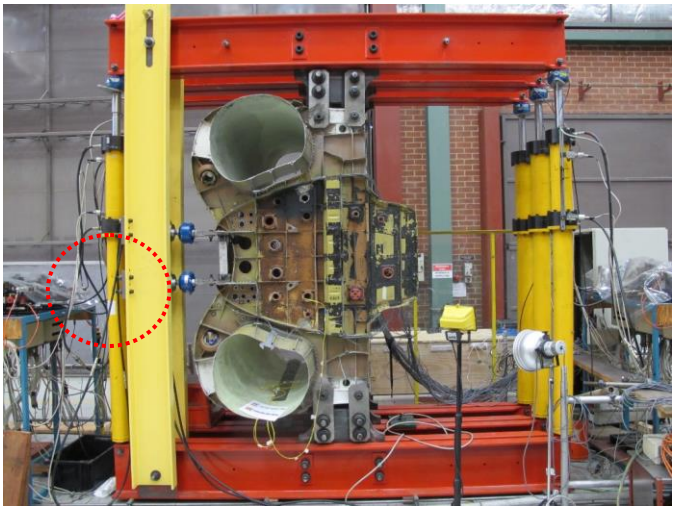

Figure 3: FINAL CB19 in the test rig at DSTO-Melbourne. Note the vertical yellow beams on the left hand side of the rig, which provide the support for the actuators (circled) to apply shear loads to the lower structure of the Y453 bulkhead.

3.4 PC-9/A Empennage and Aft Fuselage Recertification and Life Assessment (PEARLA), (G. Swanton Geoff, R. Boykett, D. Mongru and B. Dixon, [DSTO])

The Royal Australian Air Force (RAAF) operates the world's largest and oldest fleet of Pilatus PC-9 advanced turboprop trainer aircraft. Although a full-scale fatigue test (FSFT) had previously been performed, there were testing deficiencies which were thought to explain why in-service cracking had been discovered earlier than expected, or in locations not identified by the FSFT. Coupled with its fleet leader status, this meant the risk of fatigue failure at the aft fuselage and empennage were higher than desired. This led to the establishment of a collaborative effort between the RAAF, the Defence Science and Technology Organisation (DSTO) and Industry, called the PC-9/A Empennage and Aft Fuselage Recertification and Life Assessment (PEARLA) program. The aim of PEARLA was to provide information to mitigate this risk and allow operations to safely continue beyond 30 years of service.

PEARLA involved a ground and flight test program using an extensively instrumented operational loads monitoring (OLM) aircraft to identify and quantify loads associated with the most severe manoeuvres in the flight envelope. The 'ground' component activity comprised of a loads calibration test (Figure 1) and a ground vibration test and ran from January to April 2013. This was followed by an 'edge of the envelope' flight test program conducted over the July to October 2013 period.

Figure 1: PC-9/A OLM aircraft during ground load calibration testing

A detailed structural unified finite element model (UFEM) was developed specifically for PEARLA, and was validated using the ground calibration loads (Figure 2). Together with the acquisition of data at the extremes of the flight envelope, this provided the unique ability to conduct sophisticated structural fatigue analyses accounting for both dynamic (buffet) and lower frequency manoeuvre loads on the aft fuselage and empennage.

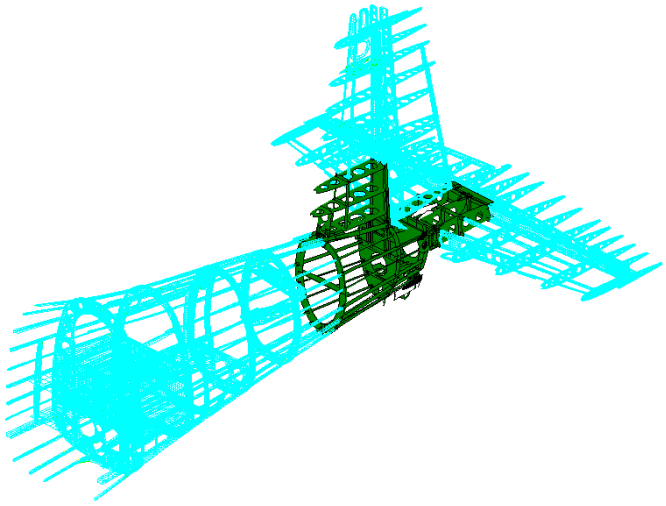

Figure 2: PEARLA UFEM with core structural region coloured in green.

The analyses involved a UFEM static stress analysis of 335 individual points in the sky representing extreme loads (including buffet) measured during the flight test program. The maximum stress resulting from any load condition was calculated for each element. The thin skins were not included in the analysis to avoid the complicated analysis needed to account for skin buckling and because they are easily inspected.

The UFEM was then used to generate stress sequences for each of the severe manoeuvres before a fatigue life was calculated for each of these stress sequences using the engineering Crack Initiation (CI) fatigue prediction methodology as outlined in Ref. B. In this manner a fatigue life was calculated for each element and those locations with fatigue lives below a chosen threshold

life, which accounted for uncertainties of the analyses methods and the requirements of the PC-9/A structural certification basis (DEFSTAN 00-970), were identified as potentially fatigue critical.

Locations identified as potentially fatigue critical were assessed against: the extant safety by inspection (SBI) program, replacement and modification programs, FSFT results, past service findings, previous assessments of component safety criticality, and the requirements of DEFSTAN 00-970. As a result of this review, 67 new locations were recommended for targeted inspection.

The PEARLA program enabled a thorough assessment of the PC-9/A fatigue life management, leading to revised inspection practices for important structural locations. These actions enhance the ability of the RAAF to safely manage the fleet to its Planned Withdrawal Date.

References

[1] Dixon, B., Mongru, D., Boykett, R., and Bandara, S., Assessment of RAAF PC-9/A Empennage and Aft Fuselage Fatigue Management for the PEARLA Program, DSTO Report DSTO-TR-3059, Dec. 2014.

[2] Quaranta, D., *PEARLA Phase 1 Fatigue Analysis Methodology*, Pilatus Report TM-09-000018, 16 June 2013.

3.5 The development of bar-coded marker band load sequences to enhance fatigue test outcomes (Burchill, Barter, McDonald [DSTO], Jones [Fortburn])

Crack growth data, from element, component or full-scale fatigue testing with the design loading spectrum is a fundamental input into validating predictive models used to monitor the accural of structural fatigue damage of many modern aircraft during service. Identifying, measuring and assessing fatigue cracks generated during testing therefore is of critical importance to aircraft operators, such as the Royal Australian Air Force (RAAF), to maintain aircraft structural integrity for the life of an airframe. The Defence Science and Technology Organisation (DSTO) commonly utilises a test enhancement methodology to mark the fracture surface of fatigue cracks, assisting in the accurate and rapid determination of crack lengths post-test. With recent improvements in the understanding of fatigue crack growth, DSTO has proven a new method by which these marks can be *bar-coded,* successfully in a range of coupon and full-scale test programs [1].

Researchers, when trying to make particular marker bands unique typically use a few (i.e. typically between one and ten) large amplitude load cycles to create individual striations, an example is shown in Fig. 1a [2]. However, accurate measurement of crack depth then relies upon counting the individual striations, which is often difficult and time consuming and usually not possible when the crack is small. The new bar-coded marker band method presented here utilise hundreds of load cycles, or *sub-blocks,* of constant amplitude (CA) each with stress ratio ($R = \sigma_{min}/\sigma_{max}$) that varies markedly from the adjacent sub-blocks, although each sub-block has the same maximum load. Such changes in the loading have been observed to change the crack path to create distinct, contrasting patterns [3]. An example of this approach is shown in Fig. 1b,

where the consecutive CA sub-blocks produce crack path changes that are visible under optical and electro-optical (as shown in Fig. 1b) microscopy.

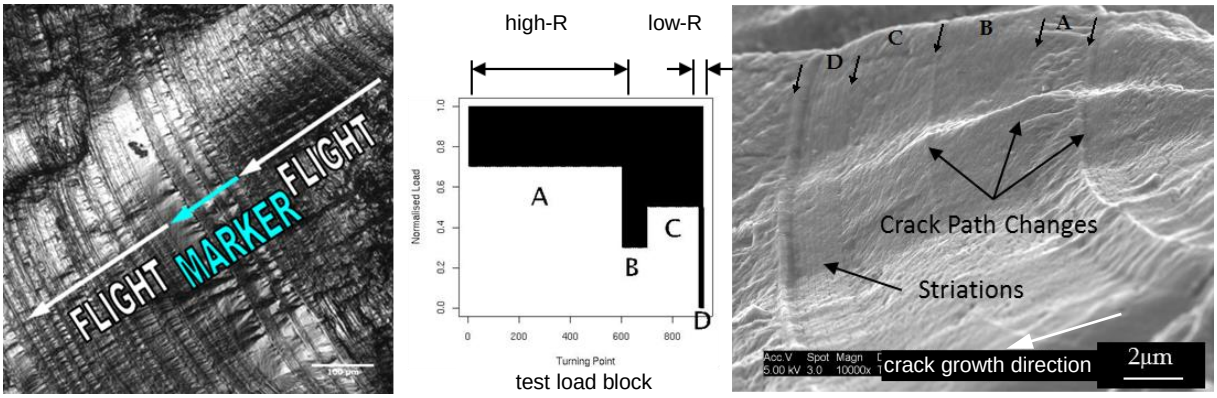

(a) (b)

Fig. 1: (a) Example of a striation-based marker band from [4], (b) example of marker band based on changes in the crack path due sub-blocks of loading with various R values [1].

The current research has extended this concept of using crack path changes, to develop a series of individual *bar-coded* marker bands, which have been successfully used on two common aircraft alloys: aluminium AA7050-T7451 and titanium Ti-6Al-4V [4-6], tested with a range of combat, transport and helicopter variable amplitude (VA) spectra. Examples of six of these bar-coded marker band load sequences are shown in Figure 2a, which produce crack growth that differs significantly from the VA crack growth, seen clearly in examples in Figure 2b and Figure 2c for aluminium and titanium alloys. From these features crack growth measurements can be made and definitely ascribed to the test time at which each marker band load sequence was applied. Since these bands are not as restricted by limitation of the observance of single striations, this method can result in accurate growth information for fatigue cracks over a large range of crack depths; and down to very short depths, <0.5mm in aluminium and <1mm in titanium alloys tested in this program.

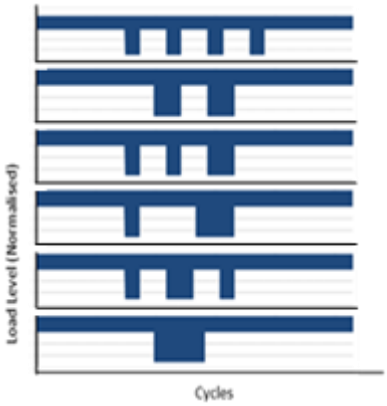

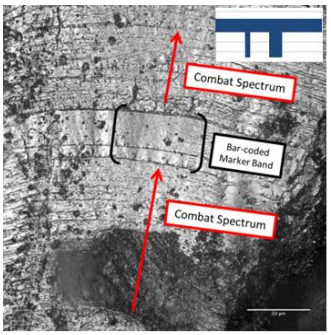

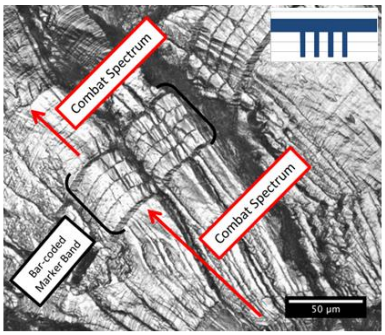

(a) (b) (c)

Fig. 2: a) Six individual bar-coded marker bands load sequences with sub-blocks of high-R and low-R CA loading, and images of marker bands as they appear on fracture surfaces in b) titanium alloy at crack depth of 1.63mm, (c) aluminium alloy at crack depth of 1.55mm

The design parameters of each marker band load sequence set typically require some fine-tuning, in the number of cycles and the maximum load level, depending on the spectrum and the test material. For coupon tests, as the stress level of the test spectrum of interest varies, it was found that the number of cycles and maximum load of the marker bands also needed to be altered. For instance, the choice of high-R and low-R cycles may not remain the same for all stress levels for the same spectrum depending on the purpose of the particular test. For full scale testing, where critical fatigue locations maybe unknown, the marker band load sequences are designed to result in between 5-10% of the crack growth of a highly stressed location failing within a given number of lifetimes of loading, typically three. As well as the extent of marker band growth, it is important to ensure that the loads of the marker band sequence do not invalidate or compromise the results from the test spectrum by inducing retardation or accelerated growth. (For this reason the marker band sequences are applied at a lower constant peak than the test spectrum's peak.) To address the finer aspects of the tuning, a set of guidelines [1] for marker band development has been proposed however more work is being carried out to investigate if a general relationship between successful marker band load sequences and test spectra can be derived.

References

[1] Burchill M, Barter S, McDonald M, Jones M. The development of bar-coded marker band load sequences to enhance fatigue test outcomes. *Australian International Aerospace Congress AIAC1*6, Melbourne, 2015

[2] Barter S, Molent L and Wanhill R. Marker loads for quantitative fractography of fatigue cracks in aerospace alloys. *25th International Congress on Aeronautical Fatigue Symposium, ICAF,* Rotterdam, 2009.

[3] White, P., Barter, S. A. and Wright, C. Small crack growth rates from simple sequences containing underloads in AA7050-T7451. *International Journal of Fatigue,* vol 31, pp 1865-1874, 2009

[4] McDonald M, Boykett R and Jones M. Quantitative fractography markers for determining fatigue crack growth rates in aluminium and titanium aircraft structures, *International Congress of the Aeronautical Sciences, ICAS2012,* Brisbane, 2012.

[5] Burchill M, McDonald M, Boykett R and Jones, M. Development of Marker Bands for Inclusion into the Full Scale Durability Testing of the JSF Conventional Take Off and Landing Variant Horizontal Tail. DSTO Technical Report DSTO-TR-2925, 2013.

[6] Burchill M, Walker K, Barter S, Wang C, and Khadka, A. Improvements to predicting fatigue crack growth rates in aluminium alloy (AA7050-T7451) loaded with a standard transport aircraft spectrum. *International Conference on Structural Integrity and Failure, APCFS-SIF*, Sydney, 2014.

3.6 Calibration and verification of analytical crack growth and fatigue life tools for use with helicopter spectra (P. Jackson, B. Krieg, W. Hu [DSTO])

Analytical crack growth and fatigue life prediction tools are key inputs to all stages of the fatigue management methodologies for conventional fixed wing aircraft, including the design and interpretation of full scale fatigue tests (FSFTs). DSTO has sought to evaluate the effectiveness of two analytical tools; FASTRAN [1] (an internationally recognised crack growth model) and FAMS [2] (a strain-life fatigue model), which have been extensively used at DSTO in support of fixed wing aircraft, when applied to materially different helicopter spectra, in this case spectra derived from flight test for a location on the helicopter airframe in the vicinity of the cabin roof. These studies have used experimental coupon test data to calibrate, verify and validate crack growth and fatigue life estimations using the FASTRAN and FAMS analytical tools as implemented in DSTO's CGAP software [3]. This experimental data was sourced from a companion spectrum truncation validation and verification coupon test program performed on 7075-T7351 aluminium consisting of some 24 centre cracked and notched (central hole) coupons [4].

Crack Growth Predictions

A calibration of FASTRAN was developed by optimising the *threshold* and *constraint loss* models of FASTRAN to minimise the error between prediction and experiment for a selected truncation load level. Using the most recently obtained crack growth rate data obtained for 7075-T7351 material, including emphasis on data in the threshold region, the model successfully predicted crack growth rates for long cracks, i.e. > 1mm) for all other truncation levels examined. The model was then extended to produce a probabilistic, full life model to predict the complete experimental fatigue lives for notched coupon test data. This model used the (0.025, 0.975) quantile values of an equivalent initial flaw size (EIFS) distribution (i.e. the input initial discontinuity size to produce a specified life) to produce crack growth predictions that would theoretically bound 95% of the experimental data. This model successfully captured the variation in fatigue lives of the coupons for the majority of truncation levels; however relied on an EIFS distribution that was significantly different from the published, physical initial flaw size distribution for similar material. This discrepancy was attributed to limitations in geometric assumptions about the crack front, and errors associated with the original calibration.

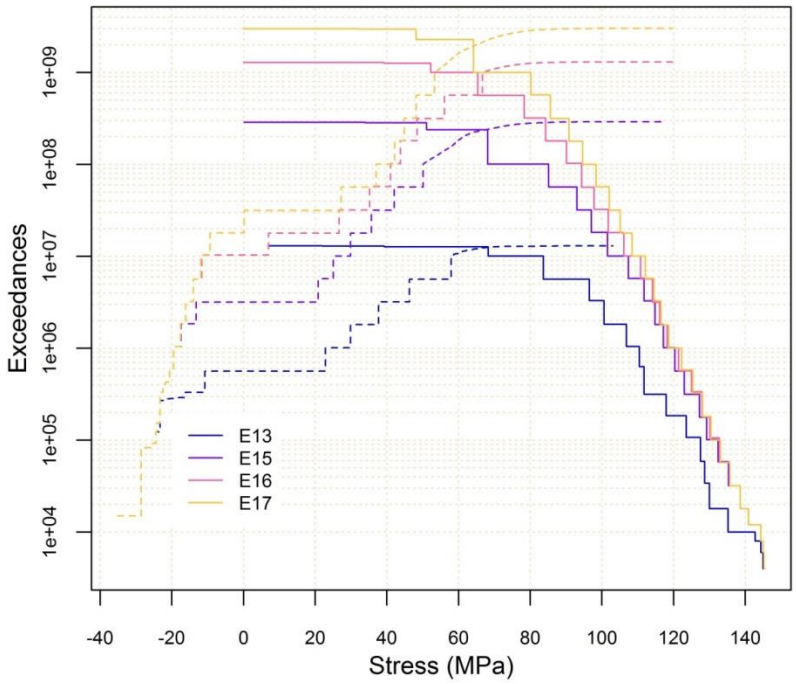

Figure 1: The various spectra used for the spectrum truncation study. Note; the spectra are for 100 flight hours and the large number of exceedances reflect the combination of manoeuvre and vibratory cycles present on a helicopter airframe.

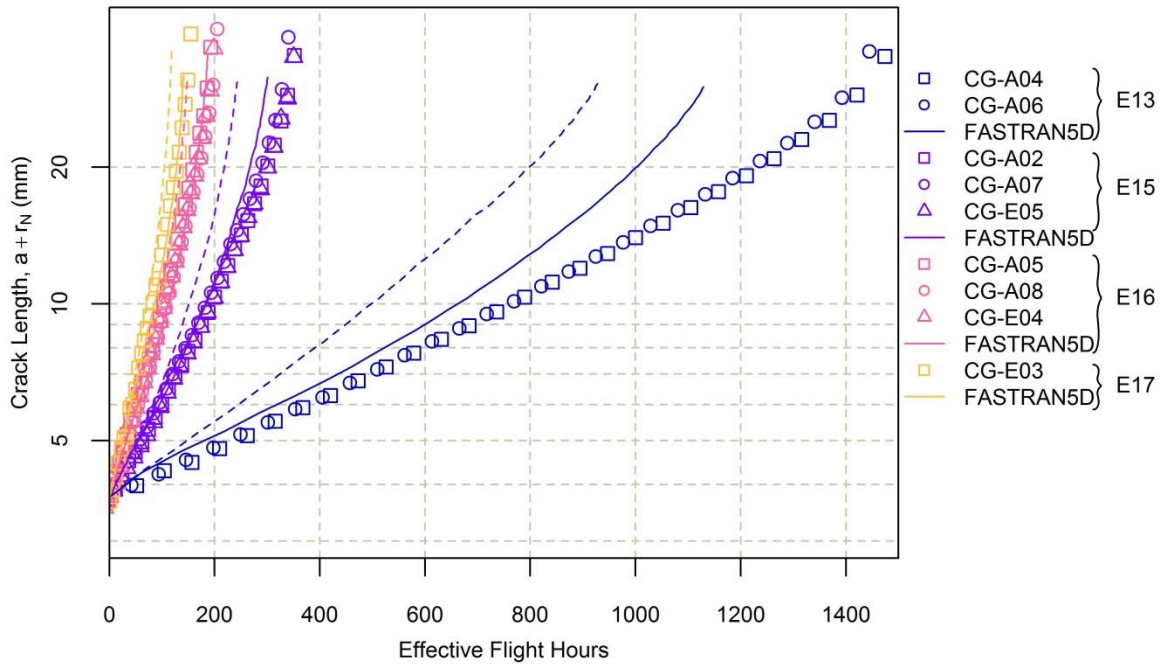

Figure 2: Comparison of prediction (dotted lines prior to calibration, solid lines after calibration) to experiment

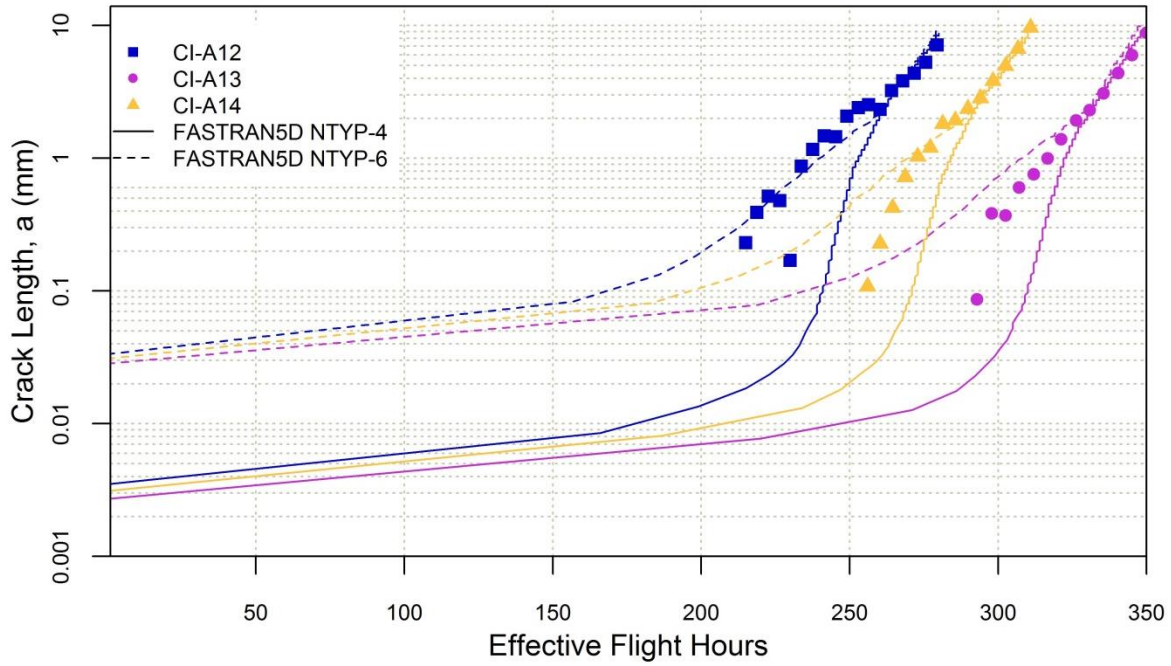

Figure 3: FASTRAN predictions for three coupons at one truncation level showing the different equivalent initial crack sizes resulting from assuming a through thickness crack shape (solid lines) and a semi-circular surface flaw (dotted lines)

Fatigue Life predictions

In its current form, the FAMS code was unable to sufficiently differentiate between fatigue lives for load sequences corresponding to different truncation levels. The input material strain-life data was limited to a maximum life of 10^7 cycles, beyond which the code assumed zero damage. In the absence of more comprehensive strain-life data, a *working* strain-life curve was developed for input in the FAMS curve by developing a numerical optimisation routine that could minimise the analytical and experimental errors on the basis of varying the strain-life relation. This methodology provides a method where a material strain-life curve can be produced from variable amplitude testing. The resulting material curve deviated from the published values indicative of a number of as yet unresolved issues inclduing a possible breakdown in the equivalent strain relation used to interpret the material strain-life curve and the distribution of loads (strain amplitudes) resulting in non-uniform weighting across the working curve. Careful examination of alternative material curve parameterisations, equivalent strain relations and additional spectra with different cycle distributions were recommended to further improve the FAMS model.

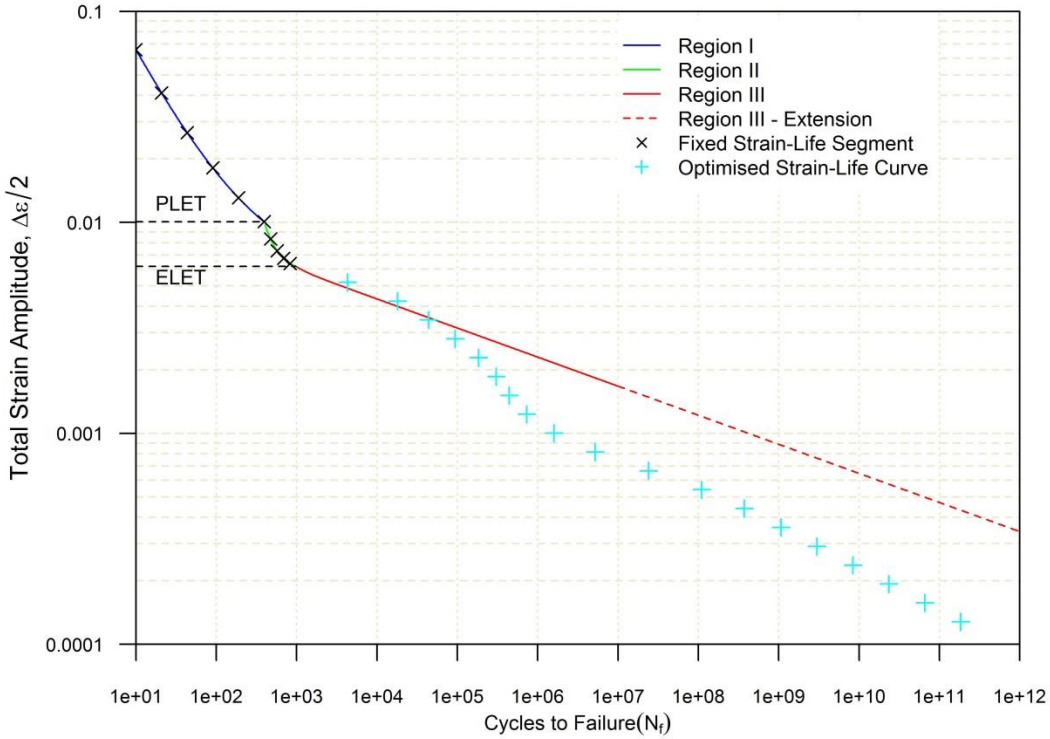

Figure 4: Optimised "working" strain life curve (blue crosses) derived from the coupon test results showing the departure from the published material curve (solid red line)

The studies documented in [5] suggest that the current generation of the FASTRAN crack growth tool is sufficiently mature for application to helicopter analytical and test spectrum development; while the FAMS fatigue life estimation tools have significantly limited utility and requires further development.

References

[1] James C. Newman, J. (1992) FASTRAN-II - A Fatigue Crack Growth Structural Analysis Program. 104159, National Aeronautics and Space Administration.

[2] Fatigue Analysis of Metallic Structures (FAMS) - A computer Program to Calculate Fatigue Damage by local stress/strain approach. (1995) Naval Warfare Center.

[3] Wallbrink, C. and Hu, W. (2010) A Strain-Life module for CGAP: Theory, User Guide and Examples. DSTO-TR-2392, Melbourne, Defence Science and Technology Organisation.

[4] Krieg, B. and Forrester, C. (2014) Coupon Test Program in Support of HAFT-TD Spectrum Vibration and Fatigue Life Estimation Tools. DSTO-TR-XXXX, [Technical Report in publication] Melbourne, Defence Science and Technology Organisation.

[5] Krieg B. & Jackson P., HAFT-TD: Calibration and verification of analytical crack growth and fatigue life tools for use with helicopter spectra. DSTO-TR-XXXX, [Technical Report in publication] Melbourne, Defence Science and Technology Organisation.

3.7 Hardware-in-the-Loop integrated Fatigue Test Simulation (HiLiFTS) (Albert K. Wong, DSTO)

The importance of metal fatigue was recognised in the early 1800s by European engineers such as Albert and Poncelet. However, the first systematic investigation on this subject was attributable to Wohler in 1860, who introduced the now universally recognised S-N curve. Wohler's contribution is hugely significant in that, for the first time, it gave engineers a predictive capability of component lives for their designs. Over the next two centuries, progressively sophisticated models have been developed, such as those to account for mean-stress, variable load amplitudes, cyclic effects, local plasticity and closure, threshold effects and multi-axial loads. However, all of these phenomenological models, which are at best augmented by quasi physics-based variations, amount to little more than curve fitting exercises. As such, robustness is often difficult to assure and limitations in their predictive capabilities are abound. This is particularly true when they are used in an extrapolative sense rather than an interpolative one – e.g., predictions in the threshold regions using long-crack data, or calculations for built-up structures under complex loads using uniaxial coupon data. From this perspective, the idea of a virtual fatigue test (Ostergard & Ibbotson [1]) to qualify an aircraft is far from reach. In fact, a NATO paper titled "Qualification by Analysis" [2] that advocates increasing reliance on analysis as a practical means to constrain program costs, concedes that:

"… Full Scale Fatigue Tests (FSFTs) continue to produce premature fatigue cracking, demonstrating the current inadequacies of the fatigue analysis process. Until a time is reached when FSFTs do not reveal significant premature failures or cracking, designers and regulators alike will not have enough confidence in analysis methods to allow deletion of full scale testing."

At the other end of the modeling spectrum, the advent of high power computers have enabled truly physics-based fatigue models to be developed on the atomic scale (White [3]). However, due to their gargantuan degrees of freedom at this scale, these models are invariably limited to idealised materials, tiny solution volumes and small number of load cycles. Whilst these models are extremely useful in shedding new light on our understanding of fatigue mechanisms, their prospective use to certify aircraft is equally unrealistic in the foreseeable future.

In this paper, a new concept is introduced that straddles these two extremes and could well have significant impact. The so-called Hardware-in-the-Loop concept is one that is much used in the field of dynamic systems or weapons modeling in which the actual critical component of interest (one that is often the most difficult to model) is integrated into the simulation. When an FSFT is conducted to certify an aircraft, we can be confident that all of its gross loading and deformations can be modeled accurately by well-known tools such as finite element analysis. If anything, finite element models (FEMs) can provide greater degrees of freedom and thus match actual flight loads better than is possible using a limited number of physical loading jacks. What cannot be confidently assured in models are: no over-simplifications compared to the real article, and importantly, the accurate prediction of fatigue behaviour at critical locations, particularly the earlier stages of fatigue that include crack initiation and propagation in the threshold regime. Both of these issues are effectively addressed if the critical regions of the model are substituted with the actual articles. Conceptually then, imagine that an FSFT is replaced by an FEM of the aircraft in which its critical regions are replaced by the actual parts, or hardware – thus the coined term Hardware-in-the-Loop integrated Fatigue Test Simulation (HiLiFTS). In reality, the hardware are separately tested by laboratory rigs in which the loading

conditions are determined by the FEM. Two challenges remain to be tackled, viz., i) ensuring all critical parts have been identified and ii) being able to apply complex boundary loads on structural parts. The introduction of DSTO's microbolometer thermoelastic stress analysis (TSA) technology (Wong [4]) has effectively paved the way to solving i, and whilst ii will not be trivial, neither will it be insurmountable as there are current technologies that can offer solutions (e.g., multi-axial test machines, piezoelectric actuators, robotic manipulators). A schematic diagram of the HiLiFTS concept is shown in Figure 1 below.

This concept includes the following significant benefits:

1. Because TSA is highly sensitive, the FSFT requires only small applied loads (typically only 10% of DLL) and it is anticipated that such tests need to be conducted only over a few weeks before all hotspots have been identified, the test article could then be returned to the production line thus resulting in no wastage of an airframe.

2. Related to the above, more than one FSFT article can be assessed, thus allowing a greater sampling representation compared to the current one test article approach.

3. Because of the much reduced size of test components, tests can be run at much greater speeds, say 20Hz cf. 0.5Hz (typical of FSFTs). This 40 fold increase in speed could potentially compress a typical 10 year test program to just 3 months!

4. Although there will be multiple component tests, these can be conducted in parallel and be widely distributed (to a number of sub-contractors around the world if necessary), thus spreading the effort and risks.

5. Similar to #2 above, #4 allows repeated tests of the same location, thus allowing greater sampling representation compared to the present.

These advantages mount a strong business case that could revolutionize the future of certification testing, and DSTO is embarking on a program to demonstrate this concept.

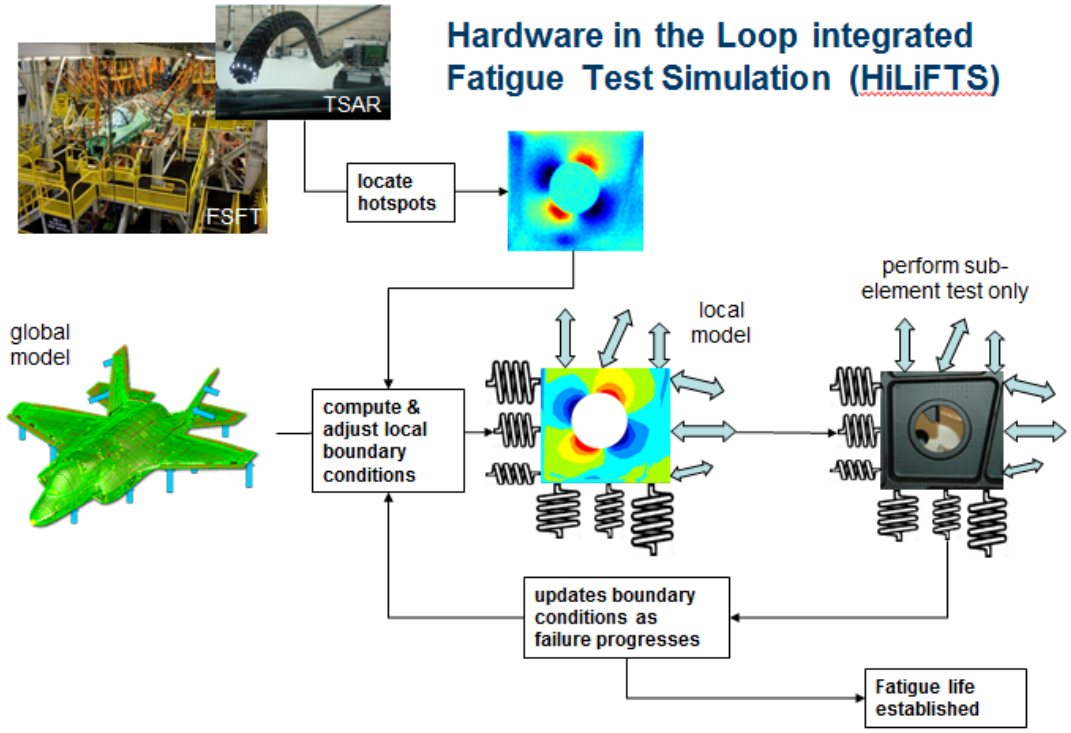

Figure 1: Schematic diagram of the HiLiFTS concept

References

[1] Ostergaard, M.G., Ibbotson, A.R. "Virtual testing of aircraft structures", CEAS Aero J, 2011, 1:83-103.

[2] NATO RTO "Qualification by analysis", NATO-RTO Rept, 2009, RTO-TR-AVT-092 AC/323(AVT-092)TP/229.

[3] White, P. "Molecular dynamic modelling of fatigue crack growth in aluminium using LEFM boundary conditions", Int. J. Fatigue, 2012, 141-150.

[4] Wong, A.K. "Seeing the invisible: Taking a look at stresses in aircraft fatigue analysis and testing", Proc. 27th ICAF Symposium, Jerusalem, 2013, 247-259.

4. IN-SERVICE STRUCTURAL INTEGRITY MANAGEMENT

4.1 Fatigue Analysis of a Virtual Airfram Structure (Chris Wallbrink, Michael Opie and Xiaobo Yu [DSTO])

Recently DSTO completed a program of work to help identify possible fatigue critical locations in the aft fuselage of the PC-9 trainer aircraft to supplement fleet condition data and past information gained through a full scale fatigue test [1]. The program aimed to deliver information to identify additional possible locations susceptible to fatigue and was conducted with limited time and significant budgetary constraints. This paper utilizes results obtained through this work program to assess the practicality of a virtual full scale fatigue test (FSFT). The virtual FSFT is appealing in potential cost savings, but relies heavily on the accuracy of the analysis.

A distributed fatigue analysis was performed over the entire finite element model of the PC-9 in an attempt to better identify fatigue critical locations as opposed to previous methods of ranking locations based on peak stress information. The identical FSFT load spectrum that was applied through the 25 jacks during the FSFT was applied to the finite element model. Every element in the model was analysed using the strain-life approach to determine a relative fatigue index to rank locations. For simplicity a multi-axial critical plane search was conducted for each element. The purpose of the critical plane search was to identify the plane which produces the minimum fatigue life and the likely crack initiation orientation. A number of control points were chosen in the analysis to serve as metrics on which to assess the methodology. These locations were chosen based on observed fatigue cracking in the FSFT and fleet.

One of several fatigue critical locations that will be discussed and was identified during the FSFT was the forward fin attachment shown in Figure 1. This figure also shows a comparison of the identified fatigue critical elements in the model and the eventual damage observed from the FSFT. The results appear to indicate a good qualitative relationship with the observed fatigue cracking in the FSFT and areas of high fatigue index in the model.

A globally refined finite element model has been used in conjunction with a strain life methodology to identify locations susceptible to fatigue. It has been demonstrated that the method does provide a qualitative correlation where fatigue is known to have occurred in the full scale fatigue test. This paper discusses the performance of the present methodology relative to several fatigue critical locations identified during the FSFT. Further, the paper discusses some advantages and disadvantages of this approach and what future work could be conducted to improve the outcomes of the analysis.

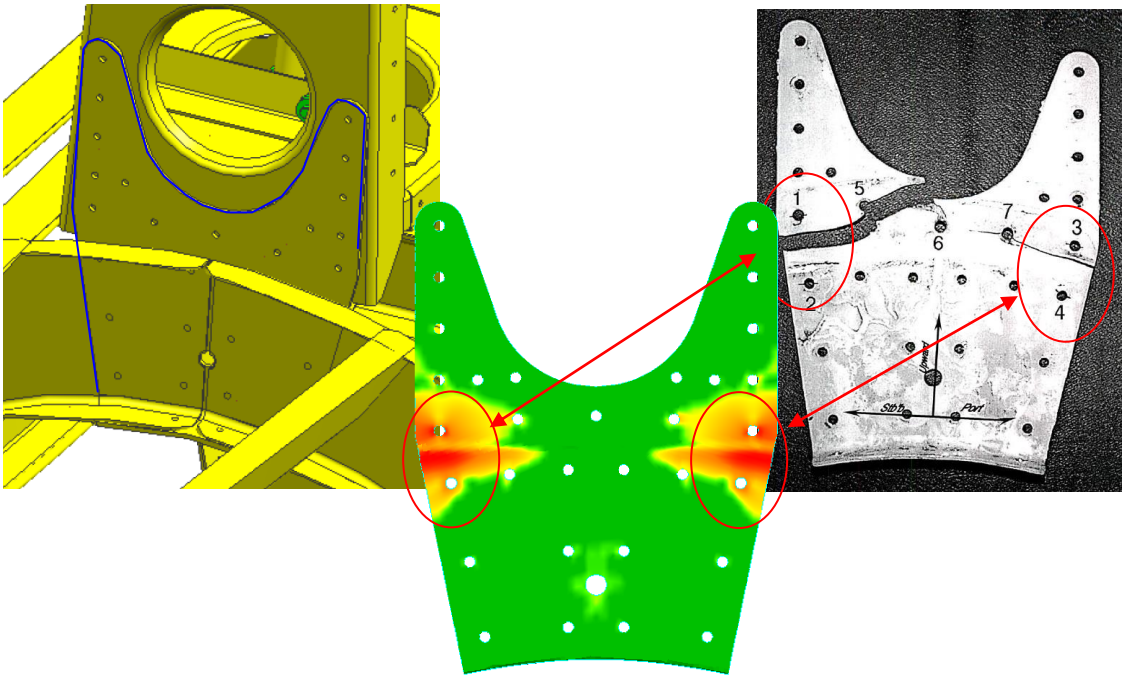

Figure 1: Comparison of the analysis and the forward fin connection strap that was removed at 100,000 flight hours in the FSFT

References

[1] C. Wallbrink, M. Opie and X. Yu,. Fatigue Analysis of a Virtual Airframe Structure. In. ICAF 2015, Helsinki, Finland: 1-5 June 2015.

4.2 Flight Manoeuvre Recognition (FMR) (Lieutenant N. Sethi [DGTA – ADF]).

Aircraft structures degrade over time as a result of fatigue and environmental induced degradation. Helicopters have many structural components in their dynamic systems that are life-limited by fatigue strength considerations. Replacement of fatigue life-limited structural components is determined using a safe-life methodology – which defines the life being reached when risk of fatigue failure is considered unacceptable[1]. This article discusses the aspects of improving fatigue management through an enhanced usage monitoring system which is a fundamental element to the Aircraft Structural Integrity Program (ASIP). Other elements are briefly discussed to provide the overall framework of the ASIP with a focus later in the article on improvements to the usage monitoring system using FMR.

Background

There are several elements which make up the ASIP and are shown in Figure 1 below. The scope of this article will mainly focus on Usage Monitoring (UM) and Fatigue Management (FM).

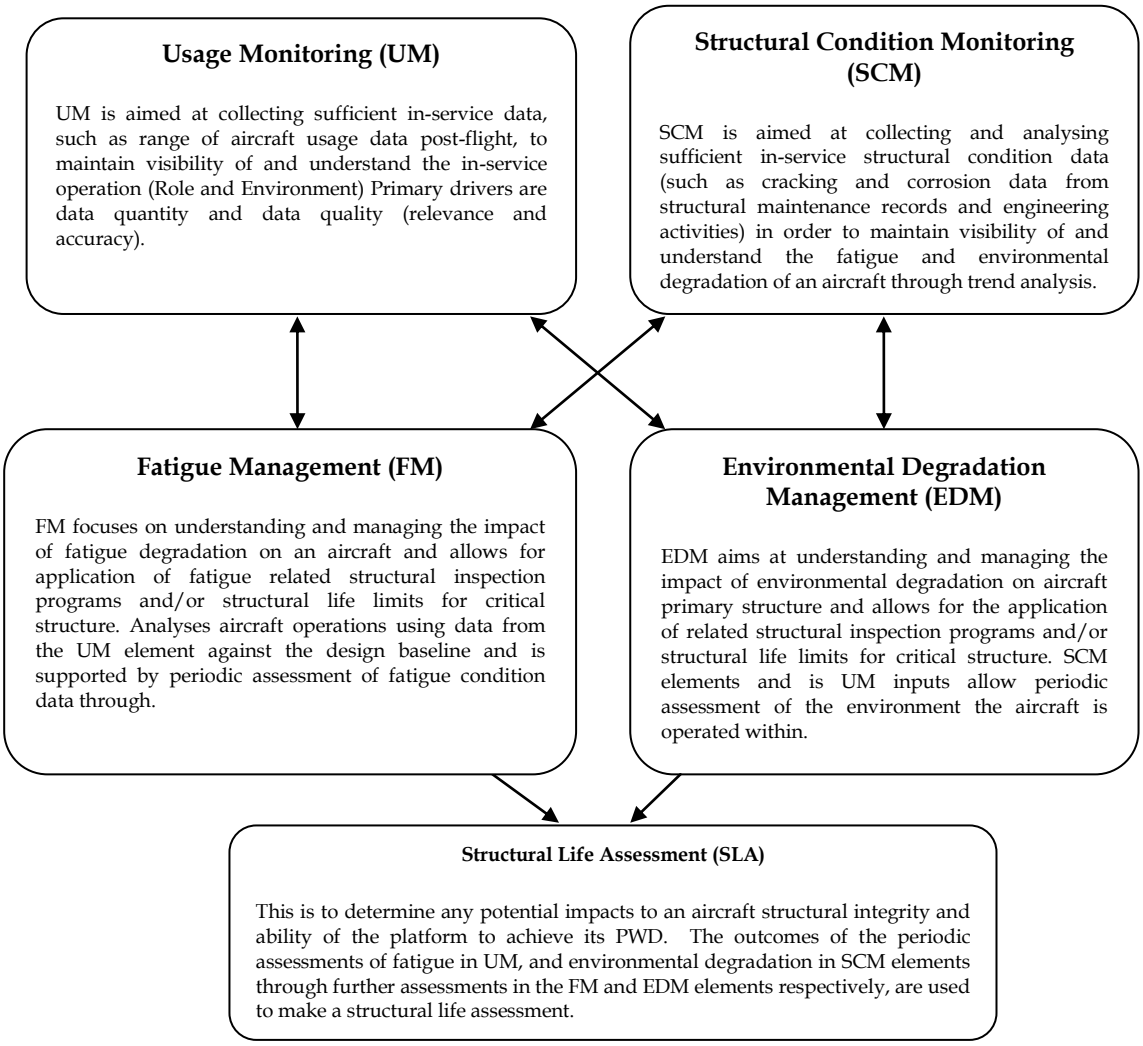

Figure 1 - Aircraft Structure Integrity Program information flow (from Reference 2)

FM allows for the identification, and reduction of risk of an aircraft structural failure through understanding and managing the impact of fatigue degradation. Most aircraft platforms have their structural life limits calculated through a fatigue damage hypothesis (predominantly Miners rule) from a combination of design Usage Spectrum (DUS) and design loads using stress-life (S-N) curves developed through a series of component fatigue tests and curve shapes based on extensive material testing[3]. DUS are generally structured, and produced by the OEM, to conservatively account for the most fatigue damaging manoeuvres through a 'worst case' approach, while loads may be applied through block loading, cycle counting, pro-rating or a combination of both.

Depending on the measured loads utilised and the endurance limit of the S-N curve used, each component will have a differing number of manoeuvres in the DUS that are considered to

accrue fatigue damage. These manoeuvres are known as the fatigue drivers for that component. Ideally, the in-service assessment of the validity of a component structural life limit would be based on the periodic assessment of the difference between actual in-service usage and the baseline DUS for each of the fatigue drivers for that component. This is based on the assumption that the design loads and material properties remain unchanged. A diagrammatical representation relating DUS, FM and UM is shown in Figure 2.

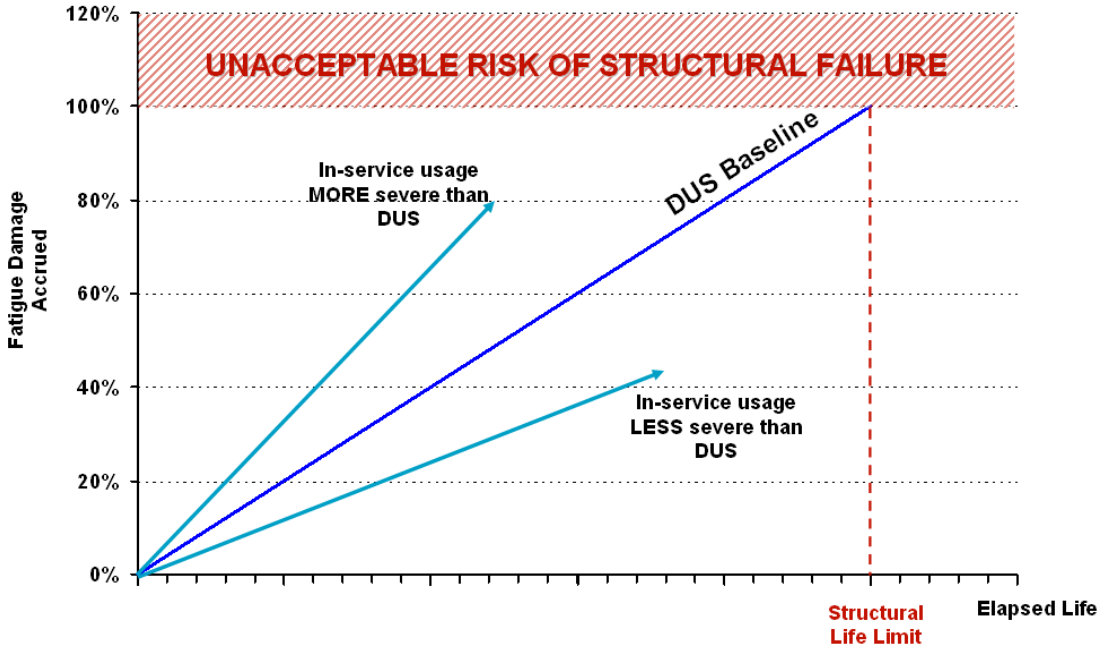

Figure 2 - Basic Fatigue Assessment Chart (From Reference 3)

An ideal UM system would capture load versus time to allow direct comparison against the S-N curves. However, noting the difficulty of implementing this, a practical solution would be to record all fatigue damaging regimes instead which would be used to determine the usage severity of fleet operations by comparing it to the DUS. Current rotary wing platforms UM systems are not at this level. QinetiQ's investigation into the current usage monitoring system identified that circa 30% of fatigue damage is captured across Rotary Wing platforms (32% and 57% on Blackhawk and Seahawk respectively, see References 5 and 6). Helicopter Structural Integrity – Directorate General Technical Airworthiness (HSI-DGTA), as the Aircraft Structural Integrity managers, moved to investigate other options for improving this value. The UM System was implemented through use of form EE360, which is a paper based form. The EE360 system is reliant on pilot recollection and, as such, the accuracy of the information recorded on the EE360 for many parameters may be questionable. This is due to either the frequency with which the events occur (eg. large control reversals), the likelihood that the pilots recognise the event is occurring (eg. 1.5g Pull-Up or Droop Stop Pounding) or the difficulty associated with accurately measuring the period for which the event occurs (eg. percentages of flight time in various altitude/airspeed bands). Identification of errors or omissions on these forms has led HSI-DGTA to incorporate the functionality of the EE360 form within CAMM2. This has allowed for the hard coding of rules to prevent omissions and some of the errors that have impacted the UM System.

The SCM System is an important input into the FM System, because an integral assumption during design is that components are pristine components free from any condition defect.

However, due to degradation, a continuous assessment of their condition is required to allow ongoing validation of this assumption. The basis of the SCM System is the requirement for good quality and quantities of data on the condition of the aircraft that lend itself to analysis. Condition data currently analysed is generally of low quality, making it difficult to analyse and draw meaningful conclusions. Further work is being conducted to ensure the quality of condition data is markedly improved to allow better trend analysis to ensure accurate capture of any degradation of critical components.

Proposed solution

Flight Manoeuvre Recognition, also known as Regime Recognition, is the process of analysing automated data collection systems, such as the Crash Data Recorder (CDR) on S-70B-2 Seahawk and S-70A-9 Black Hawk, that record flight performance data to assess the characteristics, including manoeuvres and regimes flown, for a particular flight. FMR software incorporates a set of algorithms to recognise a wide array of DUS manoeuvres/regimes. The data analysis is automated and summarises In-Service Usage in a format directly comparable to the DUS. It supports the extant UM capability for both Seahawk and Black Hawk.

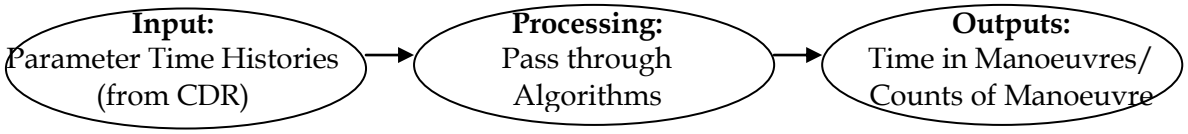

Figure 3 – Simplistic representation of FMR methodology

FMR development for the Seahawk platform was through the use of a software application utilising the Seahawk manoeuvre recognition algorithms originally developed by Raytheon Australia[4], for the purpose of identifying S-70B-2 DUS regimes in data downloaded from the CDR. Raw CDR data is downloaded directly from the aircraft and is processed through the Flight Data Systems Sensor Test and Replay System (STARS) application. STARS laptops output CDR data in a standard text format, with parameters converted to engineering data with units. These output files are then processed using QinetiQ modified manoeuvre recognition algorithms. Manoeuvre recognition algorithms provide a means of recognising occurrences of different flight manoeuvres via automated processing of flight data. Initial study was primarily to assess the fidelity of data recorded on EE360 forms against a sample of Seahawk CDR flight data. CDR flight data is however of varying quality. Seahawk CDR data reviewed contained many data inconsistencies for most of the parameters recorded. These included spikes, interruptions or malfunctioning signals. Data was manually pre-conditioned by signal improvement (i.e. removal of data spikes) and data interpolation prior to being entered into the initial FMR software version in order to better enable its processing through the algorithms. No further improvements were considered or actioned for the Seahawk platform due FDR data quality issues and the benefits of further V&V was not justifiable from a return on investment perspective noting its Planned Withdrawal Date (PWD) of 2017. Recent efforts were directed towards the S-70A-9, noting the similarity between Regime algorithms, a superior quality CDR, and that Blackhawk had longer to run to PWD. QinetiQ have identified that when combined with continued operator based reporting, FMR could increase accurate fatigue damage capture

to over 80%[7]. This capture rate is seen as a significant leap in improving UM system and now allows for creation of detailed flight profiles for all mission types allowing for a more robust assessment of the assumptions used in fatigue analysis.

Future

Development of Mission profiling – this is the next step HSI-DGTA is currently undertaking which allows the provision of detailed mission profiles which are compared to manually recorded mission types. This allows estimates for the unmonitored regimes to be derived. This in turn increases the "capture" of damaging regimes, resulting in more accurate fleet severity calculations to understand the conservatism of the current assumption of unmonitored fatigue drivers.

This allows for accurate assessment of safety, reduction in cost of ownership and increased availability which form the three pillars of Aircraft Structural Integrity Management.

The underlying algorithms driving the software tool, once full capability is recognised, could potentially be transferred across to other rotary wing platforms depending on both the availability of suitable FDR flight data and validation of the algorithms against the platform flight models. This software tool would enable HSI-DGTA to develop a comprehensive understanding of the actual usage of ADF rotary wing aircraft across a wide range of mission types and would enable a mature and thorough spectrum to be developed for future ADF Rotary Wing aircraft acquisition projects.

Conclusion

The benefits of FMR for future platforms is significant in that it allows HSI-DGTA to gain knowledge and experience for processing data to develop detailed mission profiles. Future platforms have more robust and integrated capabilities for capturing data and conducting RR. The corporate knowledge gained from FMR will allow HSI-DGTA to more capably act as the Commonwealth SME for Usage and Fatigue Monitoring. It will allow greater understanding of the future processing and analysis of automated Usage Data from new Seahawk and Chinook variants MH-60R and CH-47F. The RW FMR software tool is not intended to replace the authorised UM system but instead will augment it by characterising fleet usage in greater detail than is currently possible. Implementation of FMR software for Rotary Wing platforms serves to improve the understanding of the level of risk in the management of Structural Integrity.

Acknowledgements

Author wishes to acknowledge efforts of FMR development by members of QinetiQ Australia - A. McArlein, A. Tuck, J. Huang.

References

[1] DSTO, Importance of Reliability Assessment to Helicopter Structural Component Fatigue Life Prediction, DSTO-TN-0462, Jun 2002.
[2] DGTA-ADF, S-70B-2 Seahawk Aircraft Structural Integrity Management Plan, Issue 6, 21 November 2012.
[3] DGTA-ADF U3101324, Rotary Wing Fatigue Assessment Methodology Development, May 2012.

[4] QinetiQ-ER-S70B51-ASM963, S-70B-2 Seahawk Flight Manoeuvre Recognition and Software Verification and Validation, Rev 1, of 15 Oct 13.
[5] QinetiQ-LR 4-4-03-25.3S7148, Black Hawk Incorporation into Rotary Wing Flight Manoeuvre Recognition Software, of 06 Aug 13.
[6] QinetiQ-ER-S70B-51-ASM977, S-70B-2 Annual Fatigue Assessment, Rev 1, 0f 30 Sep 13.
[7] QinetiQ-ER-S70A-51-ASM1015, S-70A-9 Black Hawk Flight Manoeuvre Recognition Software Verification & Validation, Rev 1, of 16 Dec 14.

4.3 Tackling the Characterization of H-60 Airframe In-Flight Dynamic Response and Fatigue Loading Using Small Scale High Performance Computing (John Vine, Luther Krake, Phil Jackson [DSTO])

The Australian Defence Science and Technology Organisation (DSTO), in collaboration with the United States Navy (USN) Naval Air Systems Command (NAVAIR) and the Australian Defence Materiel Organisation (DMO), is embarking on a program which aims to demonstrate the technical feasibility of undertaking a Full Scale Fatigue Test (FSFT) on a helicopter airframe. If this can be done successfully, the way will be opened to conduct FSFTs on military helicopter airframes, providing many of the same airworthiness and cost of ownership benefits as such tests currently provide for fixed-wing aircraft.

A necessary precursor to conducting a FSFT on a helicopter airframe is a detailed understanding of the vibratory loading the airframe is subjected to in flight. To that end, DSTO has developed a novel methodology to characterize the in-flight dynamic response of a helicopter airframe. This paper describes the developed methodology and its application to the H-60 Black Hawk airframe, specifically, its use to characterize the variation in H-60 airframe response with flight condition and airframe location.

DSTO took advantage of many recent advances in computational processing when developing the methodology. The methodology integrates traditional structural dynamic analysis techniques with high performance computing and advanced data mining techniques to dramatically increase the scale of analysis achievable. The methodology characterizes in-flight response by its vibrational energy content, and associates this content by source, thereby facilitating aggregation and improved interpretation. The methodology can be summarized by the following three steps: i) In-flight response data undergoes two stages of pre-processing including a cleaning process to remove data irregularities and a resampling process to simulate a standardized main rotor speed across all data; ii) The processed data is segmented by time, and a spectral density estimation calculated for each individual segment; iii) Peaks within each spectral density estimation are associated with key expected vibration frequencies (e.g. rotor, drivetrain, natural frequencies) identified from helicopter theory and modal analysis, and the energy within each peak is calculated.

DSTO used this methodology to characterize the in-flight dynamic response of the S-70A-9 Black Hawk, which is the Australian military export variant of the UH-60A. Key characteristics of measured in-flight response data were captured in the form of Dynamic Response Signature (DRS) plots, which were used to conduct a number of example analyses. By comparing multiple DRS plots DSTO was able to quantify the variation of in-flight dynamic response of the S-70A-9

airframe by airframe location and maneuver. Comparisons were also made to generalized data in the helicopter literature that revealed good correlation.

The developed methodology characterizes airframe dynamic responses in terms of their energy content, not fatigue damage. Although energy and crack growth behavior are related (e.g. strain energy release rate G vs. stress intensity factor K) making response energy a good indicator of fatigue significance, further work is required to quantify the fatigue significance of these airframe response energies. Once established, this fatigue significance will be vital in informing the dynamic loading requirements of any future helicopter airframe FSFT.

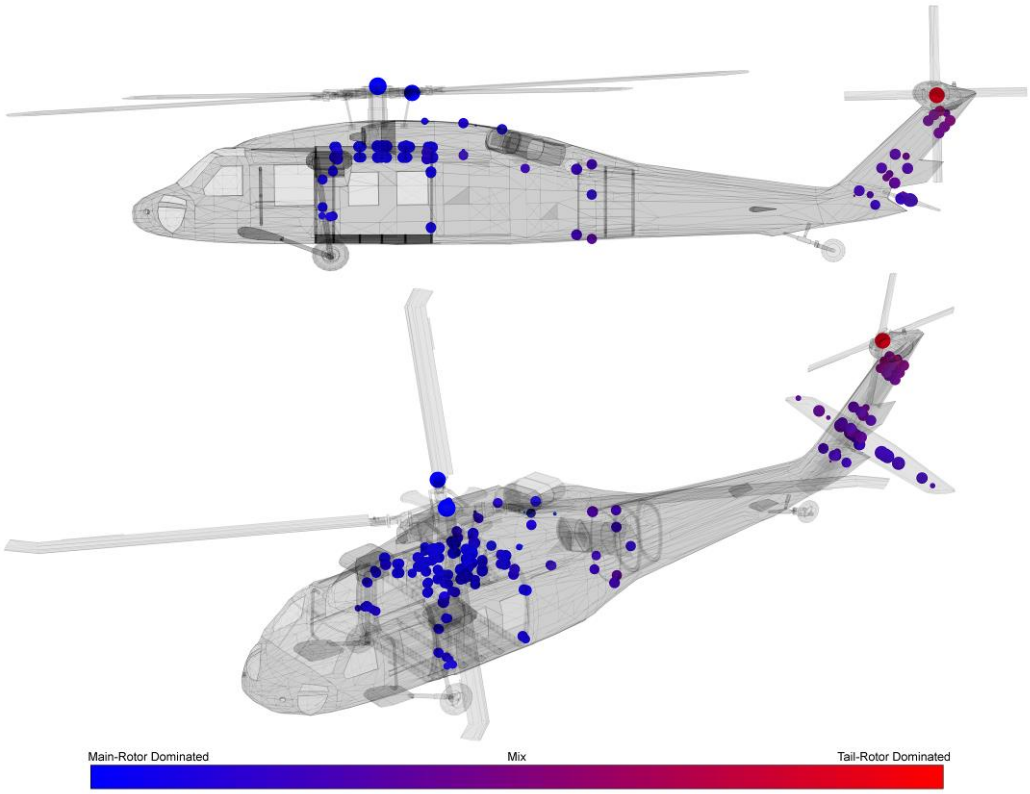

Figure 1: Distribution of vibrational energy across the S-70A-9 airframe. Each marker is sized by the amount of vibrational energy at that location and coloured by the contributing sources.

4.4 F/A-18 Life Of Type Analysis (LOTA) (S. Trezise, D. Moorhead and J. Moews [QinetiQ Australia])

To achieve operational goals the RAAF F/A-18 platform needs a life extension beyond its current certified structural LOT. The F18 is managed to multiple life limiting metrics – FLEI, DEF STAN AFHRs, SD565 AFHRs, landings and GAGs. To achieve its operational goals, Tactical Fighter Systems Program Office (TFSPO) would like an extension from 6000 to 6600 AFHRs, from 5000 to 6000 GAGs and from 8300 to 9300 Field Landings. FLEI limits will not be increased. Further, whilst LOTEX is desired on a fleet wide basis, it is understood that due to the planned approach to drawdown, only a small subset of the fleet will be required to approach the extended limits.

QinetiQ was requested to scope the activities required to achieve these extensions. It was realised early on that the scoping of the LOTEX required an assessment of the 'status' of the management of baseline primary structure with a view to indicating the actions needed to extend it to the LOTEX goals, this was called the LOTA. It was also recognised that to efficiently and effectively complete this LOTA, it needed to leverage the extensive expertise and experience held in-country predominantly by DSTO but also within ASI-DGTA, QinetiQ and TFSPO.

To achieve this outcome, a framework for the LOTA was created around the guiding construct called the 'Steering Group Committee (SGC)'. The SGC was made up of the most experienced and authoritative members of ASI, DSTO and QinetiQ and their mandate was to make decisions that would guide the scale and focus of the LOTA such that the resulting outcomes for LOTEX were the most relevant, effective and efficient that could reasonably be achieved. The SGC mechanism was exercised through a series of set meetings where QinetiQ, working to a set of identified considerations for LOTA and LOTEX, would present initial scoping, thinking and analysis and seek discussion from the wider forum and guidance from the SGC.

The LOTA is now almost 60 percent complete, and the combination of many years of RAAF relevant test data, research and experience with empowered and pragmatic decision making has meant that the LOTA will itself clear much of the AFHRs limited primary structure to 6600 AFHRs and provide a rigorous basis for either 'management' or 'guidance on further work' necessary to achieve the LOTEX goals for all other affected primary structure.

4.5 Alternative methods for derivation of safe life limits for a 7050-T7451 aluminium alloy structure (L. Molent [DSTO])

For modern agile military aircraft, the fatigue life determined via full-scale fatigue tests (FSFT) forms the basis of the fatigue structural certification programs. The service life derived from these tests is based on an interpretation of the results using a Certification Structural Design Standard (CSDSTD). The CSDSTD requires/specifies that the airframe should maintain a cumulative probability of failure (CPOF) from fatigue below a prescribed allowable value.

A Royal Australian Air Force's (RAAF) preferred CSDSTD [1] requires that the CPOF for the total airframe due to structural fatigue must be limited to 1/1000[1] aircraft for the life of type. This is principally achieved by following the CSDSTD guidelines during the structure's design and by conducting a representative FSFT. To achieve the required CPOF the fatigue lives demonstrated by the FSFT are divided by a scatter factor (SF), which is applied to account for scatter in the fatigue performance of aircraft structures and/or service loading. In the case of the RAAF's preferred CSDSTD, the FSFT article is considered to be an estimate of the mean production airframe that has been tested to a spectrum that is representative of the mean fleet usage.

The CSDSTD provides guidance on the means of deriving a SF as a ratio of the geometric mean test life (L_{mean}) to the safe aircraft life (L_{safe}):

$$SF = \frac{L_{mean}}{L_{safe}} = 10^{z\sigma\sqrt{1+1/N}} \qquad (1)$$

The variation of failure times is made up of the material variation (σ^2) and the variation in estimating the mean of the population from a limited number (N) of samples. If the time to failure of any of N identical locations on the aircraft is (log) normally distributed with a mean of and a standard deviation of , then an estimate of the mean (L_{mean}) will likewise be (log) normally distributed, with a mean μ and a standard deviation of $\sigma/\sqrt{N}$.

For values of N = 2, σ = 0.12 [(a)], and a probability of failure of 1/2000 (which gives a total aircraft probability of failure of 1/1000), z = 3.30. This results in a safe life factor of approximately 3. The value of σ is based on unspecified historical data so that its appropriateness for current production airframe cannot be altogether quantified.

Fortunately, understanding of the fatigue behaviour of metal airframes has progressed to the point where, for a fixed loading spectrum[2], stress level and material, it is known that the scatter in the fatigue performance of monolithic metallic airframes is governed by the variability in the metal's material properties and manufacturing quality. These two areas can be quantified by gaining an understanding of the variability in:

---

[1]The CSDSTD considered (or assumed) two critical items only (e.g. left and right wing) each with a CPOF = 1/2000. The validity of this assumption will not be addressed here.

[2] Note that variations in aircraft usage will also lead to significant scatter in fatigue lives. This is one reason why most military agile aircraft are fatigue usage monitored.

1. the initial material discontinuities that lead to fatigue cracking;
2. stress concentrations leading to inter-aircraft variations in local stress;
3. fit-up or residual stresses;
4. stress intensity threshold;
5. the fracture toughness of the material;
6. crack nucleation and/or initiation period; and
7. the crack growth rate of fatigue cracks in the material being examined.

Items 1 to 3 are considered to define the aircraft's build quality from a fatigue perspective. Items 4 to 7 define the metal's property variability[3]. Thus, if the variation, or influence, in these variables can be adequately quantified then a more accurate estimate of the scatter in a metal's fatigue performance can be made.

The work summarised in [2] illustrated a simple alternative approaches for determining the Safe Life Limit (SLL) for thick-section aircraft aluminium alloy 7050-T7451 plate structure, considering the material and manufacturing properties listed above. These approaches may be useful in certain circumstances, for example when no FSFT data are available but data describing the relevant material properties are available. A sample of FSFT results associated with cracking in an F/A-18 Hornet aircraft's AA7050-T7451 centre fuselage sections has been used to illustrate these alternative methods. It was found that the alternative methods provide some support to the RAAF F/A-18's CSDSTD derived SLL.

References

[1] Design and Airworthiness Requirements for Service Aircraft Volume 1 – Aeroplanes. Defence Standard 00-970, Issue 1, Dec 1983.

[2] Molent L. Alternative methods for derivation of safe life limits for a 7050-T7451aluminium alloy structure, Fatigue 2015; 74:55-64.

4.6 Damage Tolerance Analysis of the Wing Root Joint of the P-3C Aircraft (K. Watters, M.Ignjatovic and S. Pinskier [QinetiQ Australia]; C. Chauhan and J. Ayling [Airbus Group Australia Pacific])

The wing root joint in the P-3C involves a chordwise splice comprising a double shear butt joint with the centre wing and outer wing lower planks butting together, spliced with a rib cap on the inner side and a splice plate on the outer side. While the blueprint joint has been demonstrated

[3] Some aspects of item 1 (e.g. production discontinuities) may also be considered as a material processing property.

to have adequate fatigue life, it has been discovered that the fleet configurations differ significantly from blueprint. Cross sections of the joint are shown in Figure 1.

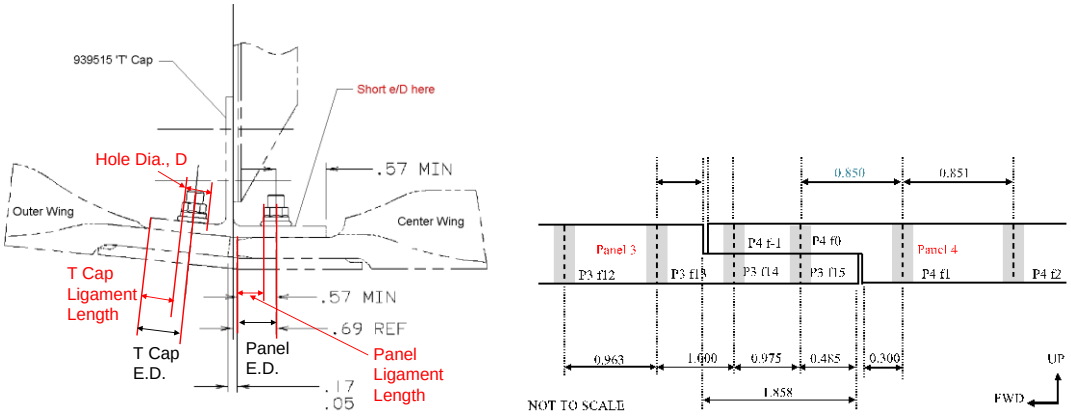

(a) Spanwise Cross Section (b) Chordwise Cross Section

Figure 1: P-3C Wing Root Joint Cross Sections

One particular Royal Australian Air Force (RAAF) P-3C was found to have a very poor configuration of the joint. This specific poor configuration is shown in Figure 1(b). It has undergone Damage Tolerance Analysis to develop inspection intervals to support its continued operation. A complex DTA was performed to determine accurate beta factors and allow for load shedding through the phases of crack growth, in order to get the best result for the RAAF. Across the wing chord there are 9 panels that are spliced together along their spans and finish in the butt joint at the wing root. A plan view of the splice between two panels is shown in Figure 2.

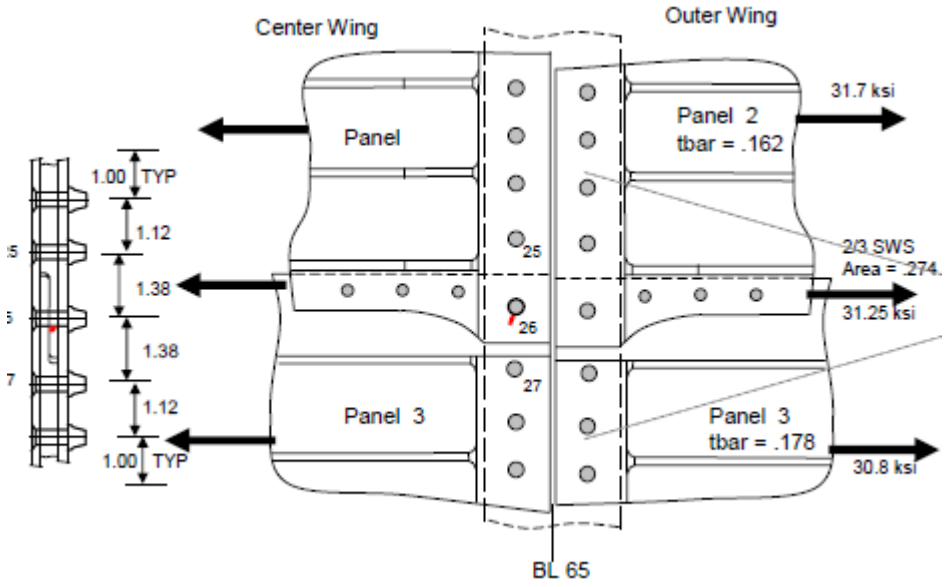

Figure 2: P-3C Lower Wing Panel Splices – Plan View

The DTA considered a crack in a panel at a hole near the edge of a splice. The crack runs in a chordwise direction, initially to the edge of the panel, and then continuing growth from the other side of the hole back into the panel. Once the crack propagates to the edge of the panel, it was considered that the load in that fastener would reduce by load shedding during phase 2 growth back into the panel.

A finite element analysis was conducted of the wing root joint with varying crack lengths to quantify the load shedding. This was achieved by developing a single finite element model representing the aircraft actual configuration. A full crack was deliberately introduced that was initially stitched at the crack faces grids utilising multipoint constraints (MPCs). Releasing the MPCs in a defined sequence allows the simulation of crack initiation and propagation first towards the edge of the panel and subsequent phase 2 growth back into the panel. Free bodied fastener loads were then extracted for each crack growth stage. The results are shown in Figure 3(a).

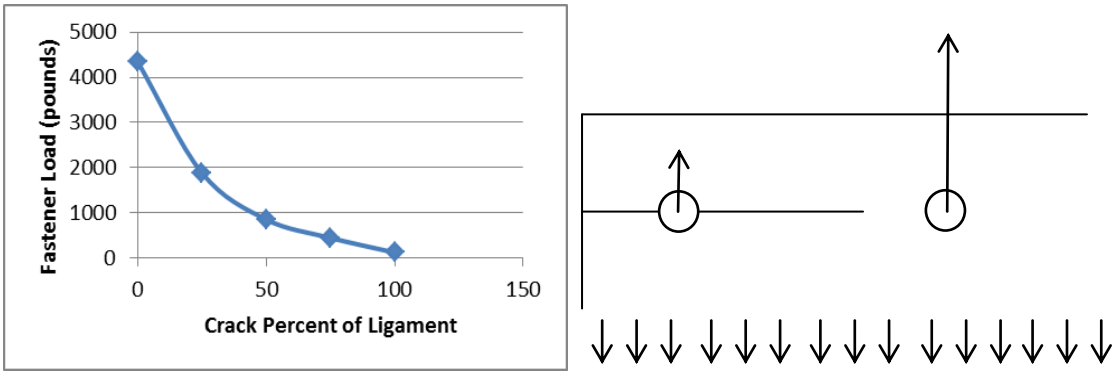

(a) (b)

Figure 3: Load Shedding During Phase 2 Crack Growth

Due to the load shedding, the load in the first fastener ceases to be the primary driver of the crack growth in the latter part of phase 2. Instead, as the crack approaches the second fastener, the stresses from that fastener, and to a lesser extent the fasteners beyond it, start to make a significant contribution to the beta factor. The crack configuration responding to those stresses is like an edge crack at a lug as shown in Figure 3(b).

Unfortunately, handbook beta solutions for an edge crack at a lug could not be found. Approximate solutions were developed by compounding and superimposing simple handbook solutions to reflect the effects of separate boundaries and loads. Even then, the available simple geometries were not all directly applicable, and a comparison to a StressCheck model of the joint showed that the compounded beta factor was low and not capturing the full flexure of the near end of the panel. The compounded solution was adjusted to match the StressCheck result and then used to model the change of beta factor with crack growth.

In the end, the DTA using a FASTRAN analysis of a representative load spectrum produced a basic crack growth life that was still insufficient for the required inspection interval. However, the RAAF had cold worked the fasteners in the joint at the time they did the configuration check. A conservative life improvement factor due to the cold work benefit was applied to the basic crack growth life and a suitable inspection interval resulted.

References

[1] QinetiQ Australia, A09-753 BL65 Damage Tolerance Assessment, ER-P3-57-ASM1004, 19 September 2014.

[2] Australian Aerospace, Finite Element Model- Lower BL65 Joint analysis Phase 2 to 4 (Qinetiq DTA), A09-ER-002690, Revision A, 8 May 2014.

4.7 Equivalent Pre-crack Sizes in Aluminium Alloy 7050-T7451 (L. Molent [DSTO])

For the most part, F/A-18 Hornet service life assessment, as for most modern fighter aircraft, involves the interpretation of fatigue tests. Many significant fatigue tests have been conducted to assist in the structural integrity management of the F/A-18 Hornet fleet. These fatigue tests comprised certification tests and fatigue validation tests conducted on various coupons, components and full-scale test articles under numerous F/A-18 structural test programs. As part of the test interpretation effort, many fatigue cracks generated during these tests have been examined using Quantitative Fractography (QF).

To date, crack growth data for more than 900 cracks found on 7050 aluminium alloys used in the Hornet airframe have been collated and analysed [1]. The analyses include the Equivalent Pre-Crack Size (EPS) derived for many of these fatigue cracks. The EPS values are an estimate of the effective size (of an equivalent fatigue crack-size) of pre-existing initial discontinuities/flaws in a material that grow fatigue cracks. The EPS was derived by back-extrapolating measured crack growth data to the estimated size at the beginning of loading using an exponential crack growth model [2]. Previous work provided EPS analyses for various surface finishes (e.g. etched, machined, peened etc) whereas this analyses considered the type of fatigue initiating defects (including: inclusion, etch pit, peening damage, mechanical damage, porosity and corrosion pits).

This paper presents statistical analyses of the EPS and covers the following topics:

1. Historical sources of Effective Initial Flaw Size (EIFS)
2. Description of EPS data samples;
3. Is EPS sensitive to varying stress levels?;
4. Probability distribution of the EPS data; and
5. Correlation of EPS and measured initial discontinuities/flaw size.

A better understanding of the key parameters i.e. EPS and initial discontinuity/flaw size that influence fatigue cracking has the potential to facilitate more accurate predictions of fatigue life, and thus the possible extension of the economic life of aircraft structures so as to reduce the cost of ownership. The results of this work are considered significant as firstly, the types of fatigue initiation sources in the 7050 aluminium alloy have been identified. Secondly, estimations of typical initial discontinuity sizes (or EPS) for use with related crack growth models have been derived and these have been shown to be largely stress level and spectrum independent. For one initiating discontinuity type, the EPS was shown to approximate a physical characteristic of the material and the surface treatment. Related work is presented in [3].

References

[1] Molent L. (Invited Review paper), A review of equivalent pre-crack sizes in aluminium alloy 7050-T7451, Fat Fract Eng Mat Struct 2014;37: 1055-74.
[2] Molent L, Barter SA and Wanhill RJH. The Lead Crack Fatigue Lifing Framework, Int Fatigue; 33 (2011) 323–331
[3] Gallagher JP and Molent L. Effect of load spectra and stress magnitude on crack growth behaviour variability from typical manufacturing defects. Advanced Materials Research Vols. 891-892 (2014) pp 100-105.

4.8 Managing airframe fatigue from corrosion pits – A proposal (Molent L, Sharp K, Crawford B and Loader C. [DSTO])

Modern military aircraft utilize highly optimized metallic structure to assist in achieving their performance objectives. Thus their structure (particularly its fracture critical components) tends to be uniformly highly stressed and thus susceptible to fatigue cracking. Despite corrosion prevention or protection schemes/treatments and corrosion prevention and control plans in-service corrosion does occur and has the potential to impact the structural integrity of the aircraft. Whilst the fatigue and environmental degradation management of the aircraft is generally well understood as reflected in typical Aircraft Structural Integrity Management Plans (ASIMP, see [1]), limited provision beyond *find and fix* exists for corrosion repair. Thus the repair of corrosion can be a major through life cost driver as well as an aircraft availability degrader. This *find and fix* policy exists largely because approved tools do not exist to accurately assess the structural significance of corrosion when it is detected (examples of recent proposals include [2]-[4]), as well as the difficulty in traditional approaches where fatigue is assumed to occur concurrently with a corrosive environment (e.g. [5]).

Investigations by Trathen [6], which presented the corrosion rates measured in internal bays in a range of Royal Australian Air Force (RAAF) aircraft, were the first to report that there appeared to be little corrosion activity occurring during flight. Barter and Molent [7][8][9] subsequently showed that for cracking in 7050-T7451 aluminium alloy (AA) in an operational RAAF F/A-18 Hornet aircraft, examination of fracture surfaces revealed that corrosion was only apparent during extended periods of downtime (inactivity). This is supported by the work of Burns et al. who state that aircraft fatigue cracking occurs in cold and dry in-flight environments [10] where corrosion activity is largely suspended[4]. Wanhill also showed that fracture surface topography from a service commercial airline fuselage lap-joint specimen and one tested in the laboratory were similar [11]. Similar findings were reported by Jones [12]. Jones and Hoeppner also showed that in some cases fatigue initiated preferentially from material discontinuities despite the presence of corrosion pits and a corrosive environment [5]. These independent findings suggest that (in general) for combat aircraft the effect of the environment on fatigue crack growth can be

[4] This may not apply for aircraft that spend extended periods flying low in hot and salty environments or cavities exposed to corrosive products. Also note that some aircraft types (e.g. fighters) spend the vast majority of the service lives on the ground.

decoupled which significantly simplifies the problem (i.e. the growth of fatigue cracks on these aircraft is not environmentally assisted[5]).

A significant proportion of aircraft corrosion can be classified as pitting corrosion which is a form of localised metal corrosion. The pits may be shallow depressions or cavities and in its early stages, pitting may have the appearance of general corrosion at a macroscopic level. Pitting may be present under white or grey powdery deposits of corrosion product on an AA metal surface and tiny holes or pits are seen after clearing away the deposit. As pitting corrosion is one form of corrosion that can lead to fatigue cracking it is specifically addressed here. It should also be stressed that not all corrosion pitting will lead to cracking (e.g. [5]).

For fatigue cracks that originate from pitting corrosion it has been found that the effective crack-like pit depth is a defining fatigue crack growth characteristic [3][8][9][15] to [19] (excluding at end grains). Coupling these findings with a robust crack growth model, such as the lead crack framework [19], provides a means of predicting the impact of pitting corrosion on the structural integrity of an airframe.

In this paper, examples of fatigue growth from corrosion pits are provided and these are followed by a framework for the management of in-service detected pitting corrosion that departs from the find and fix method. The aim of this work is to provide a fracture mechanics basis for allowing detected pitting corrosion to remain in service for a limited period of time (e.g. to the next planned or scheduled servicing). Unanticipated maintenance costs significantly more than planned and orderly maintenance (e.g. ensuring the availability of personnel and logistics). By delaying the repair of pitting corrosion until the next scheduled maintenance, it is believed that this alone will save considerable resources and improve aircraft availability.

The development of such analytical tools as reported in [20] to [22] capable of accurately assessing the effect of corrosion on the durability of a structure would be a major advance in the aircraft structural integrity management philosophy.

References

[1] MIL-STD-1530C, Aircraft Structural Integrity Program, 1 Nov 2005.
[2] Burns JT and Gangloff RP. Scientific advances enabling next generation management of corrosion induced fatigue. Eng Procedia 2011; 10: 362-369.
[3] Crawford BR, Loader C and Sharp PK. A proposed roadmap for transitioning DSTO's corrosion structural integrity research into Australian Defence Force service. DSTO-TR-2475, Oct 2010.
[4] Loader C, Crawford BR, Sharp K and Molent L. A Proposal for the Management of Detected Pitting Corrosion for the F/A-18 Hornet, DSTO-TR- 2976, Melbourne Aust, May 2014.
[5] Jones K and Hoeppner DW. The interaction between pitting corrosion, grain boundaries, and constituent particles during corrosion fatigue of 7075-T6 aluminum alloy. Fatigue 31 (2009) 686–692.
[6] Trathan P. Corrosion monitoring systems on military aircraft, Proceedings 18th International Conference on Corrosion, Perth 20th -24th November, 2011.

[5] See 00 for standard definitions of corrosion terms.

[7] Barter S.A. and Molent L. Investigation of an in-service crack subjected to aerodynamic buffet and manoeuvre loads and exposed to a corrosive environment, Proceedings 28th International Congress of the Aeronautical Sciences, Brisbane, 23-28th September, 2012.
[8] Barter S. and Molent L. Service fatigue cracking in an aircraft bulkhead exposed to a corrosive environment, Eng Fail Anal 34 (2013) 181–188.
[9] Barter S. and Molent L. Fatigue Cracking from a Corrosion Pit in an Aircraft Bulkhead, Eng Fail Anal 39 (2014) 155-163.
[10] Burns JT, Gangloff RP and Bush RW. Effect of environment on corrosion induced fatigue crack formation and early propagation in aluminum alloy 7075-T651. Proc. DoD Corrosion Conference, La Quinta Ca, 31 Jul-5 Aug., 2011.
[11] Wanhill RJH. Flight simulation fatigue crack growth guidelines, NLR-TP-2001-545. NLR, The Netherlands, 2001.
[12] Jones R. (2014) Fatigue crack growth and damage tolerance. Fatigue and Fracture of Engineering Materials and Structures, 37, 5, pp. 463-483.
[13] Corrosion Fatigue and Environmentally assisted Cracking in Aging Military Vehicles, NATO RTO AGARDograph AG-AVT-140, 2011.
[14] Hoeppner DW and Arriscorreta CA. Exfoliation corrosion and pitting corrosion and their role in fatigue predictive modelling: state-of-the-art review, J. Aerospace Eng. 2012, Article ID 191879, 2012.
[15] Molent L, Sun Q and Green AJ. Characterisation of equivalent initial flaw sizes in 7050 aluminium alloy, Fatigue Fract Engng Mater Struct 2006; 29: 916–937.
[16] Molent L. (Invited Review paper), A review of equivalent pre-crack sizes in aluminium alloy 7050-T7451, Fat Fract Eng Mat Struct 2014, doi: 10.1111/ffe.12214
[17] Smith SW, Newman JA and Piascik RS. Simulation of fatigue crack initiation at corrosion pits with EDM notches. NASA/TM-2003-212166. March 2003.
[18] Burn JT, Larseni JM and Gangloff RP. Driving forces for localized corrosion-to-fatigue crack transition in Al–Zn–Mg–Cu. Fatigue Fract Engng Mater Struct 2011; 34**:** 745–773.
[19] Molent L, Barter SA and Wanhill RJH. The lead crack fatigue lifing framework, International Journal of Fatigue 2011; 33; 323–331.
[20] Molent, L., Managing airframe fatigue from corrosion pits – a proposal, Engineering Fracture Mechanics (2014), doi: http://dx.doi.org/10.1016/j.engfracmech.2014.09.001.
[21] Molent, L. Managing fatigue from corrosion pits – a proposal. Proc. AIAC15, Melb 25-28 Feb 2013
[22] Loader C, Crawford BR, Sharp K and Molent L. A Proposal for the Management of Detected Pitting Corrosion for the F/A-18 Hornet, DSTO-TR-2976, Apr 14.

4.9 Real-time Risk Management of Aircraft Fleet Based on the Probability of Failure of Aircraft Structures (Ribelito Torregosa, DSTO)

The binary observation (i.e., benign or detrimental) in an aircraft flight history is used to update the probability of failure of each aircraft in a fleet. The DSTO developed risk analysis tool FracRisk is used to calculate the real-time risk of each fleet member and the results are shown in Fig. 1. The figure shows the fleet member identification, flight hours, the probability of failure and the binary observation.

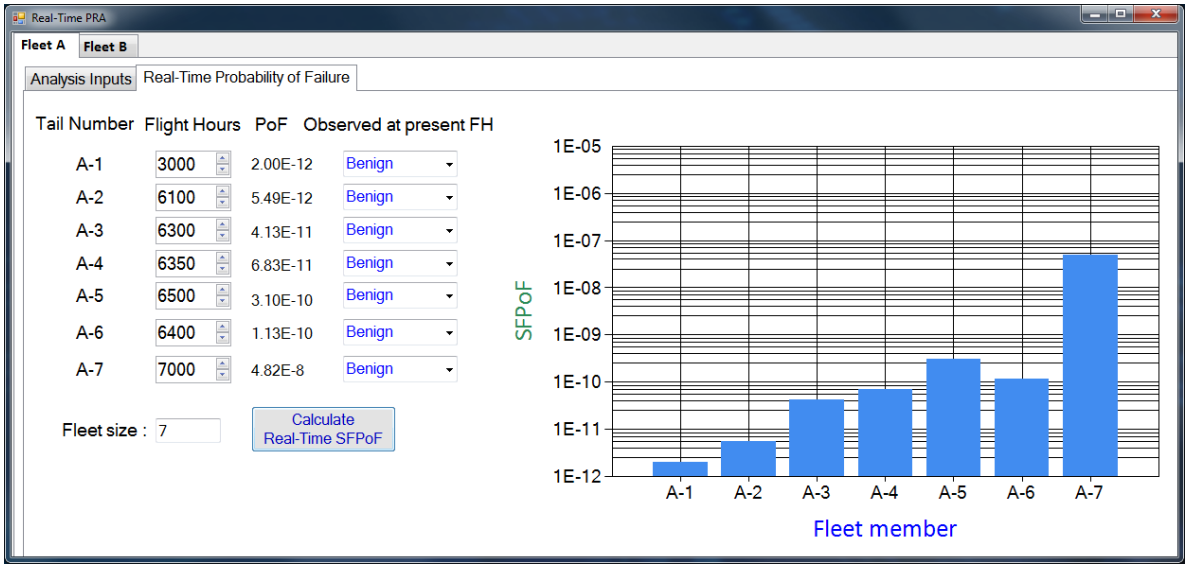

Figure 1 Real-time risk values for hypothetical fleet of seven aircraft at present flight hours

One of the advantages of real-time risk analysis over the conventional method is its ability to predict which fleet member's risk of failure is acceptable and which is not when any fleet member exhibits failure. To illustrate this, Fig. 2 shows the updated probability of failure for each fleet member when the lead aircraft fails as indicated by detrimental observation on A-7. This shows how the flight hour differences within the fleet can affect the probability of failure of each fleet member.

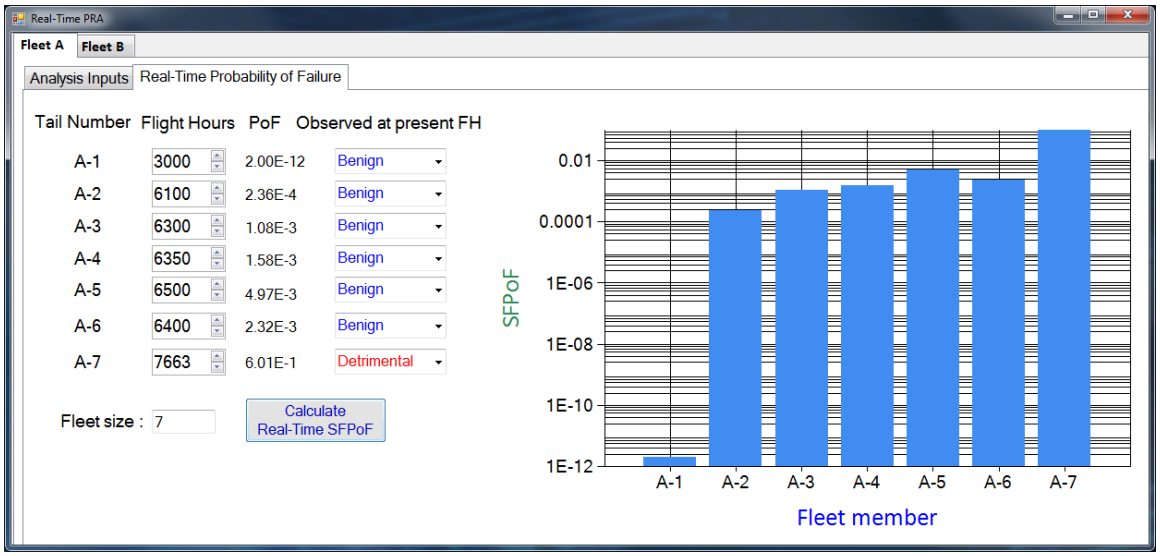

Figure 2 Real-time risk values for the hypothetical fleet of seven aircraft showing increase of risk to other fleet members when the lead aircraft fails

Based on the results of the analysis, the following is concluded:

1. Real-time risk analysis can improve the reliability of the risk prediction by progressively reducing the high uncertainties in the initial risk prediction;

2. Real-time risk analysis can be used to optimize the fleet usage;

3. Real-time risk analysis presents a framework of identifying which fleet member's risk of failure is acceptable when one fleet member fails.

References

[1] Torregosa R., *Real-time Risk Management of Aircraft Fleet Based on the Probability of Failure of Aircraft Structures*, 16th Australian International Aerospce Congress , 23-24 Feb. 2015 Melbourne, Australia.

4.10 Bayesian Updating of Aircraft Risk Assessments Using Results of Inspection (Ribelito Torregosa and Weiping Hu, [DSTO])

To illustrate how the probability of failure changes when a crack is observed during inspection, we consider a hypothetical case of a crack detected at 6000 flight hours (FH). When a crack is detected the distribution of the equivalent initial flaw size (EIFS) can be updated which will then revise the probability of failure (PoF). The updated PoF curves are indicated by the open circle symbols in Fig. 1a. Since the aircraft under consideration has already flown 6000 hours, the PoF curve segment applicable is only from 6000 FH onward. This means that for the aircraft being inspected at 6000 FH, the risk curve that has been used (i.e., up to 6000FH) and the risk curve that will be used (i.e., from 6000FH) is indicated by the solid curve. The segment of the solid curve up to 6000 FH is its past risk estimate and does not benefit the aircraft being inspected. However, the same segment of risk curve is beneficial to other fleet members with relatively low flight hours and their risk curve is the one indicated by the dashed line with open circle symbols. Fig. 1b shows different fleet risk curves for varying times of failure and the risk curve prior to the observation of failure. The updated risk discussed so far is based on one aircraft.

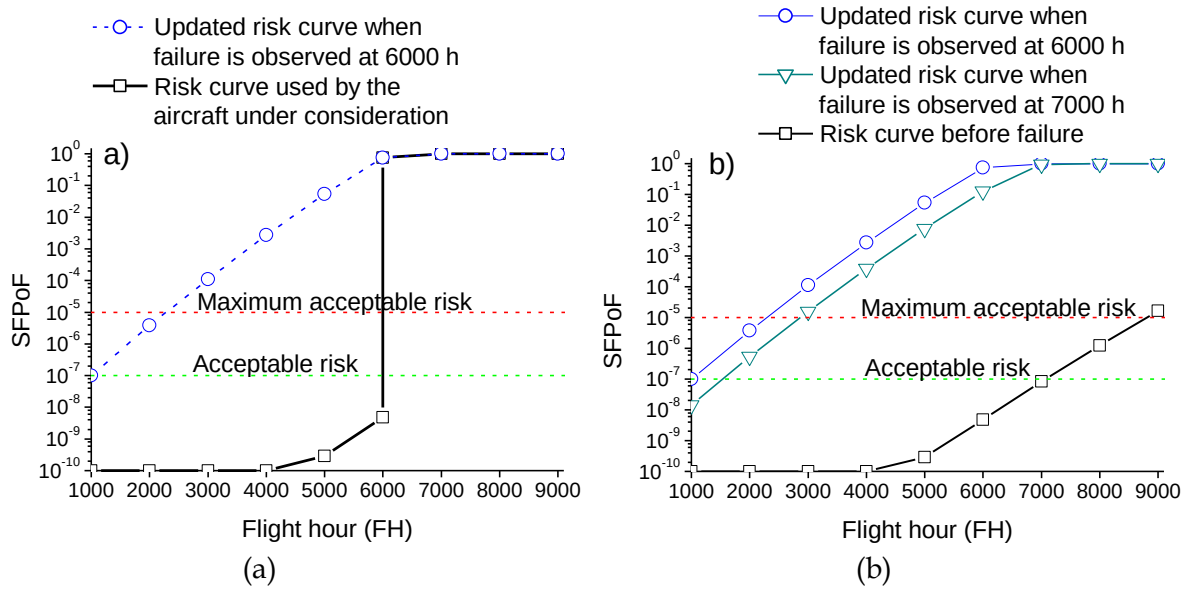

Figure 1 a) Updated risk curve when failure is observed at 6000 FH, b) Comparison of updated risk curves when failure is observed at 6000 FH and 7000 FH.

It is demonstrated how a binary observation (i.e., failure or safe) during an inspection can be used to update the risk assessment of a fleet of aircraft. The methodology presented may be useful for evaluating the PoF of each aircraft in a fleet when one fleet member has failed. The examples presented show that the fleet risk values can be very dynamic since it is a function of each individual aircraft flight hours.

Based on the cases studied, the following conclusions may be drawn:

1. The probability of failure assessment can be updated using the binary observation of a fleet member.

2. Failure in one of the fleet members will significantly affect the risk assessment of each aircraft in a fleet but depending on the flight hours of each aircraft. Whether any particular fleet member is still safe to fly would require analysis in this light amongst other factors.

3. Risk of failure is not constant over the flight history and must be reviewed when more data become available.

References

[1] Torregosa, R.F., and Hu, W. Bayesian Updating of Aircraft Risk Assessments Using Results of Inspection. in 11th International Fatigue Congress 2-7 March 2014. Melbourne, Australia.

4.11 Residual stress effects in extruded wing panels on large military transport aircraft (K. Walker, [DSTO and RMIT University Australia], and M. R. Hill, [UC Davis, CA USA])

The primary structure lower surface wing planks on the P-3C maritime surveillance aircraft are machined from either 7075-T651 or 7249-T7651 aluminium alloy extruded billets. The wing planks feature integral risers or blade stiffeners as shown in Figure 1.

Figure 1 : P-3 Wing internal structure showing integral blade stiffeners

Recent fatigue crack growth tests on specimens manufactured from the extruded billet material revealed significantly more variability in crack growth properties than expected, see Figure 2. This variability was thought to possibly be caused by residual stresses due to the manufacturing process. The objective of the work reported here was to investigate the residual stress profiles in

test coupons manufactured from sheet/plate, extruded billet, and scrap wing plank material to determine if significant residual stresses existed, and if so, determine whether they were sufficient to explain the variability in observed crack growth behaviour. Full details of the work can be found in [1].

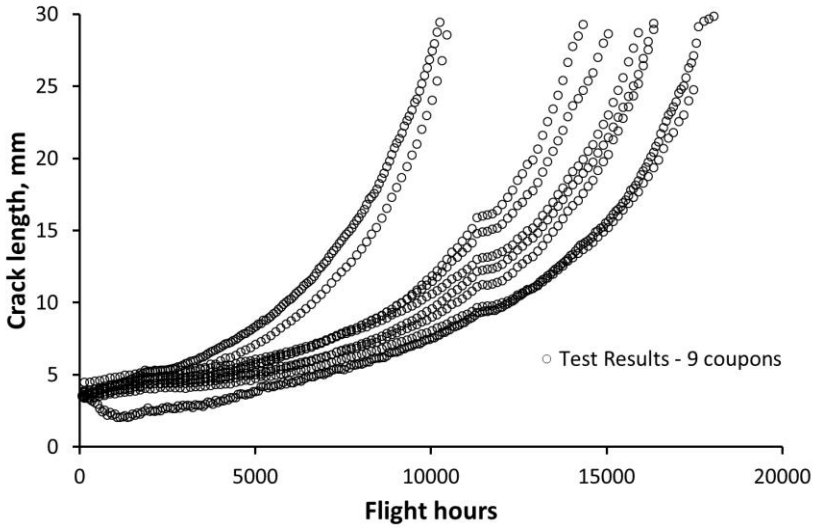

Figure 2: Crack growth variability under representative spectrum loading in test coupons manufactured from extruded billet material

The stresses vary across the plank chord (width direction). The residual stress profiles were measured here using the slitting method [2]. An example of the residual stress profile measured in an extruded billet test coupon compared with a similar coupon manufactured from sheet/plate material is shown in Figure 3. The sheet plate coupons were found to be residual stress free, which is consistent with the results in earlier coupon test programs where very little variation in crack growth properties were observed for coupons manufactured from sheet/plate. As shown in Figure 3, the residual stresses in the extruded billet coupons varied in a range of ±10 MPa across the width

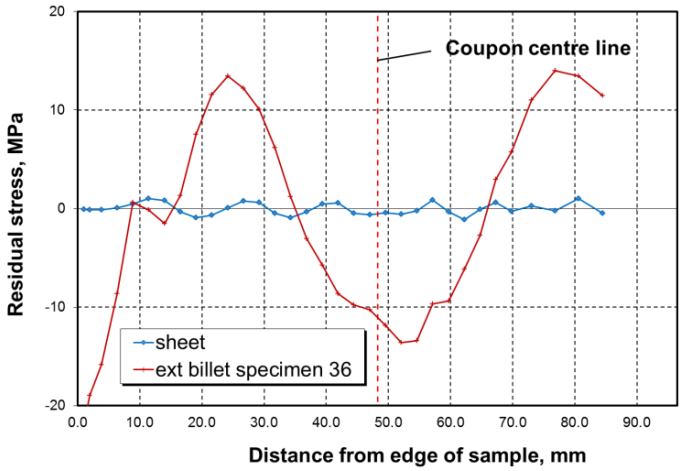

Figure 3: Example of slitting method results for residual stress profiles in extruded billet and sheet/plate coupons

Fatigue crack growth analysis was then performed using a recently updated version of the FASTRAN crack growth analysis code [3]. FASTRAN is a strip-yield model based on the Dugdale model but modified to leave a wake of plastically deformed material in the crack wake. A constraint factor (α) is used elevate the flow stress (σ_o) to account for three dimensional effects which influence the stress state ($\alpha\sigma_o$) near the crack tip. The analysis showed that residual stress variations of the order measured could explain the amount of variability in crack growth which had been observed, see Figure 4.

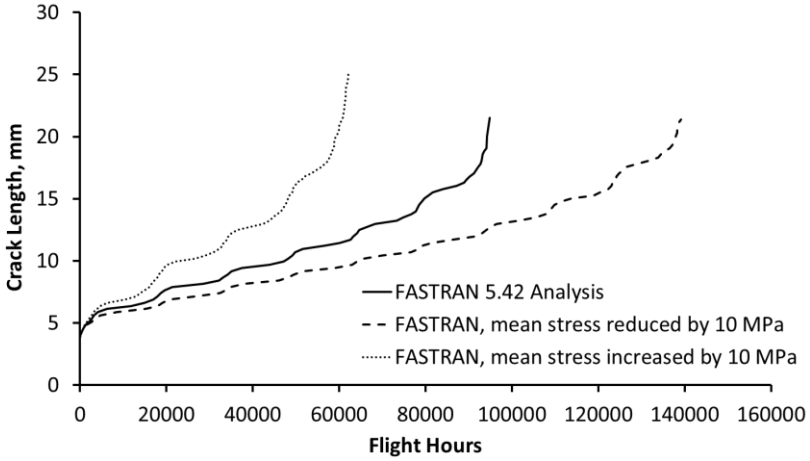

Figure 4: FASTRAN based estimate of crack growth variations possible with ±10 MPa residual stress

Ongoing work includes constant amplitude tests where the residual stress profiles will be measured using the on-line crack compliance based method [4]. The same specimen will then be subjected to the slitting approach described earlier and the results compared. The FASTRAN code is also being further developed to more accurately account for crack growth through a known residual stress profile.

References

[1] Walker, K.F., and Hill, M.R., Residual stress effects in extruded wing panels on large military transport aircraft, in 16th Australian International Aerospace Congress. 2015: Melbourne, Australia.

[2] Hill, M.R., The slitting method, in Practical residual stress measurement methods. 2013, John Wiley and Sons: UK.

[3] Newman, J.C., Jr., FASTRAN A Fatigue Crack Growth Life-Prediction Code Based on the Crack-Closure Concept Version 5.4. 2013, Fatigue & Fracture Associates LLC.

[4] Lados, D.A., D. Apelian, and J.K. Donald, *Fracture mechanics analysis for residual stress and crack closure corrections.* International Journal of Fatigue, 2007. **29**(4): p. 687-694.

4.12 Coupon Fatigue Testing of Thin Sheet Aluminium Alloy 2024-T3 Using the Direct Current Potential Drop Method (A. Gregory, DSTO)

A metal fatigue coupon testing program was conducted to produce fatigue crack growth data through enhanced and verified crack measurement techniques, applicable to thin sheet material

[1]. Crack growth measurement utilising the automated electronic Direct Current Potential Drop (DCPD) method has been refined and a robust pre-test checklist and test set-up guidelines have been established for use with thin sheet AA2024-T3 coupons. This test program demonstrated successful DCPD testing of non-standard coupon configurations, yielding excellent comparison of DCPD crack growth measurements with optical measurement. A comparison between optical (manual) and DCPD (automated) crack growth measurement is shown in Figure 1. The comparison is shown for a centre hole panel (shown on the left) and a single edge notched panel (shown on the right). The measurement techniques and the coupon test program will contribute to the verification of fatigue crack growth models and assist in the interpretation of the fatigue condition of the PC-9/A trainer aircraft fleet.

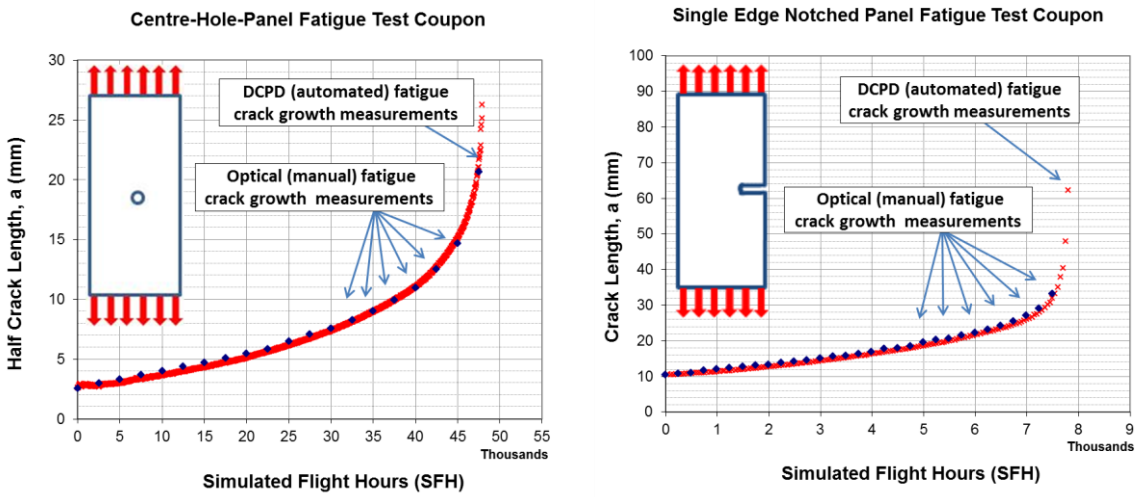

(a) (b)

Figure 1: Comparison of optical (manual) and DCPD (automated) crack growth measurements. Results are shown for a centre hole panel (left) and a single edge notched panel (right) fatigue test coupon.

4.13 Fatigue of cold expanded open hole coupons with pre-existing cracks (P. S. Baburamani, R. Ogden, Q. Liu and P. K. Sharp [DSTO])

Fatigue cracking is one of the major structural damage mechanisms limiting the structural integrity, safety, economic life and, availability of aircraft. Fastener holes have a high stress concentration at the edge of the hole, and are primary sources of fatigue crack initiation, leading to widespread fatigue damage in the airframe structure containing fastener holes. Cold working of fastener holes and autofrettaging of thick walled cylinders are commonly used techniques to extend or improve the fatigue lives of structural components [1]. The split-sleeve cold expansion (SsCx) technology is a simple and cost-effective way to improve the fatigue resistance of fastener holes by the introduction of compressive residual stresses around the holes. The mechanism by which the fatigue life enhancement occurs in cold worked holes is driven by the presence of residual compressive hoop stress around and through the hole extending radially to a length approximately equivalent of the hole radius [2], reducing the effective stress intensity factor range ΔK_{eff}. Extending the fatigue life of cracked fastener holes by established techniques such as split-sleeve cold expansion (SsCx) or hole cold working (HCW) using an oversized mandrel [3], is aimed at easing the maintenance burden by potentially extending the inspection intervals in a damage tolerant aircraft structure.

Experimental details

An experimental investigation was carried out by the Australian Defence Science and Technology Organisation (DSTO) to quantify the effectiveness of the HCW technology, in terms of fatigue life improvement factors (LIF) on a typical airframe aluminium alloy, AA7075-T7351. Open hole (zero load transfer) coupons were tested to failure in non-cold expanded and cold expanded conditions. Coupons were also pre-cracked to specified crack lengths at the open hole, and cold expanded or left non-cold expanded, and tested to failure. The pre-crack lengths investigated were 1.5 mm, 3.0 mm and 4.5 mm. The specimens were with or without a crack starter notch. The EDM crack starter notch was 400 □m long and 300 □m wide. The starter notch was wire cut by electro discharge machining (EDM) on both sides of 6.04 mm diameter central hole, and through the full thickness of the coupon. The cold expansion of open hole coupons, with and without pre-cracks was carried out by using the FTI 8-0-N standard tool diameter number (STDN) mandrel and sleeve combination, in accordance Fatigue Technology Process Specification 8101D [3]. This paper will present the results of the experimental program, involving constant and variable amplitude fatigue tests at a maximum applied net stress of 172 MPa (25 ksi).

Results

Constant amplitude fatigue tests: The log mean fatigue life results of constant amplitude fatigue tests carried out to valid failure of specimens are shown in Table 1 and Figure 1. The individual specimen test results are presented in [4] and only the log mean of fatigue life for each condition investigated are presented in Table 1. The LIFs for each condition are also given in Table 1.

Table 1 Log mean fatigue life results of constant amplitude fatigue tests [R = 0.1] at an applied net stress of 172.4 MPa and the fatigue life improvement factors due to cold expansion

EDM crack starter notch	Pre-crack length [mm]	Log mean fatigue life [cycles], NCx	Log mean fatigue life [cycles], after Cx	LIF
x	0.00 (open hole)	96,428	370,100	3.84
√	0.40	8,665	354,599	40.92
√	1.50	4,070	182,383	44.81
√	3.00	2,454	9,111	3.71
√	4.50	1,280	2,901	2.27

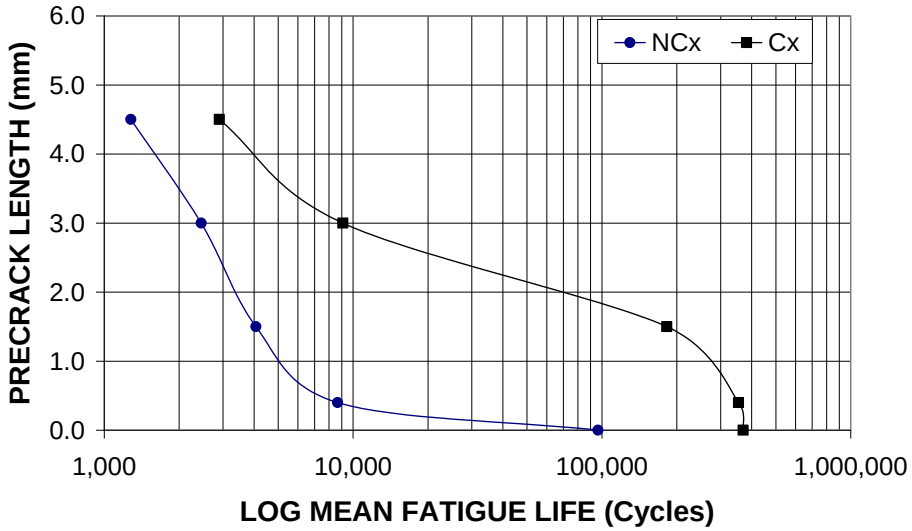

Figure 1 Effect of pre-existing cracks on the fatigue life of open hole coupons and the benefits of hole cold expansion technology. The results relate to constant amplitude loading at a maximum applied net stress = 172.4 MPa (25 ksi) and at an R = 0.1.

Fatigue Life under Variable Amplitude Spectrum Loading: Initially, the fatigue tests under variable amplitude loading were carried out at a stress level representative of a transport aircraft wing structure spectrum, 125.5 MPa (18.2 ksi), on coupons of similar configuration and conditions to those of constant amplitude testing. At the stress level used, the fatigue tests on cold expanded specimens with the pre-existing crack lengths up to 3 mm were terminated without any failure because no crack growth could be discerned even after several million segments of loading and several days of testing. The specimens with a pre-crack length of 4.5 mm, however, failed even after cold expansion, giving a life improvement factor of 16.28 for this condition. This is an encouraging test result in the context of service aircraft structures in offering a potential solution by providing an option of using corrective action early in the through-life support maintenance cycle, when the cracks are likely to be short. Testing was then continued at a higher stress level of 172 MPa or 25 ksi (the same stress level that was used in the constant amplitude tests) to achieve valid failures in the cold expanded specimens. The fatigue life improvement factors obtained in variable amplitude tests at 172 MPa for pre-crack lengths of 3.00 and 4.5 mm were 22.23and 7.77, respectively. The log mean fatigue life and pre-crack lengths results are shown in Figure 2.

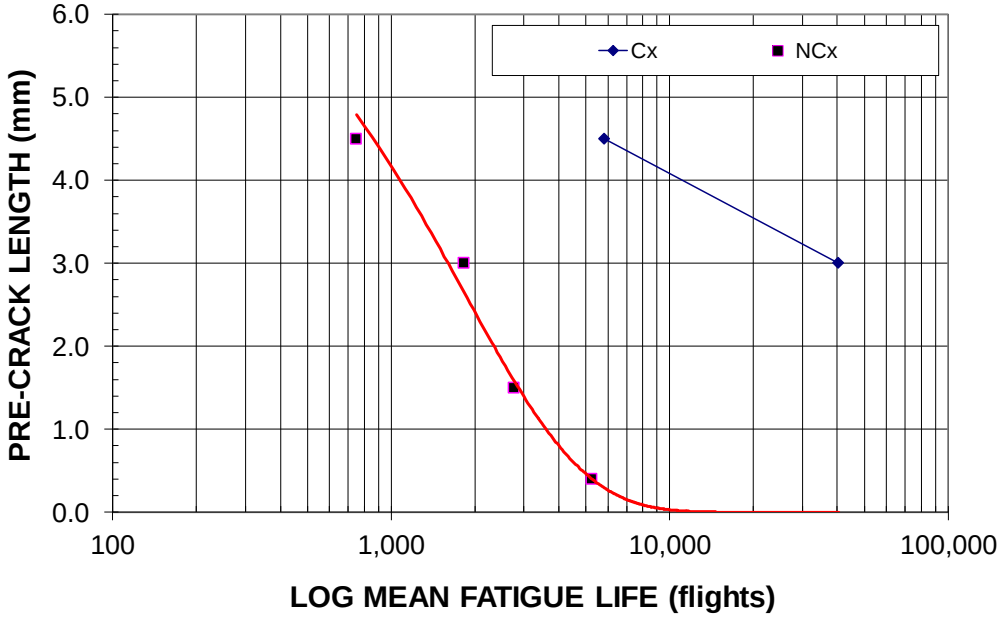

Figure 2 The effect of pre-existing cracks on the fatigue life of open hole coupons and the benefits of hole cold expansion technology. The results relate to variable amplitude loading at an applied maximum net stress = 172 MPa (25 ksi).

Summary of findings

The hole cold working technology was demonstrated to be effective and beneficial on open hole (ZLT) specimens with pre-existing cracks up to 4.5 mm in length. Hole cold working always improved the fatigue life of open hole specimens containing cracked or uncracked holes. The presence of cracks reduced the fatigue life of both cold worked and non-cold worked specimens. The LIF for specimens that contained cracks decreased with increasing pre-crack length.

References

[1] W. H. Cathey, A. F. Grandt, Jr., Fracture mechanics consideration of residual stresses introduced by cold working fastener holes, Journal of Engineering Materials and Technology, 102 (1980) pp. 85-91.

[2] L. Reid, Aging aircraft repair strategies utilizing cold expansion technologies – Part 1, The science of cold expansion, PowerPoint presentation, Ageing Aircraft User's Forum, 23-25 May, 2007, Brisbane, Australia.

[3] FTI., Cold expansion of holes using the standard split sleeve system and countersink cold expansion™ (CsCx™), FTI Process Specification 8101D, (2002)Fatigue Technology Inc., Seattle, USA.

[4] P. S. Baburamani, R. Ogden, Q. Liu, P. K. Sharp, The application of cold expansion technology to AA7075-T7351 open hole coupons with pre-existing cracks and its effect on constant amplitude fatigue life, DSTO-TN-1170, Commonwealth of Australia, 2013, 20p.

4.14 Experimental Evaluation of Supersonic Particle Deposition Technology for Aircraft Structural Repair (Wyman Zhuang, DSTO)

Supersonic particle deposition (SPD), also called cold spray, is one of the additive manufacturing technologies. It has been used to add material to repair corrosion and wear

damage in aircraft components and structures. The technology employs supersonic inert gas jet to accelerate powder particles that impact onto a substrate to form a solid-state deposit. Although the technology has already been used for the reclamation of various metallic components [1, 2], it was mainly for dimensional restoration and environmental protection [3, 4, 5]. The technology has not been certified and accepted as an aircraft structural repair for restoring structural strength of load-bearing components or improving fatigue preformance. In recent years, there have been studies to develop the capabilities of the SPD technology for the restoration of aircraft structural integrity of primary and secondary structure [6, 7].

Considering the stringent airworthiness standards for the certification of aircraft structural repairs, the main objectives of this research program are to conduct experimental assessments, ranging from coupon to full-scale fatigue tests (*Figure 1*), and to provide a body of evidence for evaluating technology readiness levels for restoring structural strength in accordance with relevant airworthiness requirements. Currently only aluminium alloy powders have been considered. As the tests are still under way some of the preliminary results are discussed below.

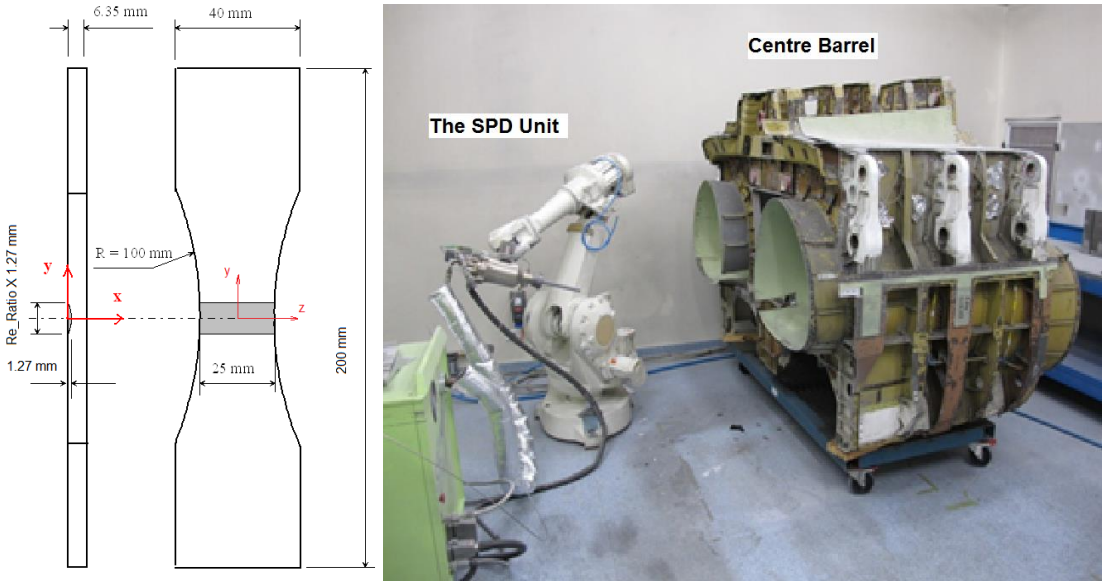

(a) (b)

Figure 1: (a) The SPDed coupons and (b) full-scale test article.

Figure 2 shows the effect of corrosion damage repair blend-out ratio (Re_Ratio = blend-out length/depth as shown in *Figure 1* (a)) on fatigue life of the SPDed coupons. It indicated that increasing the repair blend-out ratio will increase the fatigue life of the SPD repaired coupons. A variable amplitude spectrum representative of fighter aircraft wing root loads was applied at a loading frequency of 5 Hz.

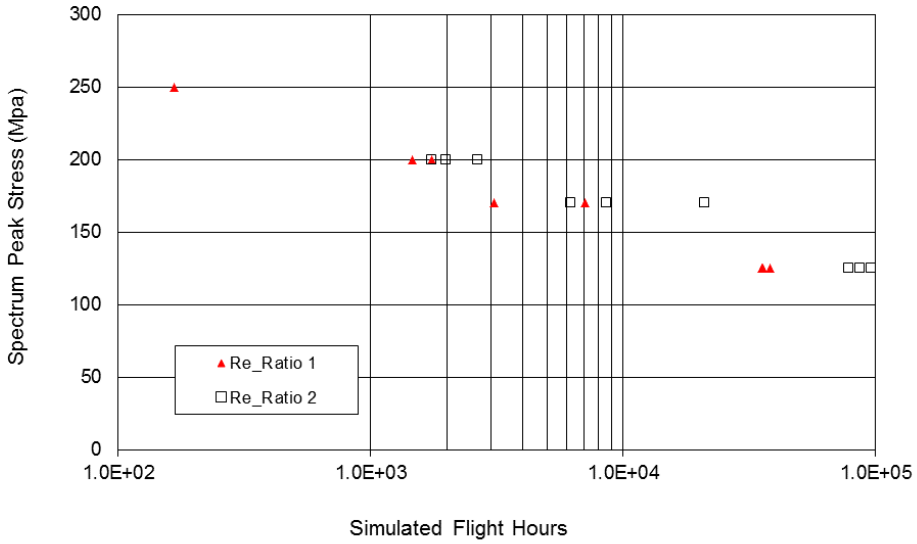

Figure 2: The effect of blend-out ratio (Re_Ratio 1 < Re_Ratio 2) on fatigue life of SPDed coupons.

For the technology assessment using full-scale fatigue test, two ex-service F/A-18 centre barrels were coated by the SPD technology in several locations. The full-scale fatigue tests have so far demonstrated that there is no indication of the failure of the SPD coatings on one centre barrel after two simulated lifetimes using the non-destructive inspection techniques while the SPD coatings on the other centre barrel failed in the early stage of the fatigue testing. The failure analysis is currently under way.

References

[1] A. Papyrin, V. Kosarev, S. Klinkov, A. Alkimov and V. Fomin, Cold Apray Technology, *Elsevier*, 2007.

[2] P. F. Leyman and V. K. Champagne, Cold Spray Process Development for the Reclamation of the Apache Helicopter Mast Support, *ARL-TR-4922*, Army Research Laboratory, 2009.

[3] D. Gerrard et al, Cold Spray Coating Technology for the Corrosion Protection and Repair of JSF / Aerospace Components, *ASM TSS Cold Spray*, USA, 2007.

[4] V. K. Champagne, P.F. Leyman, and D. J. Helfritch, Magnesium Repair by Cold Spray, *ARL-TR-4438*, US Army Research Laboratory, 2008.

[5] Department Of Defense, Department of Defense Manufacturing Process Standard: Materials Deposition, Cold Spray, *MIL-STD-3021*, USA, 2011.

[6] N. Matthews, R. Jones and G. C. Sih, Application of Supersonic Particle Deposition for Enhancing the Structural Integrity of Aircraft Structures, *International Conference on Airworthiness & Fatigue - 7th ICSAELS Series Conference*, Beijing, China, 25-27 March, 2013.

[7] R. Jones, L. Molent, S. Barter, N. Matthews, D. Tamboli, Supersonic particle deposition as a means for enhancing the structural integrity of aircraft structures, *International Journal of Fatigue*, Vol. 68, pp. 260–268, 2014.

4.15 Automated Ultrasonic Non-Destructive Inspection Capability Validation for the C-130 Centre Wing Lower Surface (M Khoo, C. Rowe, A. Smith – [DSTO])

The issue of widespread fatigue damage (WFD) may become relevant for the structural integrity management of the Royal Australian Air Force (RAAF) C-130J-30 fleet in coming years. Following on from the 2011 inspection of a C-130J wing fatigue test article in Cambridge, UK [1], a capability validation of the inspection procedure was carried out to assess widespread fatigue damage detection performance in the second-layer centre wing lower surface structure (CWLS) [2]. Ultimately, the intent is to validate this capability for use on the C-130J wing fatigue test and the RAAF C-130J-30 fleet.

Two ex-service C-130 CWLS sections from different sources were used in this study and the ultrasonic amplitude attenuation distributions due to the faying surface, or interface, between the structural layers were characterised using back face reflector slots.

The effect of the ultrasonic attenuation on the relationship between defect size and ultrasonic indication area was then characterised using artificial defects inserted in the fastener holes of an aluminium specimen representative of the aircraft wing structure. By convoluting these data with the ultrasonic attenuation distribution observed in the C-130 wing panels, the probability of detection (POD) of second-layer defects could be calculated, see Figure 1, using a method adapted from the MAPOD study previously conducted for the RAAF F-111 lower wing skin [3].

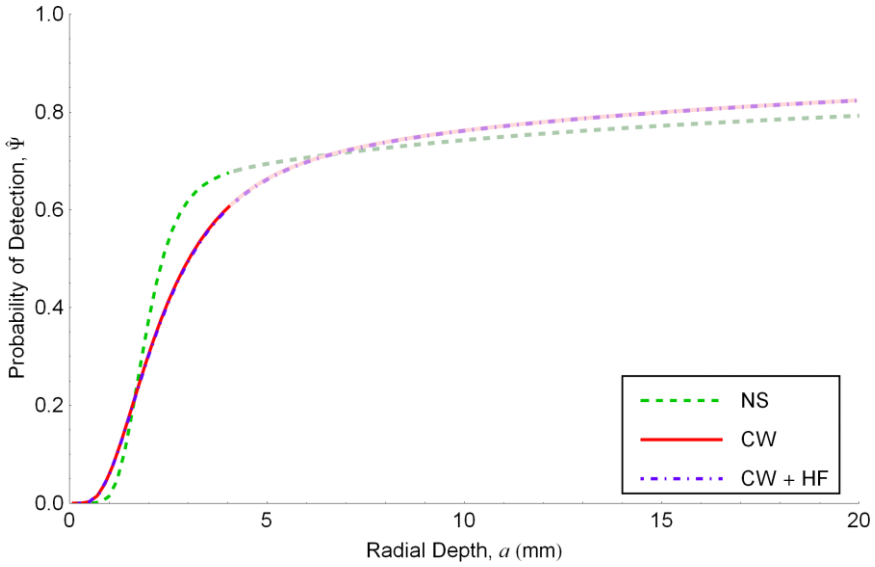

Figure 1 POD curves for baseline case of artificial notch detection in second layer of simple geometry (NS) as well as fatigue cracks in wing structure (CW) and CW with human factors included (CW+HF) (5 MHz ultrasound, faded line denotes extrapolated data)

While the 5 MHz ultrasonic inspections were shown to achieve higher penetration into the second-layer wing structure than higher frequency 15 MHz ultrasound, the variability in the faying surface condition adversely affected the overall performance of the ultrasonic inspection at both inspection frequencies. In addition to the baseline case of artificial notches in simple geometry, several POD-influencing factors were considered, including the effect of fatigue

cracks in complex wing structure, human factors and the change in attenuation distribution observed between different sides of the hole relative to the stringer hat section.

Based on the results of the POD assessment, automated ultrasonic inspections of the CWLS second layer do not appear to perform as well as the surface-scan eddy current inspections currently prescribed for C-130 WFD inspections. It must be noted that the results of this study are based on the ultrasonic attenuation distributions observed in ex-service wing sections which are assumed to be representative of high-time C-130 CWLS structure and thus care must be taken when interpreting the results for fleet inspections.

Contact email: Matthew.Khoo@dsto.defence.gov.au

References

[1] D. Hartley, M. Khoo, G. Hugo and J. Duncombe, 'Automated Ultrasonic Non-Destructive Inspection of the C-130J Wing Fatigue Test Article Centre Wing Lower Surface', Report No. DSTO-TR-2718, Defence Science and Technology Organisation, Australia (2012).
[2] M. Khoo, C. Rowe and A. Smith, 'Automated Ultrasonic Non-Destructive Inspection Capability Validation for the C-130 Centre Wing Lower Surface', Report No. DSTO-TR-3029, Defence Science and Technology Organisation, Australia (2014).
[3] C. A. Harding, 'Methods for Assessment of Probability of Detection for Nondestructive Inspections', Thesis, Department of Mathematics and Statistics, The University of Melbourne, 2008.

4.16 Ultrasonic Inspectability of Multi-Layer Aircraft Structure: Normal-Incidence Ultrasonic Inspections for Sealant Quality Assessment (A. Smith, M. Khoo - DSTO)

The detection of fatigue cracks in multi-layer aircraft structure is a challenging problem for ultrasonic non-destructive inspections, but it is also a potentially valuable capability for the Royal Australian Air Force (RAAF) to possess for the fatigue-life management of its aircraft. An automated ultrasonic inspection of the Centre Wing Lower Surface (CWLS) of a C-130J wing fatigue test article was previously trialled for the detection of widespread fatigue damage [1]. During the subsequent capability validation of the automated ultrasonic inspection procedure [2], an investigation was carried out to determine whether or not normal-incidence ultrasonic inspections can be used to assess the quality of the faying surface for ultrasonic transmission and thus the effectiveness of angle-beam ultrasonic inspections of wing structures beyond the external wing skin [3].

Three visual inspection methods were used to investigate the correlation between normal-incidence ultrasonic response and the four possible faying surface sealant conditions of the ex-service C-130 CWLS sections that were proposed to exist (Figure 1).

The three methods included:

1. visual inspection of the faying surface sealant presence around the edges of extracted fastener hole coupons and comparison with corresponding normal-incidence ultrasonic C-scans

2. visual inspection of the sealant distribution along separated fastener rows and comparison with corresponding normal-incidence ultrasonic C-scans (Figure 2)

3. visual inspection of the faying surface sealant presence around the edges of an extracted a fastener hole coupon and comparison with corresponding normal-incidence contact-probe spot measurements from both sides of the coupon

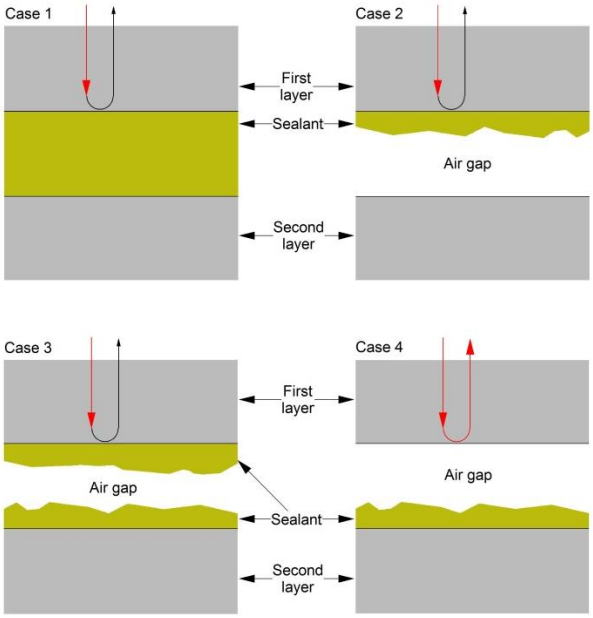

Figure 1 A schematic diagram showing the four possible sealant conditions (excluding no sealant presence) in the faying surface of a two-layer wing structure. Note that the vertical arrows in the diagram represent the predicted amplitude of the incident and reflected normal-incidence ultrasound.

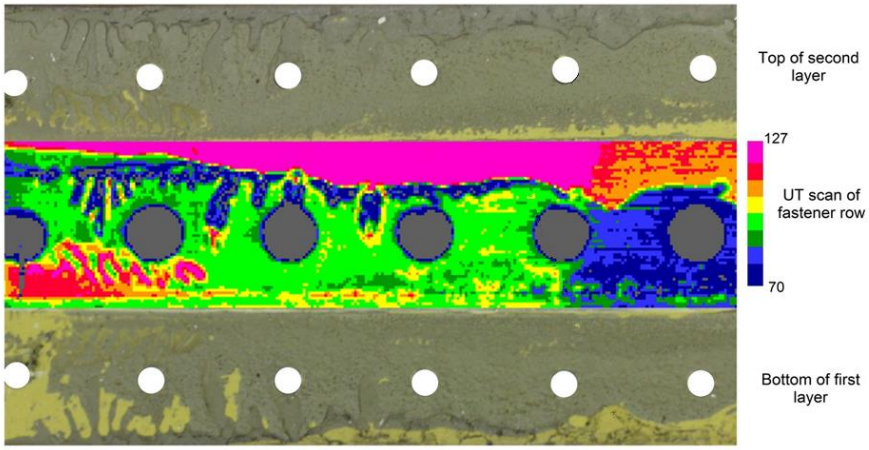

Figure 2 Comparison of a normal incidence ultrasonic C-scan with photographs of separated two-layer C-130 wing structure. Note that many of the features in the ultrasonic C-scan correspond to the sealant distribution in the wing structures.

The results showed that normal-incidence ultrasonic inspections provide only a limited amount of information about the faying surface condition. While patterns in the sealant distribution could be observed in the normal-incidence ultrasonic C-scans (Figure 2), a detailed analysis of the ultrasonic response from each sealant condition showed that normal-incidence ultrasonic inspections could not be used to comprehensively assess the quality of the faying surface for ultrasonic transmission. Based on these findings, it was concluded that it is not currently feasible to use normal-incidence ultrasonic inspections to assess the effectiveness of angle-beam ultrasonic inspections for fatigue-crack detection in the C-130 multi-layer wing structure.

The knowledge gained from this study will help the RAAF to better understand the feasibility and future challenges of employing ultrasonic inspections for widespread fatigue-crack detection in multi-layer aircraft structure.

Contact email: adam.smith@dsto.defence.gov.au

References

[1] D. Hartley, M. Khoo, G. Hugo and J. Duncombe, 'Automated Ultrasonic Non-Destructive Inspection of the C-130J Wing Fatigue Test Article Centre Wing Lower Surface', Report No. DSTO-TR-2718, Defence Science and Technology Organisation, Australia (2012).

[2] M. Khoo, C. Rowe and A. Smith, 'Automated Ultrasonic Non-Destructive Inspection Capability Validation for the C-130 Centre Wing Lower Surface', Report No. DSTO-TR-3029, Defence Science and Technology Organisation, Australia (2014).

[3] A. Smith and M. Khoo, 'Ultrasonic Inspectability of Multi-Layer Aircraft Structure: Normal-Incidence Ultrasonic Inspections for Sealant Quality Assessment', Report No. DSTO-TN-1377, Defence Science and Technology Organisation, Australia (2014).

4.17 Damage Tolerance Analysis - PA-31-350 Spar Life Extension (Aviation Engineers Pty Ltd, Millard Kwan)

The Piper Chieftain PA-31-350 Aircraft (Figure 1) was developed on May 3, 1972 with production of the aircraft in 1973. The Piper Chieftain was a modified version of the Piper Navajo which was certified under CAR 3 and included the lengthening of the fuselage by 2 ft. with more powerful engines with counter rotating propellers. Since then, 40 years down the track, these aircraft remain serviceable and continue to fly.

Figure 1: Piper Chieftain PA-31-350 Aircraft

Due to the continued development on fatigue evaluation on structures within the same time of certification, the Civil Aviation Safety Authority (CASA) Australia required that the Piper Aircraft Corporation perform a Fatigue Evaluation on their Piper Navajo and Chieftains prior to being eligible for an Australian Certificate of Airworthiness.

On the 31st March 1975 Civil Aviation Safety Authority (CASA) Australia released the original issue of the Airworthiness Directive (AD/PA-31/37) which comprised of a retirement schedule on the aircraft's Wing Main Spar Lower Cap.

Since the original release of the AD, CASA has allowed operation beyond the retirement limit on the condition that an inspection program be developed which incorporates a Damage Tolerant analysis of critical parts per FAR 23.573(b).

Aviation Engineers Pty Ltd was engaged by Flying Fighters Pty Ltd to conduct a damage tolerance analysis to extend the life limitation implemented by the AD for continued flight of the aircraft beyond the specified limit.

To perform the detailed damage tolerance analysis on the main wing lower spar cap assembly Aviation Engineers required a thorough investigation on the wing assembly of the aircraft. Aviation Engineers acquired a previously serviceable Piper Chieftain Wing to gain the required knowledge to perform the analysis. Using the Piper Chieftain Wing, material chemical analysis and hardness testing of parts was used to determine the original material layup of the Main Spar Cap Assembly. Wing skins were removed to view the dimensional characteristics of the spar assembly and attaching structures, web reinforcements, ribs and nesting angles.

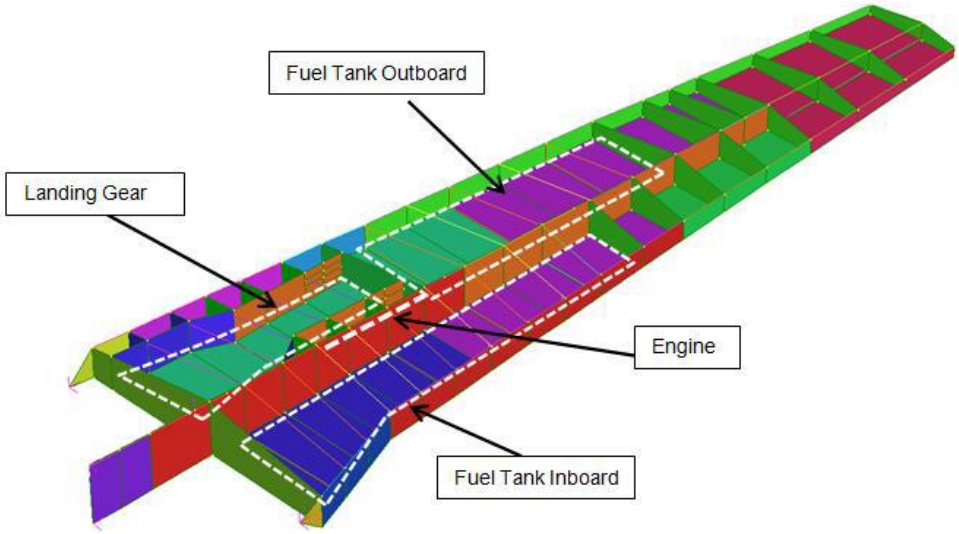

Figure 2: Finite Element Model

The project was aimed to maintain a conservative analysis using the "Rough Diamond" approach (Site, Scenario, Detectable, Dangerous and Duration) developed by Steve Swift of the Civil Aviation Safety Authority, Australia and Bob Easton of the Federal Aviation Administration, USA, as the basis for the damage tolerance analysis. Fracture mechanics forms a large portion of the damage tolerance analysis. However, damage tolerance does not only comprise of a fracture mechanics analysis, it is a detailed evaluation which also involves reviewing all modes of damage including corrosion or accidental damage.

The FAA Advisory Circular AC23.13A was utilized during the project to provide conservative Ground-Air-Ground cycles which is based on statistical analysis for similar aircrafts. Using all the information gathered throughout the life of the project in conjunction with Structural Stress Analysis, Finite Element Modeling (Figure 2), and Fracture Mechanics - Crack Growth Modeling (using AFGROW), a safe inspection interval was determined.

From the detailed investigation, stress analysis, flight strain surveys, finite element and fracture mechanic tools, a damage tolerance analysis was used to provide the inspections and modifications necessary to ensure the continued structural integrity of the airplane beyond the retirement schedule specified in the AD.

5. FATIGUE INVESTIGATIONS OF IN-SERVICE AIRCRAFT

5.1 Failure Analysis Examples in Military Aircraft - Nick Athiniotis, (DSTO)

5.1.1 RAAF Hawk 127 In-Flight Engine Failure- Low Pressure Turbine Blade Failure.

The pilots of a RAAF Hawk MK127 aircraft heard a loud bang followed by airframe vibrations. The aircraft landed safely. The Forensic investigation concluded that the LPT blade had failed as the result of a fatigue crack arising from a high nominal stress at the rear acute corner with other contributing factors. The crack propagated over numerous flights driven by engine start/stop cycles, engine partial cycles and likely engine vibration. The Investigation found no material abnormalities that indicated the life of the failed blade fell outside the normal population and therefore this failure did not represent an anomalous event.

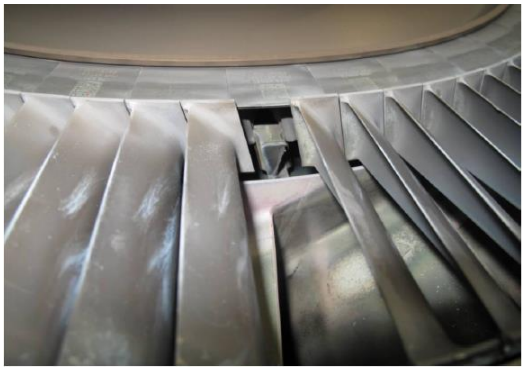

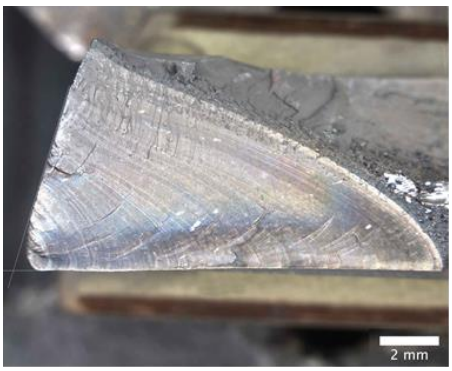

5.1.2 AS350BA Gimbal Joint Throttle Rod Assembly Failure

Following loss of pilot throttle authority, examination of the pilot's throttle twist grip assembly discovered that the upper 'beak' of the gimbal to the lower control rod had fractured.

The Forensic investigation determined that failure was due to intergranular cracking through the case hardened surface, which led to the propagation of fatigue cracks before final failure occurred. Since no surface damage was associated with the crack and no material defects were observed, it was likely intergranular cracking was due to problems encountered during the case hardening process.

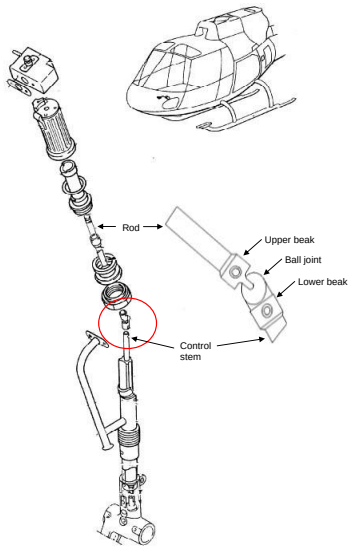

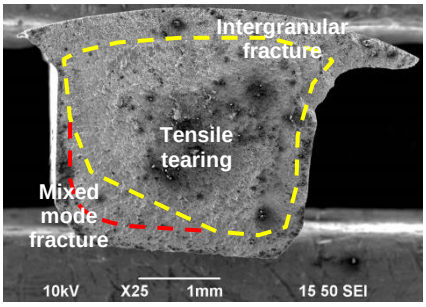

SEM photograph of the upper beak with the different fracture regions

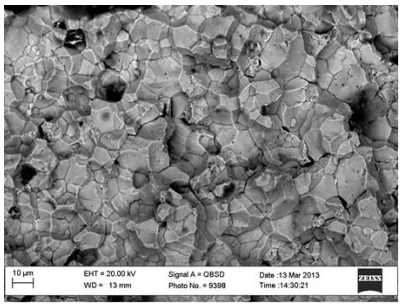

SEM image of intergranular cracking

5.1.3 Black Hawk Tail Wheel Failure

The aircraft had returned from a flight and was being towed back to the maintenance hangar when the wheel failure occurred. Failure of a Black Hawk tail wheel was found to be due to fatigue cracking at the bead seat. Fatigue cracks had initiated from silicon particles in the microstructure which had fractured under load. The bead seat radius is typically a region of high bending stress, and is therefore prone to initiation and growth of fatigue cracks. In this case, the wheel experienced loads that were sufficient to fracture the silicon intermetallic particles, and fatigue cracking propagated from these cracked particles via loading from operational stresses arising during aircraft landing and taxiing.

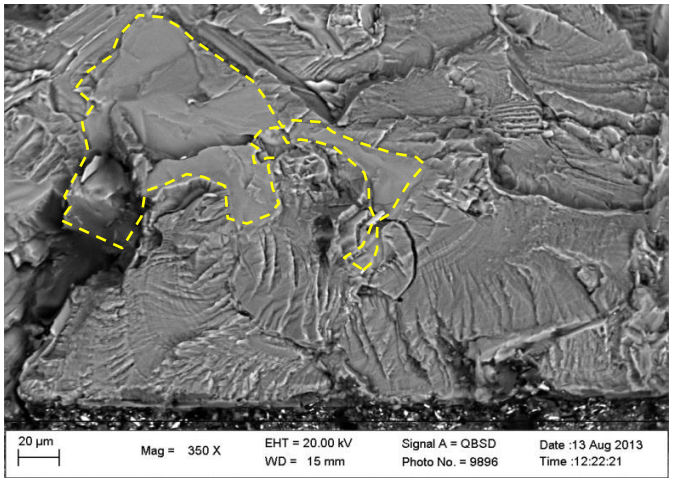

Photograph of the failed wheel and liberated wheel fragments, which encompassed approximately 75% of the circumference

SEM photographs showing fatigue cracks originating from fractured silicon intermetallic particles, outlined in dashed yellow

5.1.4 AP-3C Orion Bleed Air Duct Swivel Joint Failure

The swivel joint, a bleed air manifold, attaches aircraft bleed air ducting at the engine firewall to the engine Failure resulted in aborted take-off and engine change. The examination revealed that the flange failed due to a combination of stress-corrosion cracking and fatigue. The weld joint configuration resulted in crevices in which moisture and environmental contaminants were able to collect. Localised stress-corrosion cracking likely initiated due to the combination of joint design, environmental ingress, temperature, a susceptible material and the presence of sustained stresses.

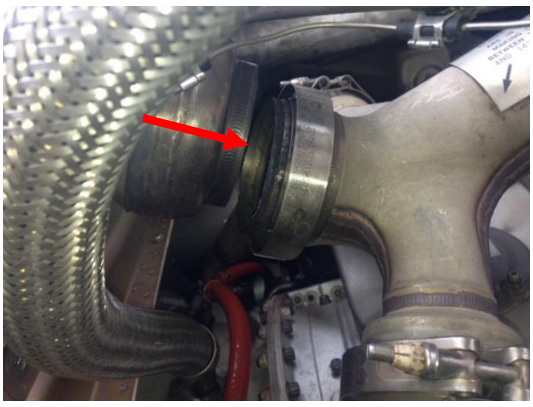

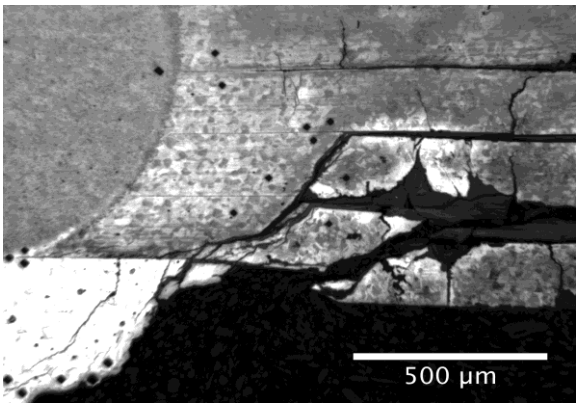

Photo of Bleed Air Duct Swivel Joint failure in-situ.

Photomicrograph of a section of the completely failed seam welded joint emanating from the root of the crevice formed between the innermost piece of the material and the first layer of the flexible bellows.

5.2 In-Flight Break-up of a de Havilland DH82A Tiger Moth (Australian Transportation Safety Board, preliminary report AO-2013-226)

On 16 December 2013, at approximately 1215 Eastern Standard Time, a de Havilland DH82A (Tiger Moth) aircraft, registered VH-TSG, took off from the operator's airstrip at Pimpama, Queensland with a pilot and passenger on board. The purpose of the flight was to conduct a commercial joy flight in the Gold Coast area. At about 1224, 1 minute after the pilot commenced aerobatics, the left wings failed and the aircraft descended steeply; impacting the water about 300m from the eastern shoreline of South Stradbroke island. The aircraft was destroyed and the two occupants were fatally injured.

Preliminary examination indicated that both of the aircraft's fuselage lateral tie rods, which join the lower wings to the fuselage, had fractured at areas of significant, pre-existing fatigue cracking in the threaded section near the join with the left wing.

The ATSB has not, at this preliminary stage of its investigation, determined whether the failure of the fuselage lateral tie rods, or another mode of wing structural failure, was the initiator of the left wing separations. However, the Preliminary Report included a safety issue that advises of the JRA-776-1 tie rod fatigue cracking and included a Safety Advisory Notice to Tiger Moth operators about this safety issue.

Up until 1997, there were no requirements for inspecting or replacing lateral tie rods in Tiger Moth aircraft. However, in July 1996, during a routine maintenance activity in the UK on a UK-registered DH82A aircraft, it was found that a lateral tie rod had fractured at the thread root. Subsequent examination found that there was significant pre-existing fatigue cracking at the point of failure. At the time of the failure, the aircraft had accrued 7,556 hours in service. A subsequent Technical News Sheet (TNS) CT (MOTH) No 29 Issue 3 called for both lateral Fuselage Tie Rods to become "lifed items" restricted to a service life of 2000 flying hours or 18 years. The service life of the two JRA-776-1 fuselage lateral tie rods fitted to de Havilland DH82A Tiger Moth, were significantly less than this limit as they were about 7 years old and had accrued about 1,300 flight hours

Figure 1: the aircraft

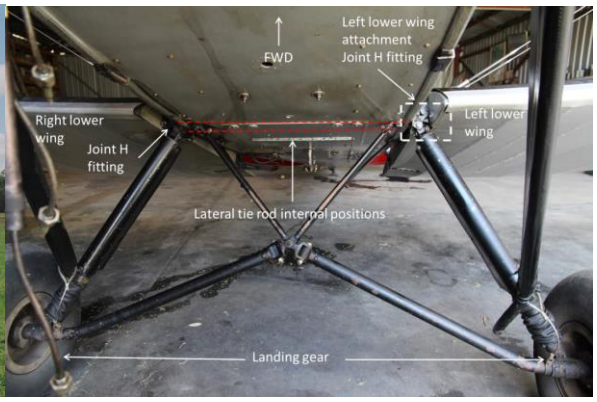

Figure 2: The position of the tie rods

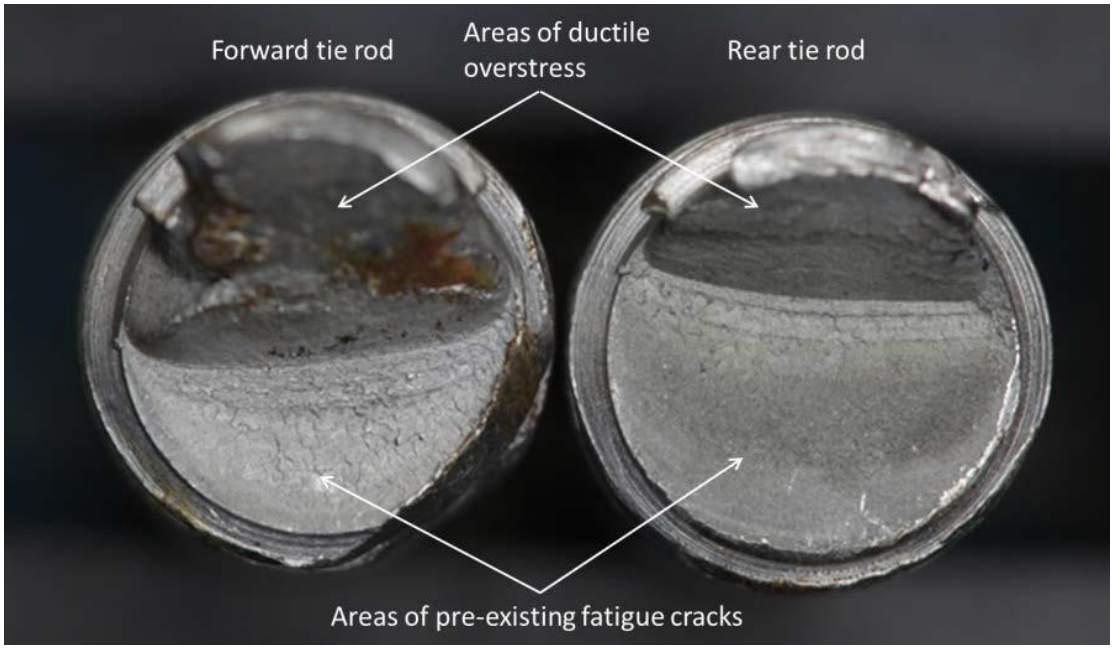

Figure 3: The tie rod failure cross-sections at the base of the LHS threaded sections


Figure 4: Threaded section of the tie rod. The black line in the base of the first thread is the crack

Both lateral tie rods fractured at an area of pre-existing fatigue cracking (Figure 3) within the threaded section. The rear tie rod cracking extended across approximately 70 per cent of the total rod cross-sectional area and the forward rod cracking extended across approximately 50 per cent. The remainder of the fractures on both rods was consistent with ductile overstress. No significant corrosion was evident at or surrounding the points of fracture. Pre-existing fatigue cracking was also evident in the threaded section of the right end of the forward lateral tie rod (Figure 4). The crack had propagated in the same thread-root area as the left side, although the rod had not completely fractured in that area. The crack extended across about 40 per cent of the cross-sectional area.

The aircraft carried a video camera mounted in front of the front occupant which captured the in-flight event.

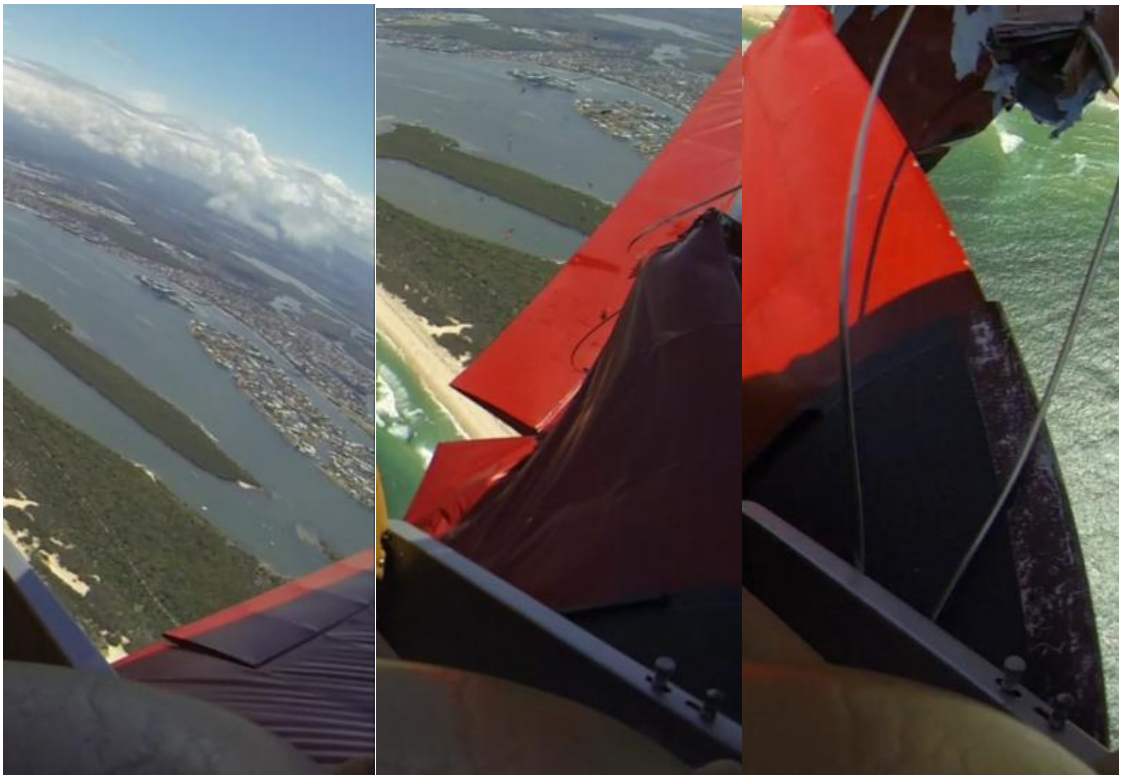

Frame 1: Failure Initiation *Frame 2: 0.15 of a second* *Frame 3: 0.35 of a second*

Figure 4: Frames from the aircraft mounted video camera.

In it's preliminary report, the ATSB cited the following associated factors that were under investigation:

1. That the tie rods were not manufactured by the OEM (the origin of the failure upon which inspections and service life limits were set) but were made in Australia to specified (but not exactly the same) material and manufacturing processes.

2. That the Australian aircraft had been undertaking considerable aerobatic flying which may not have been equivalent to the usage associated with the original failure and may have adversely affected the initiation and growth of cracking.

3. That the supplementary inspections specified to be carried out for adverse incidence such as a heavy landing would not have found rod end thread cracking of the nature existing in the Australian aircraft.

References

[1] ATSB Transport Safety Report, Aviation Investigation AO-2013-226, Preliminary – 24 February 2014 "In-flight break-up involving de Havilland DH82A Tiger Moth, VH-TSG 300m east of South Stradbroke Island, Queensland, 16 December 2013" atsbinfo@atsb.gov.au

5.3 In-flight breakup involving PZL Mielec M18A Dromader aircraft, VH-TZJ, 37 km west of Ulladulla, NSW on 24 October 2013 (Australian Transportation Safety Board, Interim report AO-2013-187)

On 24 October 2013, at about 0940 Eastern Daylight-saving Time, the pilot of a PZL Mielec M18A Dromader, registered VH-TZJ, took off from Nowra Airport to conduct a firebombing mission in the Budawang National Park about 37 km west of Ulladulla, New South Wales. At about 1004, while the aircraft was approaching the target point, the left wing separated. The aircraft immediately rolled left and descended, impacting terrain. The aircraft was destroyed by impact forces and the pilot was fatally injured.

Preliminary examination indicated that the left outboard wing lower attachment lug had fractured through an area of pre-existing fatigue cracking in the lug lower ligament.

Figure 1: The crash scene.

Figure 2: The aircraft

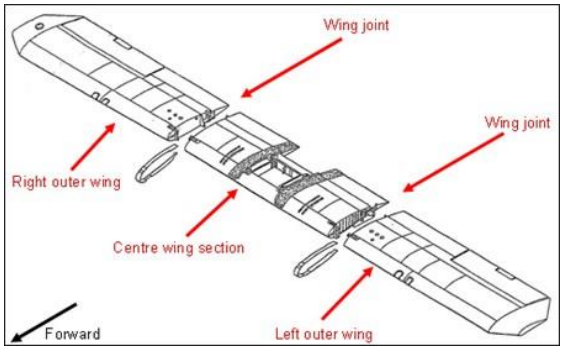

Figure 3: The wing sections

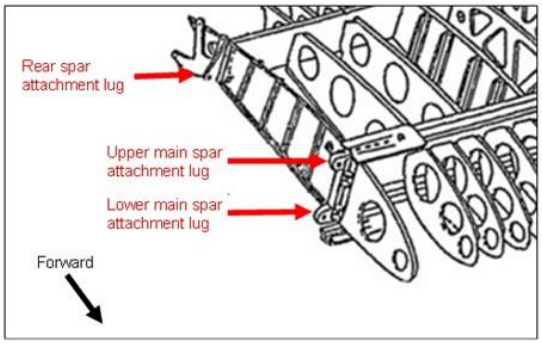

Figure 4: Close-up of the wing lugs

Figure 5: The left hand wing spar and lower attachment lug as found at the crack scene

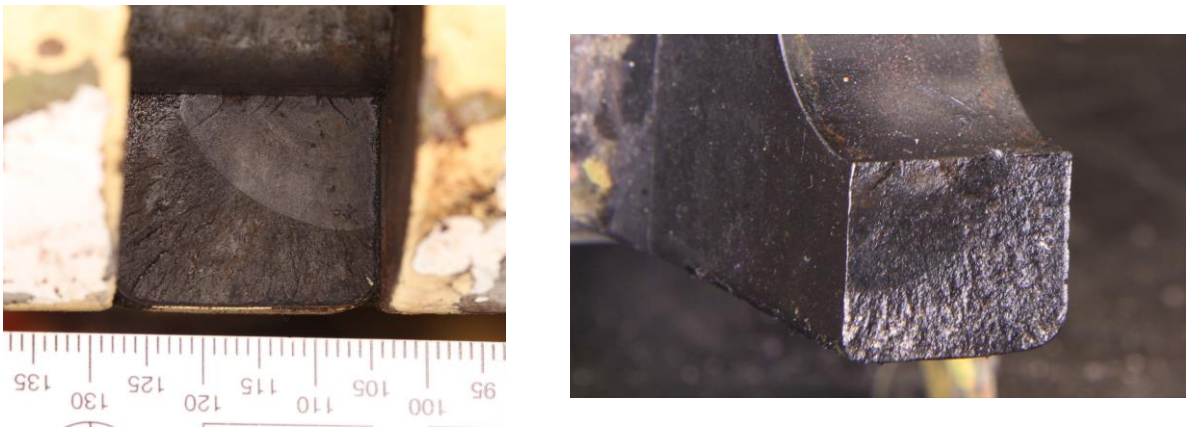

Figure 6: The mating surfaces of the fatigue crack in the left hand lower lug

Following M18 Dromader accidents that occurred in the United States involving in-flight wing separation, in September 2000, the United States Federal Aviation Administration issued Airworthiness Directive (AD) 2000-18-12. This AD required repetitive inspections of the centre wing to outer wing attach joints for 'cracks in the lugs, corrosion in the main holes, and ovalization of the main holes'. On 19 October 2000, the Australian Civil Aviation Safety Authority (CASA) issued AD/PZL/5 with the same basic inspection requirements.

In accordance with AD/PZL/5, inspections were required every 500 hours time in service or every 12 months, whichever came first. The wings of VH-TZJ were last inspected on 8 August 2013. Up to 17 October, the aircraft had accumulated about 110 hours time in service since the last wing inspection.

The investigation is continuing and will include examination of the:

1. wing inspection requirements

2. inspection methods

3. history of the aircraft's operations and maintenance.

The ATSB issued an Interim Report in order to highlight a safety issue that had been identified after the release of the Preliminary Report on 2 December 2013, vis:

Operators of some Australian M18 Dromaders, particularly those fitted with turbine engines and enlarged hoppers and those operating under Australian supplemental type certificate (STC) SVA521, have probably conducted flights at weights for which airframe life factoring was required but not applied. The result is that some of these aircraft could be close to or have exceeded their prescribed airframe life, increasing the risk of an in-flight failure of the aircraft's structure.

References

[1] ATSB Transport Safety Report, Aviation Investigation, Interim report AO-2013-187, In-flight breakup involving PZL Mielec M18A Dromader aircraft, VH-TZJ, 37 km west of Ulladulla, NSW on 24 October 2013

6. NEW ZEALAND

6.1 Application Of Digital Flight Data For RNZAF C-130H(NZ) Usage Monitoring (C. J. Barnes, Defence Technology Agency c.barnes@dta.mil.nz)

Currently the RNZAF tracks its C130 usage based on manual logbook entries from the aircrew. The logbook information includes parameters such as flight duration, landings, mission code etc. Usage tracking using the traditional approach often leads to coarse approximations of actual usage and therefore a high degree of conservatism is necessary in any usage analysis for fatigue life assessments.

As part of the RNZAF's C130 Life Extension Project (LEP) a flight data monitoring system was installed to track fatigue consumption with greater fidelity. The system hardware is mature and is commonly used in commercial aviation; however the current supporting software is limited to decoding the raw data from a proprietary format into a human readable format. Moreover the supporting software is unable to analyse the raw data. DTA has developed customised algorithms to decode and analyse the data with the aim of exploiting the available data for higher fidelity usage tracking.

The current method to determine fatigue life consumption is to categorise each flight from the logbook data into one of many predefined mission profiles. There are a range of profiles that cover logistics missions, parachute missions, low-level tactical missions and training flights. The aircraft OEM attaches a severity factor to each mission profile which is a measure of the fatigue damage accumulation. Broadly speaking the higher the severity factor the more fatigue damage is accrued. The service life for the wings is defined by an Equivalent Baseline Hours (EBH) limit, with EBH being the multiple of the profile severity factor and the actual flight duration. The severity factors were developed by the OEM from historical crack growth analysis and instrumented flight testing on USAF aircraft.

In practice, the categorisation process is only completed once using the available logbook data which results in average severity factors derived from the historical usage which are then taken forward and used for future assessments.

Digital flight data at 1Hz was recorded through the RNZAF monitoring system. A method was investigated to use this data to directly establish flight severity factors rather than 'pigeon holing' the flights into pre-defined profiles, and the approximations and assumptions that this incurs. The method used the mean airspeed, altitude and aircraft weight for each 60 second period of the flight and calculated the severity factor throughout the flight. The intention is not to use the method authoritatively at present, but is intended to highlight the potential benefits, in terms of life extension, that could be possible by using higher fidelity data.

Figures 1 and 2 show the results of the direct method (labelled SFD method) compared with the OEM method. Additional validation was also carried out with the available digital data; where actual flights closely matched one the predefined profiles then the severity factor from the direct method could be compared against the severity factor from the OEM. In general, the direct method provided conservative severity factor values.

When the direct method was applied to the approximately 2700 hours of available flight data across three aircraft, the average severity factors were lower than those from the traditional methods resulting in less overall EBH accrual.

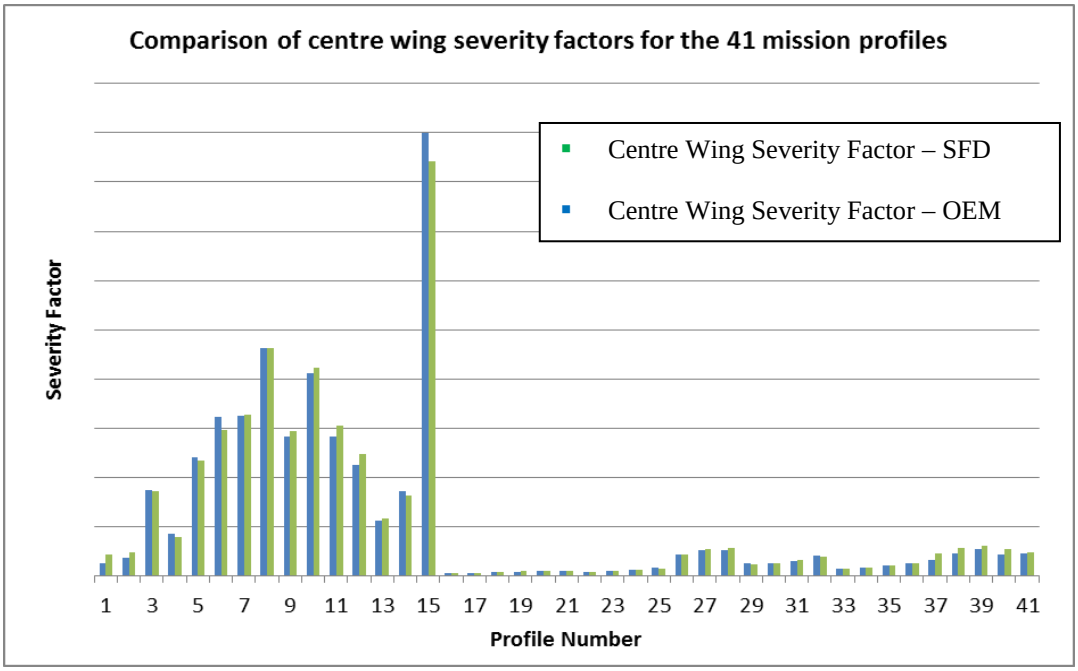

Figure 1. Comparison of the SFD results against OEM severity factors for the 41 mission profiles[6]

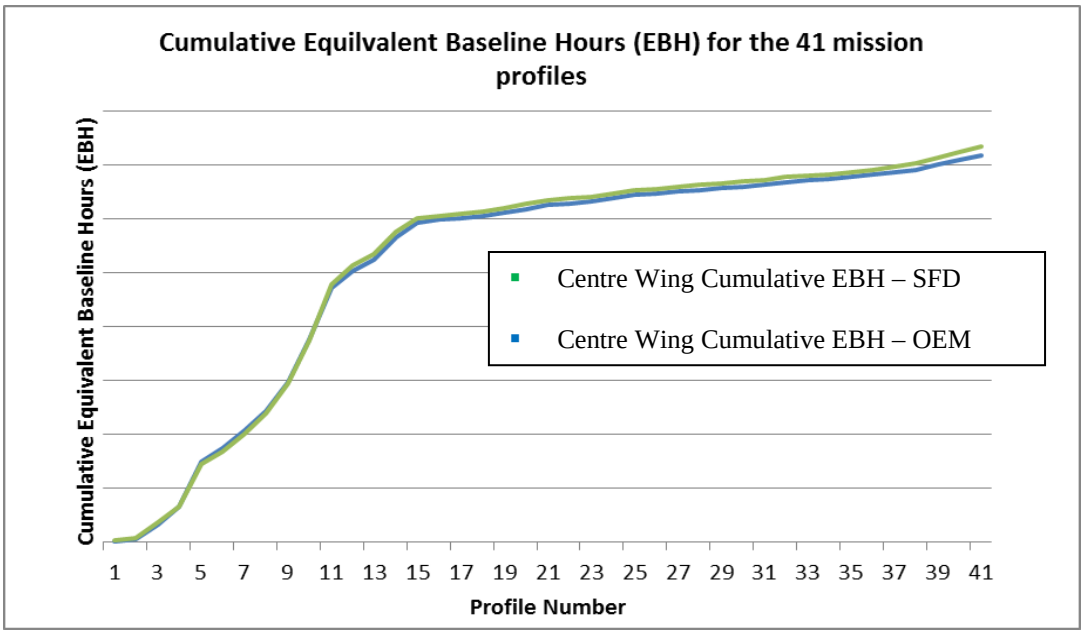

Figure 2. Comparison of the cumulative Equivalent Baseline Hours (EBH) for the 41 mission profiles i.e. the summation of EBH if each profile was flown once.[7]

[6] Note: Actual severity factor values and EBH values removed

6.2 The Effect of Gas Turbine Fuel and its Additives on Composite Materials (Ryan Brookes, Defence Technology Agency r.brookes@dta.mil.nz)

Composite materials are increasingly being used in modern lightweight aircraft and helicopter structures. As design processes mature and operational experience grows, these composite structures are being increasingly refined, further reducing design margins. Such structures have less resilience to unanticipated degradation in service, including that caused by the environment.

Hot-wet environments and also gas turbine fuel have been identified by previous research as potentially damaging to some composite material systems. Military gas turbine fuel in particular contains additives not present in fuels used by the civil aviation community. Previous work has identified one of those additives - diethylene glycol monoethyl ether (DGME) icing inhibitor – as potentially damaging. Products formed when such fuels age have also been noted as potentially degenerative to some epoxy matrix systems. Therefore, the need exists to quantify the effect of these aggressors on actual composite material systems in service.

Four composite material systems taken directly from service platforms across the TTCP nations have been subject to prolonged conditioning in DGME, aged gas turbine fuel and in hot-wet environments. Both compression and shear test coupons were tested as it is known that the compression and shear properties of composite material systems are most significantly influenced by changes to the epoxy matrix when aged in aggressive environments. Results are presented in Figure 1.

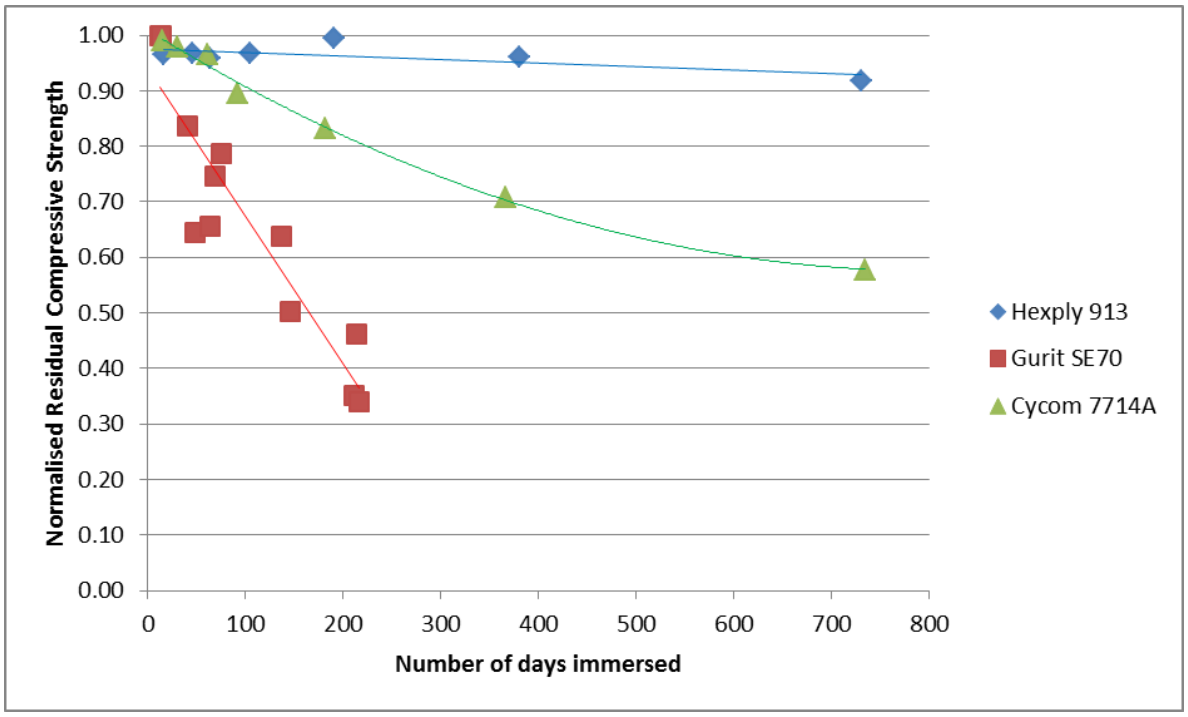

Figure 1: Normalised Residual Compressive Capacity after Prolonged Immersion in Pure DGME

[7] Note: Actual severity factor values and EBH values removed

It was found that each aggressive environment affected each epoxy system differently. The hot-wet environment degraded all material systems considered however the relatively modern Hexply 913 material system of the Cormorant helicopter was most severely affected. Pure DGME by comparison had relatively little effect on the Hexply 913 material system but very severely degraded the CYCOM 7714A material system taken from the B757 aircraft. Dilute DGME had little effect on all material systems, which may be due to the formation of a layer of sludge like 'apple jelly' on the coupon surfaces.

The key lesson taken from this research programme was that specific environments affect different epoxy systems differently. A seemingly benign hot-wet environment for example, that had little effect on some materials, most noticeably degraded another material system. It is therefore clear that each material system must be individually tested against the environments and aggressive materials to which it may be exposed in service. It is not enough to cross read the effect from one material to another.

Equally, new system fluids should also be tested before introduction to service to ensure they do not degrade legacy structures. The accuracy of the environment is also important. Dilution of an aggressor may drastically change the effect it may have on a material system. Likewise, a short period of exposure may not be adequate to disclose the full magnitude of degradation that may occur during prolonged exposure.

Through understanding the degenerative effects of various environments on material systems which are currently in service, measures can be taken to minimise effects. The information may also be of use for informing future design, evaluation and acquisition decisions.

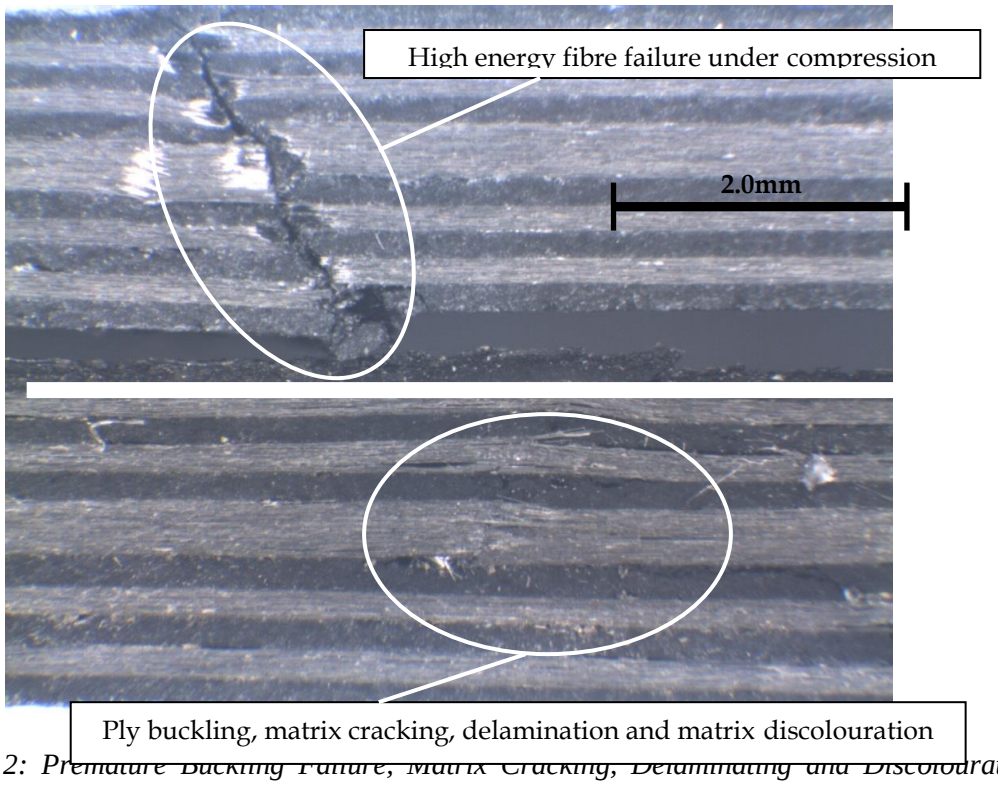

Figure 2: Premature Buckling Failure, Matrix Cracking, Delaminating and Discolouration of Epoxy Matrix after Immersion in DGME FSII for 216 Days (Lower coupon exposed to DGME, upper coupon is control)

6.3 Evaluation of RNZAF C-130H acceleration data (S. J. Bradley, Defence Technology Agency)

The Royal New Zealand Air Force (RNZAF) operates a fleet of five Lockheed Martin C-130 military transport aircraft. As part of their structural life management programme, the RNZAF installed a trial Usage Monitoring System (UMS) on a single C-130 aircraft. The UMS was developed by the Defence Technology Agency (DTA). It records a number of aircraft parameters and engineering data from sensors installed specifically for the UMS trial.

Lockheed Martin Aeronautics Company (Lockheed) was contracted to assess the data extracted from the aircraft over a four year period (2006-2010) in order to ascertain the severity of the RNZAF C-130 operational acceleration spectrum. Lockheed's assessment determined that the RNZAF's vertical acceleration spectrum is more severe than the worldwide average. The results were used as part of a wider usage assessment to determine RNZAF C-130 Equivalent Baseline Hours (EBH) and remaining airframe lifetime.

The five C-130 aircraft have recently been passed through a Life Extension Program (LEP) in which critical structures were replaced, thereby increasing the remaining life of the aircraft. The LEP also contains a significant upgrade to the mission systems, which could potentially change the operational usage of the aircraft. Each LEP aircraft has been installed with a FaMS (Fatigue Monitoring System, another form of a UMS) allowing for continuous monitoring of individual aircraft and to gain a more accurate lifetime assessment.

DTA has created an algorithm that replicates the results of the Lockheed vertical acceleration data processing software. As with the Lockheed software, this algorithm processed the trial UMS raw data and produced acceleration exceedance curves for total, manoeuvre, and gust accelerations. The DTA algorithm can now be used to analyse aircraft usage data and determine if the post LEP acceleration spectrum is more or less severe than pre LEP embodiment. Any change to the spectrum will alter the severity factors used within lifing calculations and hence residual life.

The DTA algorithm further analysed the trial UMS data and quantified gust response by GPS location for New Zealand airspace. The output is a visual representation of gust responses, portrayed as a contour map over New Zealand. The gust occurrence plots will allow more informed decisions to be made with respect to where the RNZAF conducts certain C-130 operations, with the aim of reducing gust driven fatigue.

Contour plots displaying the gust response in New Zealand were also successfully produced by the DTA algorithm. For each altitude band (high vs. low altitude), four plots were produced as follows:

- A contour map of flight time spent at locations within New Zealand.
- A contour map of New Zealand showing the locations of minor gusts (0.2g - 0.5g).
- A contour map showing the locations of severe gusts (>0.5g).
- A contour map of estimated gust fatigue damage.

Figures 1 and 2 show these contour plots.

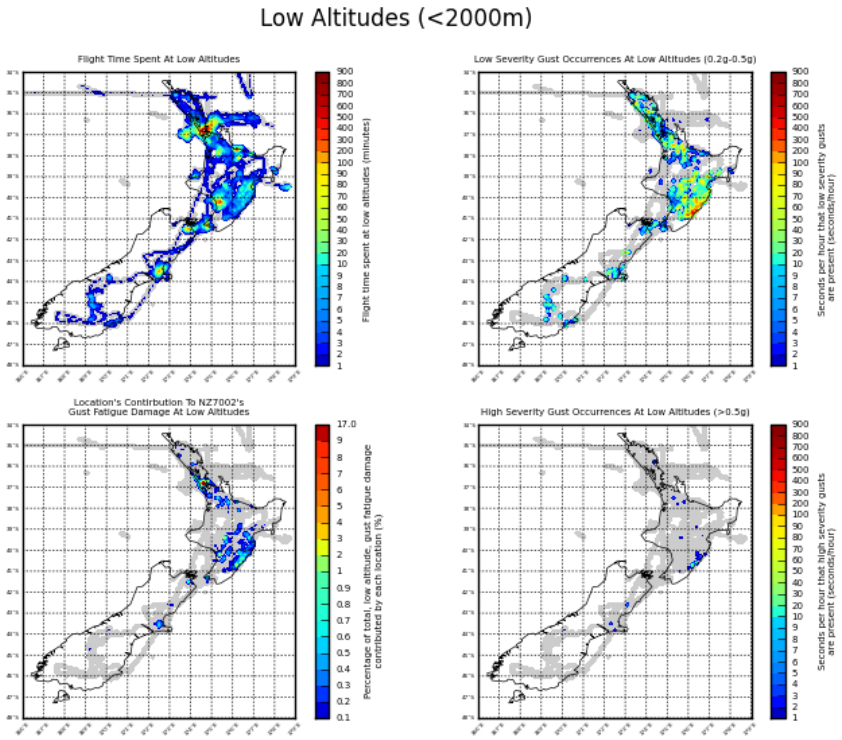

Figure 1. Geographic gust severity and frequency plots for low altitude flight.

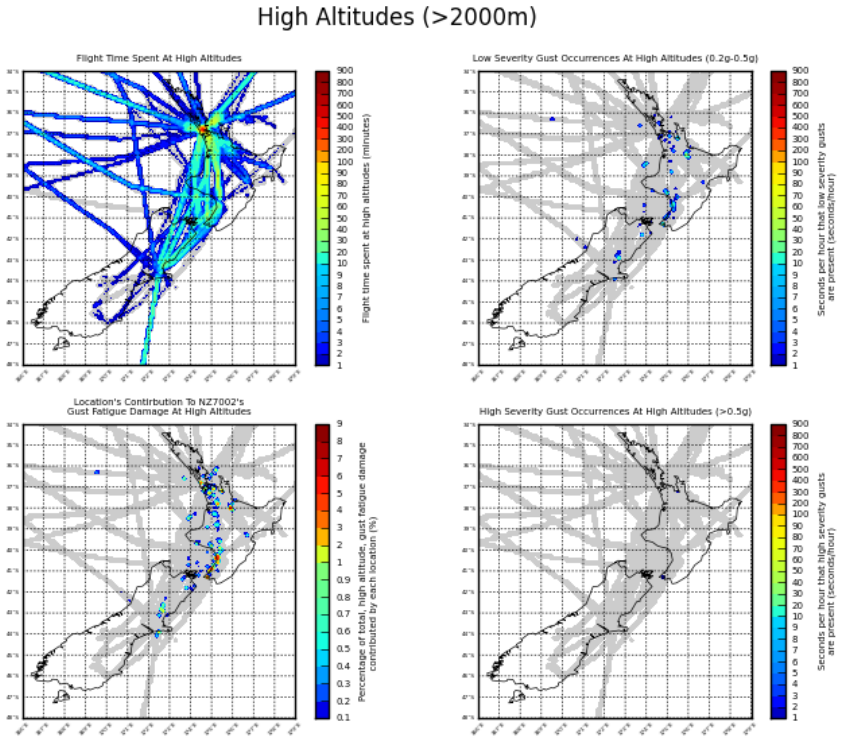

Figure 2. Geographic gust severity and frequency plots for high altitude flight.

Email: S K Campbell (s.campbell@dta.mil.nz)